Phenotypic, Functional, and Developmental Characterization of a Mouse Model for Virtual Memory $CD8^+$ T cells

by Katherine Roth Stagliano

B.S. in Biology, and Philosophy, May 1999, University of Scranton, PA, USA
M.Sc. in Plant Genetic Manipulation, August 2000, University of Nottingham, England, UK

A Dissertation submitted to

The Faculty of
The Columbian College of Arts and Sciences
of The George Washington University
in partial fulfillment of the requirements
for the degree of Doctor of Philosophy

August 31, 2017

Dissertation directed by

Arthur A. Hurwitz
Senior Director, Agenus

David Leitenberg
Associate Professor of Microbiology, Immunology, and Tropical Medicine

The Columbian College of Arts and Sciences of The George Washington University certifies that Katherine Roth Stagliano has passed the Final Examination for the degree of Doctor of Philosophy as of May 12th, 2017. This is the final and approved form of the dissertation.

Phenotypic, Functional, and Developmental Characterization of a Mouse Model for Virtual Memory $CD8^+$ T cells

Katherine Roth Stagliano

Dissertation Research Committee:

Arthur A. Hurwitz, Senior Director, Agenus, Dissertation Co-Director

David Leitenberg, Associate Professor of Microbiology, Immunology, and Tropical Medicine, Dissertation Co-Director

Conrad Russell Cruz, Assistant Professor of Pediatrics, Committee Member

Patrick Hanley, Assistant Research Professor of Pediatrics, Committee Member

© Copyright 2017 by Katherine Roth Stagliano.
All rights reserved

Dedication

For my sister.

Acknowledgements

This journey for me definitely took a village or three. You all know who you are, if you are reading this and I didn't list your name, I apologize. I love you and you were important to this process. I admit to making fun of people with long acknowledgement sections, but I really couldn't help myself. THANKS, EVERYONE!

My amazing, steadfast, true-hearted and fearless husband has been by my side for all the ups, downs and arounds that this process required. I would not be here without him. Thank you, Dave, for making sure my dreams came true. Thanks to Andy Hurwitz for providing a lab home for me at NCI. Andy, you will always stand out to me as an example of personal and scientific integrity in the face of unreasonable circumstances. Thank you for always choosing the true and the good. There are no words to describe the depth of love and gratitude I have for my Science Divas. Kim Shafer-Weaver, Nicole Gerlanc and Marty Sklavos, you carried me when I couldn't walk. Thank you for the sanity checks, the wine and the cursing. Sarah Cramer, you fill my soul. Love you forever. Miranda Hanson-Baseler, you take my breath away every time I'm with you. I don't know how I lived on this earth before knowing you. Lindsay Garvin, you amaze me. Thank you for saying yes when I told you I wanted to be friends with you. Majda Haznadar and Leigh Greathouse, thanks to each of you for being fine examples of strong, independent and successful female scientists and for being my friends. Robin Winkler-Pickett and Sheryl Brining have individually served as faithful mentors and friends to me for years. Thank you both for the monthly lunches and coffees.

These were/are vital to my sanity. Steve Cuss, thank you for being unflinching in the face of adversity. A true scientist seeks truth in all things, which is what you do. Thank you for your friendship. Jenn Shoe, I adore you. Thank goodness you were part of our team at NCI. You are a saint. Special thanks to everyone else in the animal facility at NCI who helped with my experiments. Special shout out to Jen Waters and Chris Perella. My interns!!! Bonnie Douglas, Cherish Ardinger, Ashley Babyak, Dahlia Kronfli, Troy Shuman, Avilash Das, Erin O'Connor, and Smaraki Dash – you made my survival possible, and enjoyable. I'm so proud of each of you. Thank you for letting me be part of your journey as well.

To Mom and Dad, thank you for passing on the value of valuing education and learning for learning's sake. Thank you for supporting me in my own particular interests which were different from everyone else's. I would not be here without you. Love you both! Chris, I got my degree before you got yours, HA! My parents, Dave's parents, all of our brothers, sisters, nieces and nephews have been a source of unrelenting support to both me and Dave during my journey. All of our nieces and nephews have been born while I was in school for one degree or another. You are each a source of joy to me. I love you all. Special thanks to Jess Tinsman for being an inspiration on how to follow your dreams and to never give up. Aunt Kathy, thank you for being a travel buddy for me when Dave was deployed. You are the easiest travel companion I know. I look forward to many more adventures with you. Dianne, there are no words for the role that you play in my life. Thank you for being my lifeline whenever I need you. Thank you for savoring with me every moment of goodness and happiness that life has offered to us. Alicia, Charlotte, Stacey, and Anita and all of your girls, thank you for being my life outside of work.

You are all so precious to me and so important to my happiness. Donna Moga, thanks for always loving me and being a witness to my life. To Maureen Petersen, and Pat and Kim Hickey, thank you for the dinners, wine, board games and reference points to sanity and stability. Josh Olsen and Cheryl Miller, thank you for our long-standing friendship. Kayleen Baguley Pemberton Stanek, thank you for changing my life. Thank you for being a huge part of my life outside of the lab. Misty Gilbert, thank you for being my weekly accountability buddy and my friend. Thank you for encouraging me when I need(ed) it. Anna Trivett, thank you for always being lovely, positive and encouraging. Rachel Eberly – I have cherished every pedicure we have gotten together and every bottle of wine that we have consumed. LOVE YOU! Allison Poore – you light up my life whenever we connect. The sun shines brighter, the air is purer, and the grass is greener in your presence.

All of my scientific mentors since high school had major impacts on my journey and deserve recognition here. Sister John Ann Proach and Rita Tomlinson at Conwell-Egan were foundational forces for me. I thought after I took that AP Bio test I would never study Immunology ever again. Little did I know. Kathy Dwyer at Scranton, June Nasrallah at Cornell, my colleagues and teachers at Governor's School at Carnegie-Mellon, and those I met during my Fulbright year at Nottingham were instrumental in training me in Molecular Biology which I will always consider my first and true love in science. When I'm roaming the halls of Building 10 on Saturdays in my t-shirt, jeans and flip-flops I always think of running into Jan Chlebowski at VCU on the weekends during my time there. I got my grounding in Biochemistry from some excellent professors at VCU. There were

important people who kept the fire burning for me during my interregnum - Yasir Skeiky and Chuck Scanga at Aeras and John Risinger in Savannah.

My time at NCI was full of wonderful experiences and important conversations. Special thanks to Giorgio Trinchieri, Jo Oppenheim, Scott Durum, Julie Hixon, Howard Young, Ming Dai and everyone else in CIP. No one ever turned me away if I needed help with questions or reagents. Special thanks to Devi Gurusamy, Jake Hocker, Ziqiang Zhu, and Vinod Singh for being excellent lab mates. Thanks to Cheryl Lamb and everyone else who keeps the CIP and NCI in Frederick running. Thanks to everyone I met in the FYI-CCR, you are all incredible. Thanks to Cristina Bergamaschi for help with the IL-15 mouse, and helpful conversations. Thanks to Rob Leighty and Nicole Gerlanc for help with statistics. A thousand thanks to Roberta Matthai and Kathleen Noer in the Flow Core for the late hours they spent sorting for me. They always went above and beyond the call of duty. This work would have been impossible without their expertise.

Most recently, I've made my home at the Center for Human Immunology at NIH. It is a complete honor and a source of immense joy to me to come to work every day with our entire team. It is impossible for me to adequately thank my Board of Directors for their guidance, mentorship and support – Neal Young, Giorgio Trinchieri, Ron Germain, Pam Schwartzberg, John Tsang, Chris Hourigan, Gregoire Altan-Bonnet and Steve Holland have all been exceptional people and scientists to know and have each been essential to my success. I've received fierce and relentless support and cheerleading from Caroline Iciek, Maria Conner,

Tiffiany Jones, Jessica Mann, Ange Biancotto, Brian Sellers, Marc Langweiler, and the entire CHI team. Thanks to my colleagues and professors at GW. Special thanks to Linda Werling for her open door policy. I don't know if you know how much your kindness and your support meant to me and everyone else who came through IBS under your watch. Thanks to Marc Wittlif for making me feel like I was his favorite.

Finally, thanks to my thesis committee. BJ Fowlkes, Patrick Hanley and Russell Cruz all stepped forward when called upon to serve on my thesis committee. Thank you for your input and valuable conversations. Thanks to Crystal Mackall for serving on my research committee while she was at NIH. HUGE thanks to Dave Leitenberg for generally being awesome and for being available to me since I started at GW. Thanks for being close by during this last part of the process. Kristin Tarbell, you were an essential part of me actually getting done. Thank you for continuing to check up on me during the last 1.5 years and making sure I actually crossed the finish line. THANK YOU.

Thanks to everyone for their encouragement and support so that I could finally get **Ph**inishe**D**.

Abstract of Dissertation

Phenotypic, Functional, and Developmental Characterization
of a Mouse Model for Virtual Memory $CD8^+$ T cells

Virtual memory (VM) cells exist in the steady-state in unimmunized mice as memory phenotype, antigen-specific $CD8^+$ T cells. VM cells display phenotypic and functional similarity to antigen-driven memory cells, however they exist at vanishingly low frequencies making them challenging to isolate, characterize, and study functionally. Our lab generated a mouse model of $CD8^+$ VM cells that allows us to characterize the phenotype, function and developmental requirements of this normally rare cell population. The mouse model, called very low avidity (VLO), harbors $CD8^+$ T cells that express a very low avidity transgenic TCR specific for an epitope of Tyrosinase Related Protein-2 (TRP-2). TRP-2 is an endogenous protein in C57BL/6 mice, and is a tumor antigen expressed in murine melanoma. Phenotypic characterization of VLO cells by flow cytometry shows that their memory signature, $CD44^{hi}$ $CD49d^{lo}$ $Eomesodermin^{hi}$ $T\text{-}bet^{hi}$, is consistent with previous reports of VM T cells that originate from a lymphopenia-induced pathway. We hypothesize that VLO cells develop in a unique manner resulting in their acquisition of a memory-like phenotype and innate-like function and may serve as model for non-antigen-induced memory cells. VLO mice exist in a state of severe lymphopenia. When lymphopenic conditions are relieved the frequency of VLO cells expressing a VM phenotype lessens, indicating that cell extrinsic factors are involved in directing acquisition of the VM phenotype. VLO cells proliferate weakly and produce low levels of interferon gamma (IFNγ) in response

to antigen stimulation, but respond dramatically to pro-inflammatory cytokines by proliferating robustly and expressing high levels of IFNγ. These responses are consistent with what has been reported for VM cells. *In vivo* examination of the response of VLO cells to a lymphopenic environment revealed that VLO cells proliferate rapidly, which is consistent with a VM phenotype. When VLO cells were used in an adoptive transfer model for treatment of B16 melanoma they did not control tumor any better than a control group statistically, but further studies are warranted. To gain an understanding of the role of antigen in the development of the memory phenotype of VLO cells, our lab generated a TRP-2 knockout mouse. When VLO cells developed in the absence of their cognate antigen they retained their memory phenotype, but also had increased cell numbers in the periphery suggesting that cognate antigen plays a role in deletion of VLO cells. Using mouse models, we demonstrated that VLO cells are able to develop in the absence of IL-15 or the absence of IL-7. Our data suggest that IL-7 plays a role in the homeostatic maintenance and/or survival of these cells. Taken all together these data support the idea that VLO cells behave consistently with what has been reported about VM cells. We suggest the VLO mouse is a useful model to study the behavior and development of VM cells.

Table of Contents

Dedication iv

Acknowledgements v

List of Figures xv

List of Abbreviations xviii

Chapter 1: Introduction 1

1.1 Adoptive Cell Therapy 1

1.1.1. History of cancer immunotherapy 1

1.1.2. Adoptive cell therapy 2

1.1.3. Improvement of ACT 3

1.2. Development of Mouse Models to Study ACT 6

1.2.1. Overcoming T cell tolerance to improve ACT 6

1.2.2. TCR functional avidity may affect susceptibility to tolerizing conditions 7

1.2.3. Mouse models to study TCR avidity in ACT 10

1.3. Memory $CD8^+$ T cells 18

1.3.1. Antigen-induced memory cells 18

1.3.2. Innate memory cells 19

1.3.3. Use of memory $CD8^+$ T cells in ACT 26

1.4. Hypothesis and Specific Aims 26

Chapter 2: Methods 29

2.1. Mice 29

2.1.1. Recipient mice: C57BL/6, B6.$Rag^{-/-}$, B6.$Rag^{-/-}$ $Thy1.1^+$ and $CD45.1^+$ 29

2.1.2. TCR Tg mice: VLO, LO and HI 29

2.1.3. KO mice used for developmental studies: $Il\text{-}7^{-/-}$, $Il\text{-}15^{-/-}$ and 30

Dct-Exon $1^{-/-}$ 30

2.1.4. Generation of Dct-Exons 2-$6^{-/-}$ mice 30

2.1.5. Generation of bone marrow chimeras 34

2.2. Generation of memory phenotype LO cells 34

2.2.1. In vitro method 34
2.2.2. In vivo method 35
2.3. Peptide, cytokines and antibodies 35
2.3.1. Peptide 35
2.3.2. Cytokines 35
2.3.3. Antibodies 35
2.4. Flow cytometry and cell sorting 38
2.5. In vitro assays 38
2.5.1. Proliferation assay 38
2.5.2. IFN-γ ELISPOT assay 39
2.6. In vivo experiments 39
2.6.1. CFSE dilution 39
2.6.2. Adoptive transfer of Tg T cells to treat subcutaneous B16 tumor 39
2.6.3. Generation of dendritic cell vaccine 40
2.7. Statistical analysis 40
2.7.1. Statistical analysis for in vitro studies and cell counts 40
2.7.2. Statistical analysis for tumor studies 40
Chapter 3: Aim 1 - Phenotypic Characterization of VLO 42
3.1 Phenotypic analysis of VLO cells by flow cytometry 42
3.2 VLO cells express high levels of memory markers and low levels of CD49d on their surface 46
3.3 VLO cells express high levels of the transcription factors Eomesodermin and T-bet 49
3.4 VLO cells express higher levels of Ly6C and lower levels of CD3 on the cell surface 53
3.5 Severe lymphopenia of VLO mice compared to other TRP-2 Tg mice 56
3.6 Generation of BM chimeras to investigate VLO lymphopenia 59
3.7 Mixed BM chimerism relieves memory phenotype of VLO cells 62
Chapter 4: Aim 2 - Functional Characterization of VLO 67
4.1. VLO cells proliferate less than HI or LO in response to higher doses of TRP-2 peptide 69
4.2 VLO cells produce less IFNγ than HI and LO in response to TRP-2 peptide 73

4.3. VLO cells proliferate more than HI and LO in response to proinflammatory cytokines in the absence of TCR stimulation 76
4.4. VLO cells secrete more IFNγ than HI and LO in response to proinflammatory cytokines in the absence of TCR stimulation 81
4.5. VLO undergo rapid homeostatic proliferation 85
4.6. VLO cells proliferate more than HI and LO in response to IL-15 in the absence of TCR stimulation 91
4.7. IL-15 stimulated proliferation is not coupled with IFNγ production 94
4.8. VLO cells do not efficiently control B16 melanoma tumor in an adoptive transfer model 97
Chapter 5: Aim 3 - Investigation of the Developmental Requirements for the Memory Phenotype of VLO Cells 105
5.1. VLO retain memory phenotype when developing in the absence of TRP-2 antigen 105
5.2. Generation of DCT KO mouse model by deleting Exons 2 through 6 110
5.3. VLO Dct-Exon 2-6$^{-/-}$ retain memory phenotype while alleviating lymphopenia in the periphery 115
5.4 VLO develop in the absence of IL-15 and retain memory phenotype 119
5.5. VLO develop in the absence of IL-7 in contrast to HI 123
5.6. VLO retain memory phenotype and lymphopenia in the absence of IL-7 127
5.7. Lymphopenia of VLO mice worsens with age in the absence of IL-7 130
Chapter 6: Discussion 134
6.1 VLO phenotype is consistent with virtual memory cells 134
6.2 VLO cells develop independently of IL-15, and IL-7 138
6.3 VLO cells respond robustly to proinflammatory cytokines 140
6.4 Treatment of tumors via adoptive transfer of VLO cells requires optimization 141
6.5 Overall summary 142
6.6 Future studies 143
Chapter 7: Bibliography 146

List of Figures

Figure 1.1: Murine model to explore T cell avidity in ACT. 12

Figure 1.2: VLO cells express high levels of CD44 and Ly6C on their cell surface compared to HI, LO and wild-type cells. 16

Figure 1.3: Summary of pathways that generate innate and antigen-induced $CD8^+$ memory T cells. 24

Figure 3.1: Gating strategy used for phenotypic analysis by flow cytometry. 44

Figure 3.2: VLO cells express high levels of CD44, CXCR3, CD122 and low levels of CD49d on their cell surface compared to HI, LO and wild-type cells. 47

Figure 3.3: VLO cells express high levels of T-bet and Eomesodermin. 51

Figure 3.4: VLO cells upregulate Ly6C and downregulate CD3 on the cell surface. 54

Figure 3.5: VLO mice are severely lymphopenic compared to other TRP-2 Tg mice. 57

Figure 3.6: BM chimeras were generated to investigate VLO lymphopenia. 60

Figure 3.7: Mixed BM chimerism relieves memory phenotype of VLO cells. 64

Figure 4.1: VLO cells proliferate less than HI and LO in response to TRP-2 peptide. 71

Figure 4.2: VLO cells produce less IFNγ in response to TRP-2 peptide. 74

Figure 4.3: VLO cells proliferate more than HI and LO in response to proinflammatory cytokines in the absence of TCR stimulation. 78

Figure 4.4: VLO cells secrete more IFNγ than HI and LO in response to proinflammatory cytokines in the absence of TCR stimulation. 82

Figure 4.5: VLO undergo rapid homeostatic proliferation. 88

Figure 4.6: VLO cells proliferate more than HI and LO in response to IL-15 in the absence of TCR stimulation. 92

Figure 4.7: IL-15 stimulated proliferation is not coupled with IFNγ production. 95

Figure 4.8: VLO cells do not efficiently control B16 melanoma tumor in an adoptive transfer model. 99

Figure 5.1: VLO retain memory phenotype when developing in the absence of TRP-2 antigen (*Dct*-Exon $1^{-/-}$). 108

Figure 5.2: Generation of *Dct* KO mouse model by deleting Exons 2 through 6. 112

Figure 5.3: VLO *Dct*-Exon $2\text{-}6^{-/-}$ retain memory phenotype while alleviating lymphopenia in the periphery. 117

Figure 5.4: VLO cells develop in the absence of IL-15 and retain their memory phenotype. 121

Figure 5.5: VLO develop in the absence of IL-7 in contrast to HI cells. 125

Figure 5.6: VLO cells develop in the absence of IL-7 and retain their memory phenotype. 128

Figure 5.7: VLO lymphopenia worsens with age in the absence of IL-7. 131

List of Tables

Table 2.1: Primers used to screen prospective clones for presence of homologous recombination of the DCT knockout construct 32

Table 2.2: Primers used to screen mice to confirm deletion of *Dct* gene. 33

Table 2.3: Antibodies used for flow cytometry experiments. 37

Table 4.1: Observed differences in xmid parameters and p values for the pairwise xmid contrasts. 1022

List of Abbreviations

^{o}C – degrees Celsius

µCi - microcurie

µM – micromolar

^{3}H – tritiated

ACT – adoptive cell therapy

ANOVA – analysis of variance

APC – antigen presenting cell

bp – base pairs

BM – bone marrow

CAR – chimeric antigen receptor

CD – cluster of differentiation

CFSE - carboxyfluorescein-diacetate succinimidyl ester

CPM - counts per minute

DC – dendritic cell

DCT – dopachrome tautomerase

DNA – deoxyribonucleic acid

ELISPOT - enzyme-linked immunospot

Eomes – eomesodermin

FBS – fetal bovine serum

FSC-A – forward scatter area

FSC-H – forward scatter height

GM-CSF - granulocyte macrophage colony-stimulating factor

hi – high

HI – high avidity mouse model or $CD8^+$ T cells from that mouse

HLA – human leukocyte antigen

HP – homeostatic proliferation

IFNγ – interferon gamma

IL – interleukin

IMP – innate memory phenotype

IV - intravenously

KO - knockout

lo - low

LO – low avidity mouse model or $CD8^+$ T cells from that mouse

MEM - Minimum Essential Media

mESC – mouse embryonic stem cells

MFI – mean fluorescence intensity

MHC – major histocompatibility complex

mL - milliliter

mM - millimolar

Neo - neomycin

ng - nanograms

NK – natural killer

PCR – polymerase chain reaction

pMHC – peptide-MHC

RAG – recombination-activating gene

RPMI - Roswell Park Memorial Institute

SSC-A – side scatter area

STAT - signal transducer and activator of transcription

T_{CM} – central memory T cells

TCR – T cell receptor

T_{EM} – effector memory T cells

Tg - transgenic

TGF-β - transforming growth factor beta 1

TILs – tumor-infiltrating lymphocytes

TMMML - Transgenic Mouse Model Laboratory

T_N – naïve T cells

Treg – regulatory T cell

T_{RM} – tissue-resident memory T cells

T_{SCM} – T memory stem cells

TRP-2 – tyrosinase related protein-2

TSLP - thymic stromal lymphopoietin

VLO – very low avidity mouse model or $CD8^+$ T cells from that mouse

VM – virtual memory

WT - wildtype

Chapter 1: Introduction

1.1 Adoptive Cell Therapy

1.1.1. History of cancer immunotherapy

In the late 1800s, William B. Coley, M.D., a bone sarcoma surgeon, injected a bacterial preparation composed of Streptococcus and Bacillus into a patient with a malignant tumor. He observed durable regression of the tumor, and spent the remainder of his career using "Coley's Toxins" as a treatment for bone and soft-tissue sarcomas [1, 2]. His work is considered to be one of the first examples of immunotherapy. With the emergence of radiation therapy and chemotherapy in the early and mid-1900s, Coley's methods, which produced less reliable outcomes, fell out of fashion [1]. As inbred laboratory animal models became available during the 1940's and 1950's, controlled studies examining the interaction of the immune system and cancer became possible [3]. In the late 1950's, as a result of these types of studies, Burnet proposed the hypothesis of cancer immunosurveillance, the idea that the immune system is constantly defending against threats, both foreign (infections) and domestic (cancer) [4]. In the 1970's, the investigation of immunotherapy gained popularity with the success of Bacillus Calmette–Guerin to treat bladder cancer [5]. The mechanism of action of this treatment modality is immune-mediated but is still incompletely defined, nonetheless it is still considered to be an effective local treatment for superficial bladder tumors [3, 6]. During the following decade, the use of intravenously administered cytokines was explored as a cancer therapy in humans using interleukin (IL) -2 and interferon alpha [7, 8]. These cytokine therapies and others have been refined over time, and

are still used for successful treatment of specific cancers [9, 10]. By the early 2000's, the concept of immunosurveillance was refined to the idea of cancer immunoediting which results in tumor elimination by, tumor equilibrium with, and tumor escape from the immune system [11]. In 2011, cancer was quasi-officially recognized as an immunological disorder when Hanahan and Weinberg expanded their six hallmarks of cancer to include "evasion of immune destruction" as an essential tenant of their conceptual framework [12]. In 2013, Science recognized cancer immunotherapy as its "Breakthrough of the Year" [13].

1.1.2. Adoptive cell therapy

Modulation of the immune system to fight cancer encompasses an array of approaches including: cancer vaccines, oncolytic viruses, cytokines, monoclonal antibodies, Toll-like receptor agonists, immune checkpoint modulators, and adoptive cell therapy (ACT) [14-21]. ACT can include transfer of T cells, Natural Killer (NK) cells, NK-T cells and antigen presenting cells (APC) [17, 22-24].

ACT made headlines in 2010, with the FDA approval of sipuleucel-T (PROVENGE®) manufactured by Dendreon [22, 25]. PROVENGE is a an autologous cellular immunotherapy used for the treatment of metastatic hormone refractory prostate cancer [22, 25]. The methodology of this therapy involves purifying a patient's peripheral blood mononuclear cells, which are then cultured *in vitro* in the presence of a recombinant human protein composed of prostatic acid phosphatase fused to granulocyte macrophage colony-stimulating factor (GM-CSF) which promotes the growth and differentiation of dendritic cells (DC)

[26, 27]. The results of this therapy are clinically modest, with only a 4-month increase in median survival, but are still considered promising [22, 25-27].

ACT utilizing T cells has not been approved for commercial development and remains in the clinical trial realm. The typical methodology involves isolating $CD4^+$ and $CD8^+$ T cells from a patient's blood or tumor, expanding these cells *ex vivo,* manipulating them in some fashion, and then reinfusing them back into the immunodepleted patient often including IL-2 which functions as a T cell growth factor [28, 29]. T cells isolated from resected tumors are termed "tumor-infiltrating lymphocytes (TILs)". T cell receptors (TCRs) with a desired specificity can be selected from a pool of TILs, and can then be targeted for expansion [28]. This strategy is based on the idea that T cells that are isolated from a tumor are in fact tumor-specific and have been functionally impaired by the immune suppressive tumor microenvironment [28, 30, 31]. Adoptive T cell therapy has shown hopeful, and in some cases dramatic, clinical results especially when used for the treatment of metastatic melanoma with overall response rates of approximately 50%, and complete response rates around 20% after at least five years of follow up [28, 32, 33]. Despite these encouraging results there remains an overwhelming need to continue to improve ACT for both melanoma and for other types of cancers. For the remainder of this dissertation reference to ACT will exclusively mean adoptive T cell therapy.

1.1.3. Improvement of ACT

One area that has increased the success of ACT is the use of immunodepleting regimens to prepare the patient prior to reinfusion of the cell

therapy. Immunodepletion can be accomplish by total body irradiation and/or chemotherapy. These treatments decrease the burden of endogenous regulatory T cells (Tregs) which are thought to inhibit the activity of anti-tumor $CD8^+$ T cells [34]. Gattinoni *et al* (2005) demonstrated using mouse models that lymphodepletion increases available levels of IL-7 and IL-15, leading to increased function of adoptively transferred T cells [35]. This observation was recapitulated in human studies which showed an increase in both IL-7 and IL-15 after lymphodepleting regimens [36, 37]. Higher response rates were associated with greater lymphodepletion [36-38].

Another area of focus for the improvement of T cells used in ACT is genetically modifying them with a chimeric antigen receptor (CAR). CARs are now in their fourth generation of development. Generally speaking, they are engineered receptors composed of an antibody that targets an extracellular tumor antigen, a CD3-derived immunoreceptor tyrosine-based activation motif signaling chain, and a co-stimulatory signaling domain [39-41]. These domains are fused together resulting in a chimeric receptor that functions in an human leukocyte antigen (HLA)-independent fashion [41]. CARs have been used successfully in a variety of cancers with the most encouraging results in hematologic malignancies [41-43].

Another method of improving ACT is the genetic modification of a patient's T cells to express a tumor antigen-specific TCR. This is achieved by cloning the genes for the alpha and beta chains of the desired TCR [44]. This method has mediated cancer regression in animals models and in patients [44-47]. Typically,

only highly avid receptors are selected [44-47]. Drawbacks of this modality include potential toxicity as a result of self-reactive TCRs, and unexpected specificity caused by pairing between endogenous alpha and beta subunits with the genetically engineered subunits [48]. This method also requires that the tumor being treated expresses the appropriate cognate HLA allele and the target antigen [49]. Efforts are being made to reduce off-target toxicity by introducing structural modifications to the TCRs and choosing target antigens that are tumor-specific [49-52].

Studies in animal models and in humans have provided indications that T cell differentiation status (naïve, memory or effector) may play a significant role in therapeutic efficacy of T cells used for ACT. The current consensus in the literature, led mainly by the laboratory of Nicholas Restifo at the National Cancer Institute, is that the T cells with a less differentiated phenotype prior to adoptive transfer are more effective after transfer. In murine studies, central memory T cells (T_{CM}) which were derived from naive T cells (T_N), were more potent in ACT compared to effector memory T cells (T_{EM}) [53]. Likewise, mouse studies conducted by Sommermeyer *et al* (2016), compared CAR-T cells generated from T_N and T_{CM} subsets to those created from T_{EM} subsets [54]. Again the less differentiated subsets, T_N and T_{CM}, demonstrated more potent antitumor activity. Studies in mice have compared $CD8^+$ T cells derived either from naïve cells or memory cells for use in ACT. Cells derived from naïve cells expanded, persisted and exhibited better control of tumor growth [55]. T_N cells must be physically purified away from antigen-experienced and memory T cells in order to preserve

their therapeutic potential because memory cells will induce naive cells to differentiate [55].

1.2. Development of Mouse Models to Study ACT

1.2.1. Overcoming T cell tolerance to improve ACT

Despite the potential of ACT as an effective cancer immunotherapy, studies in mice and humans have demonstrated that regression of tumor is most often followed by uncontrollable relapse [56, 57]. A significant obstacle that is thought to lead to failure of tumor control is T cell tolerance. Tolerance is simply defined as "failure to respond to antigen" [58]. T cell tolerance is a natural and required aspect of the immune system. Central tolerance eliminates self-reactive T cells in the thymus by negative selection [58]. Peripheral tolerance occurs outside of primary lymphoid organs and regulates self-reactive T cells through a variety of mechanisms including anergy, programmed cell death, alterations to phenotype, as well as control by Tregs and DC [58, 59]. The tumor microenvironment itself can lead to tolerization of T cells.

Tumors have developed complex mechanisms to evade and suppress the immune system. Tumor cells downregulate peptide major histocompatibility complex (MHC)-I [60, 61], express inhibitory receptors [62-64] upregulate expression of antiapoptotic molecules [65, 66] and activate death receptor signaling pathways [67, 68]. The tumor microenvironment can secrete immunosuppressive factors including transforming growth factor beta 1 (TGF-β), vascular endothelial growth factor, IL-10, C-C motif chemokine ligand 21, and indoleamine 2,3-dioxygenase [69-73]. These immunosuppressive factors, in turn,

promote the recruitment, differentiation, and expansion of suppressive cells such as Tregs, myeloid-derived suppressor cells and tumor-associated macrophages and tolerogenic DCs [74, 75]. All of which can act upon T cells and impair their ability to effectively recognize and respond to tumor [15, 59].

1.2.2. TCR functional avidity may affect susceptibility to tolerizing conditions

TCR functional avidity may affect the susceptibility of adoptively transferred T cells to the tolerizing conditions of the tumor microenvironment. TCR "avidity" is often confused with "affinity" and "functional avidity". Affinity is a pure biochemical definition of the on- and off- rate of a ligand for its receptor. In the case of a TCR, its ligand would be peptide-MHC (pMHC) class I [76-79]. Avidity includes affinity, but also takes into account the strength of multiple TCRs interacting with multiple pMHCs. Essentially, it is a measurement of multimeric interactions [79, 80]. Functional avidity describes how T cells functionally respond to antigen. It describes antigen sensitivity of T cells and takes into account TCR affinity, avidity, expression of coreceptors (CD4 or CD8), expression of inhibitory receptors and other signaling molecules [79, 81]. For the purposes of the studies that I will be discussing "TCR avidity" will be referring to the functional avidity of the TCR in question.

Generally speaking, high avidity T cells are preferred over low avidity cells for ACT because they are thought to be more effective in mediating regression of tumor in both human and mouse [44, 45, 47, 80, 82-88]. Extensive work has gone

into increasing the avidity of TILs used in ACT using a wide array of molecular and cell-based techniques (reviewed in [89]).

Despite this attention to high avidity T cells for use in ACT, there is evidence that intermediate and low avidity TCRs may be a more effective strategy for ACT. Irving *et al* (2012) conducted an *in vitro* assessment of $CD8^+$ T cell responsiveness by varying TCR affinity up to 1400-fold different from wild-type [90]. They found that intermediate binding results in maximal $CD8^+$ T cell responsiveness *in vitro*. The authors extrapolate that lower avidity TCRs may be more effective for use in ACT because of the low density of target antigen expressed on tumors [90]. Zhong and colleagues (2013) conducted a detailed analysis of TCR affinity threshold using *in vitro* and *in vivo* measures of T cell responses [91]. They found that high affinity TCRs did not lead to great antitumor activity. Instead, their results demonstrated the existence of a plateau of maximal effectiveness of affinity, above which increases in affinity were not productive. When taking this model into account, and considering the risk of self-damage resulting from autoimmunity of highly avid TCRs, the authors suggest that low to moderate affinity TCRs may be better options for ACT [91].

There is also evidence that suggests that high avidity T cells may be more prone to becoming tolerized in the tumor microenvironment. Janicki *et al* (2008) described the loss of function of high avidity $CD8^+$ T cells after they infiltrated their target tumor [92]. Lower avidity T cells with the same antigen specificity were not as easily tolerized [92]. Our lab had the same observation using a mouse model of

melanoma and comparing a high avidity TCR with a low avidity TCR targeting the same tumor-specific antigen.

Our lab has found that not only do adoptively transferred $CD8^+$ T cells become tolerized by the tumor microenvironment, but they can also be converted into a suppressive phenotype. Using a transgenic (Tg) mouse model of prostate cancer, tumor-antigen specific $CD8^+$ T cells were adoptively transferred into tumor-bearing mice [93]. The transferred $CD8^+$ T cells trafficked to the tumor, and were isolated as TILs. These cells were tested for suppressive activity *ex vivo* and were found to inhibit the *in vitro* proliferation of naïve $CD8^+$ T cells and $CD4^+$ T cells. Our lab found that the suppressive phenotype is governed, at least in part, by TGF-β. When TGF-β was blocked in the *in vitro* assays, suppression of proliferation was relieved [93].

Suppressive $CD8^+$ T cells have been described in humans as well. These are sometimes described as a $CD8^+$ Tregs or suppressive $CD8^+$ T cells. It is unclear whether these are distinct populations, but their functional descriptions in the literature are similar. The suppressive phenotype is usually described as $CD8^+$ $CD28^-$, and the $CD8^+$ Treg is usually described as $CD8^+$ $CD25^+$ $FoxP3^+$ [94-99]. Typically these cells are isolated and tested *ex vivo* for their ability to impact the proliferation and cytolytic capacity of naïve and/or effector $CD8^+$ T cells. Reduction of these functions is considered a hallmark of the suppressive $CD8^+$ T cell. The $CD8^+$ Treg or suppressor cell has been found to be present in the metastatic lymph nodes of a number of cancers as described by Filaci *et al* (2007) [94]. While these studies do not directly address avidity of the suppressive or Treg

$CD8^+$ T cells, unpublished work from our lab using mouse models suggests that higher avidity $CD8^+$ T cells are more likely to become tolerized and suppressive than lower avidity $CD8^+$ T cells. These observations are supported by published reports of similar observations [92].

1.2.3. Mouse models to study TCR avidity in ACT

Given the evidence suggesting that higher avidity $CD8^+$ T cells used for ACT are more prone to tolerization and conversion to a suppressive phenotype in the tumor microenvironment, our lab was motivated to generate a mouse model to study TCR avidity in the context of ACT. The lab built the model around the melanocyte differentiation antigen Tyrosinase Related Protein-2 (TRP-2) which is an endogenous protein in C57BL/6 mice, and is a tumor antigen expressed in the B16 murine melanoma cell line. TRP-2 is also known as dopachrome tautomerase (DCT). Historically, the DCT designation is used when the enzymatic function of the protein is being referenced, while the TRP-2 designation is used when the antigenic properties of the protein are being discussed. The terms are used interchangeably throughout this body of work.

The lab generated three $CD8^+$ TCR Tg mouse lines whose TCRs recognize the identical immunodominant epitope of TRP-2, peptide 180-188, but with different avidities. This epitope is presented by H-$2K^b$ in mice and HLA-A*0201 in humans [100]. C57BL/6 mice were vaccinated with TRP-$2_{180\text{-}188}$, and T cells were isolated from peripheral lymph organs and expanded *in vitro*. Three T cell clones were identified based on their functional response (high, low, and very low) to graded doses of antigen. Vα and Vβ chain usage was determined by spectratype

analysis [101]. The high avidity clone expressed Vα5 and Vβ7. The low avidity clone expressed two Vα chains, Vα3 and Vα17, and one beta, Vβ11 [102]. The very low avidity clone expressed Vα8 and Vβ5.2. The genes for TCR-Vα and TCR-Vβ were cloned from these candidates and expressed as transgenes under the control the human CD2 promoter. The linearized construct was injected into embryos and Tg founders were generated using standard techniques. The mice were created on a C57BL/6 background and were crossed to homozygously delete them for recombination-activating gene (*Rag*) 2 by crossing with B6.$Rag^{-/-}$. The mice were named HI for the high avidity TCR, LO for the low avidity TCR, and VLO for the very low avidity TCR.

HI, LO and VLO $CD8^+$ T cells were tested extensively using *in vitro* and *in vivo* functional assays to confirm that they respond to the same epitope of TRP-2 with differing avidity. As shown in Figure 1.1A, single cell suspensions made from the peripheral lymph nodes of wildtype (WT) C57BL/6, HI, LO and VLO mice were assessed for TRP-$2_{180\text{-}188}$ tetramer binding and CD8 expression by flow cytometry. WT $CD8^+$ cells respond to tetramer at a vanishingly low frequency. $CD8^+$ HI cells respond uniformly and robustly to tetramer. LO $CD8^+$ cells bind tetramer less strongly, while VLO cells bind weakly. Coat color of adult mice aged 8-12 weeks was examined as shown in Figure 1.1B. HI mice experience autoimmune depigmentation.

Figure 1.1: Murine model to explore T cell avidity in ACT. Three $CD8^+$ TCR Tg mouse lines were engineered by our lab to recognize the identical immunodominant epitope, TRP-$2_{180\text{-}188}$, but with different avidities. The mice were named HI for the high avidity TCR, LO for the low avidity TCR, and VLO for the very low avidity TCR. The mice were created on a C57B/L6 background and were crossed to B6.$Rag^{-/-}$ until the lines were homozygously deleted for *Rag*. (A) Single cell suspensions of peripheral lymph nodes of WT C57B/L6, HI, LO and VLO mice were assessed for TRP-$2_{180\text{-}188}$ tetramer binding and CD8 expression by flow cytometry. (B) Coat color of each mouse is compared. Mice were unmanipulated and were aged 8-12 weeks.

A.

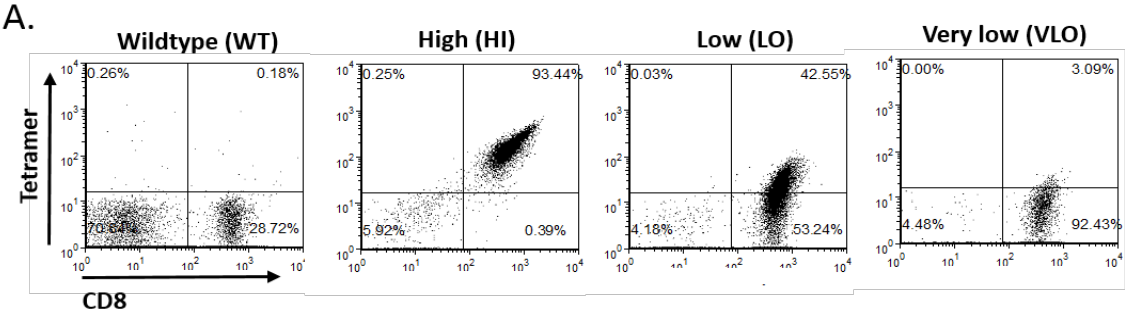
Wildtype (WT)
High (HI)
Low (LO)
Very low (VLO)
Tetramer
CD8
0.26%
0.18%
28.72%
0.25%
93.44%
5.92%
0.39%
0.03%
42.55%
4.18%
53.24%
0.00%
3.09%
4.48%
92.43%

B.

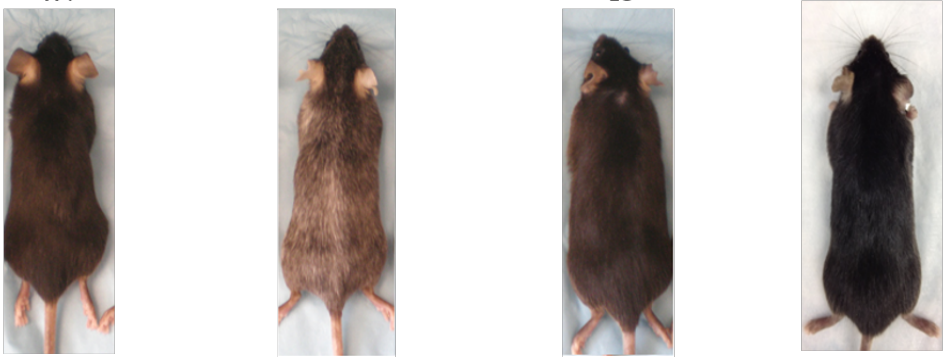
WT
HI
LO
VLO

Once the mouse lines were established, they were used as part of ACT for treatment of B16 melanoma. A typical ACT experiment using this model involved generating a melanoma tumor in a host animal by subcutaneous injection of B16 melanoma which was typically permitted to grow for several days. Meanwhile, $CD8^+$ T cells from the HI, LO or VLO lines were isolated from the lymph nodes of the TCR Tg mice. Once the tumor was established, the tumor-bearing animals were treated with intravenous injection of the HI, LO or VLO cells as ACT. Tumor burden was then measured over time.

Studies from our lab show that HI $CD8^+$ T cells are able to slow B16 tumor growth but become tolerized in the tumor microenvironment [103]. Phenotypically, HI cells contain a portion of their population that is $CD44^{hi}$. We presume that these cells are responding to endogenous TRP-2 which would be consistent with the depigmentation that is observed in these mice. LO $CD8^+$ T cells do not control B16 tumor well [102, 103]. The mice bearing the LO TCR do not develop autoimmune depigmentation and the LO cells maintain a naïve phenotype despite the presence of TRP-2 in the coat of the animals. This suggests that these cells are ignorant of endogenous TRP-2. VLO cells unexpectedly display an activated or memory phenotype and are $CD44^{hi}$ $Ly6C^{hi}$. Interestingly, these mice maintain their coat color. The memory phenotype of VLO cells could be the result of cross-reactivity to a self-antigen or be a result of some other mechanism that generates a memory phenotype. Mice from four different founder lines were tested and they each expressed the same memory phenotype. Figure 1.2 compares the phenotype of WT, HI, LO and VLO $CD8^+$ T cells isolated from lymph nodes of the

corresponding mice and tested for expression of CD44 and Ly6C by flow cytometry. VLO cells (red) express high levels of CD44 and Ly6C. In contrast, LO cells (green) display a naïve phenotype with low levels of CD44 and modest expression of Ly6C. HI cells (blue) show a range of CD44 expression and a bimodal distribution of Ly6C indicating a distinct subpopulation of HI cells that are antigen experienced. WT cells (black) are shown as a control.

Figure 1.2: VLO cells express high levels of CD44 and Ly6C on their cell surface compared to HI, LO and wild-type cells. Cells were isolated from the lymph nodes of the indicated mice, labeled for the indicated markers and analyzed by flow cytometry. Cells were gated on $CD8^+$ singlet lymphocytes before being analyzed for expression of indicated markers. This is representative data from more than three experiments.

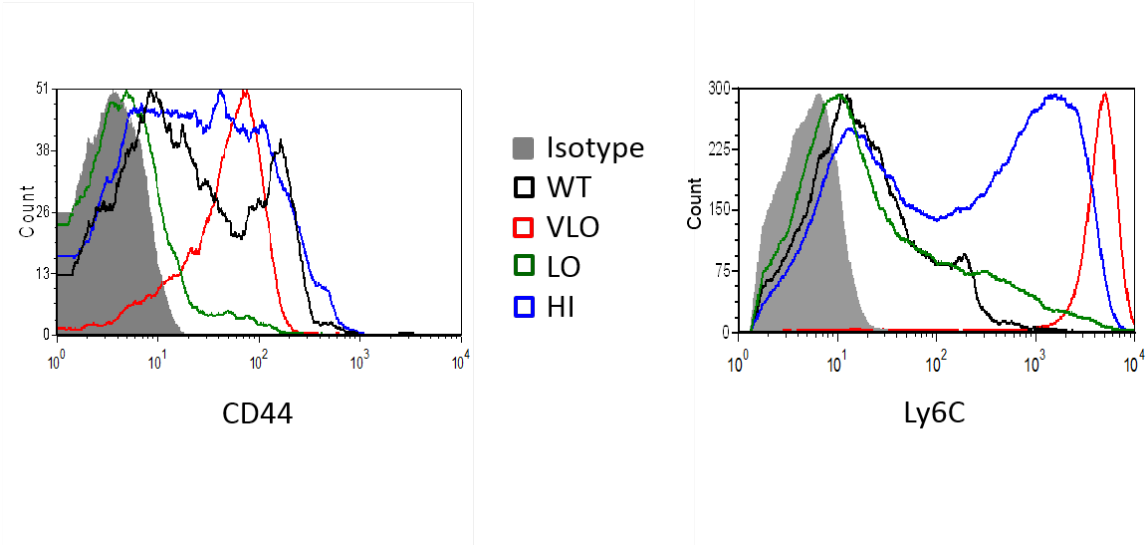
Count
51
38
26
13
0
10^0
10^1
10^2
10^3
10^4
Isotype
WT
VLO
LO
HI
Count
300
225
150
75
0
10^0
10^1
10^2
10^3
10^4

CD44

Ly6C

1.3. Memory CD8$^+$ T cells

1.3.1. Antigen-induced memory cells

Retrospective review of ACT clinical trials for the treatment of metastatic melanoma indicate that persistence of adoptively transferred cells is associated with tumor regression [33, 104, 105]. Memory CD8$^+$ T cells have the ability to self-renew and can remain for decades, thus making them an attractive target for use in ACT.

The traditional model of antigen-induced memory involves a naïve CD8$^+$ T cell experiencing foreign antigen being presented by MHC-I in the context of costimulation and stimulation by cytokines. After this priming phase, the naïve cell undergoes expansion and acquires effector function. After the effector phase, the majority of T cells die during the contraction phase, with a small fraction maintained as memory T cells [106-108]. These long-lived memory T cells persist in the repertoire. CD8$^+$ T memory cells are broadly characterized into T_{CM}, T_{EM}, T memory stem cells (T_{SCM}) and tissue-resident memory T cells (T_{RM}) [109-111]. T_{CM} recirculate through the blood stream to lymph organs, in contrast T_{EM} migrate to non-lymph tissue [109, 112]. T_{SCM} are distinguished by their multipotency and self-renewal capacity [113-116]. T_{RM} are a slow-moving population of cells that are sequestered in the tissue in which they were generated [111, 117]. The different human and mouse T cell memory subsets are distinguished by phenotypic markers, functional ability, and cytokine expression which are discussed and reviewed in detail elsewhere [112, 118, 119].

1.3.2. Innate memory cells

In addition to antigen-induced memory, there are other populations of memory $CD8^+$ T cells that fall into the category of "memory-like" including innate memory, bystander memory, homeostatic proliferation (HP) memory, and VM. These cell populations are described in the literature using different names. In order to maintain consistency, the nomenclature of innate memory T cells as rationalized by Jameson *et al* (2015) will be followed as closely as possible in this dissertation [120]. Jameson and colleagues describe $CD8^+$ T cell memory populations broadly by dividing the memory cells into "antigen-induced memory" and "innate memory" classes [120]. Figure 1.3 summarizes the pathways that result in innate and antigen-induced $CD8^+$ memory T cells. In Jameson's convention, innate memory $CD8^+$ T cells are divided into at least subclasses: 1) IL-4-induced memory cells 2) lymphopenia-induced memory cells and 3) steady-state VM cells [120].

1.3.2a. IL-4-induced memory

IL-4-induced memory cells include a range of memory subtypes. One of the best described memory subtypes is IL-4-induced innate memory phenotype (IMP) $CD8^+$ T cells. IMP $CD8^+$ T cells are a class of nonconventional αβ T cells [121-124]. They are phenotypically characterized by the expression of memory markers CD44 and CD122 (IL-2Rβ) [125, 126]. Functionally, they are able to secrete IFNγ [125, 126], and are capable of early response to antigen without primary stimulation [121-124]. Hu *et al* (2007) provided evidence that IMP $CD8^+$ T cells can help clear infectious diseases using a Listeria model [127]. Other studies have shown that innate $CD8^+$ T cells can support host defense against other infections

including Salmonella and Mycobacterium [123]. These cells are found to be increased in frequency when they develop in the absence of Tec kinases, and certain transcription factors [122, 127-133]. IL-4 is known to be involved in their development, while IL-15 is thought to be required for their homeostatic maintenance [134, 135]. The mechanism by which IMP $CD8^+$ T cells develop and their specific role in the immune system is incompletely understood. Some studies suggest they develop via selection from hematopoietic MHC-I [128, 130], while other studies suggest they develop via nonhematopoietic nonthymic MHC-I [136]. IMP $CD8^+$ T cells share markers with classical Ag-induced memory $CD8^+$ T cells and homeostatic memory $CD8^+$ T cells [137] but are distinct from these two populations [138].

1.3.2b. Lymphopenia-induced memory

Studies by Huang *et al* (2013), confirmed that the IMP phenotype is distinct from $CD8^+$ T cells that have arisen by homeostatic expansion [138]. Naïve $CD44^{lo}$ $CD8^+$ T cells undergo HP when they are transferred into a lymphopenic environment. Lymphopenia can be induced by irradiation or via a genetic deficiency such as in *Rag* knockout (KO) mice [139-141]. Some reports describe a natural phase of lymphopenia that occurs in neonatal mice [142-144]. During expansion naïve CD8 T cells acquire a phenotype that is similar to antigen-driven memory $CD8^+$ T cells with increased expression of CD44, lymphocyte function-associated antigen 1, Ly6C, and CD122 [139-141]. TCR engagement with cognate pMHC is not required for this type of expansion, nor for acquiring the memory phenotype [145-147]. Although engagement with self-peptide MHC is reported to

be a requirement for the development of this cell type [148]. HP memory $CD8^+$ T cells develop in response to IL-7 and IL-15, cytokines that signal a lymphopenic environment and trigger homeostatic expansion. During lymphopenia there are fewer cells competing for these cytokines, so the existing cells experience higher levels which then triggers their proliferation. Low-affinity TCR ligands and other cytokines are also thought to play a role in this process [149-152].

In addition to acquiring a memory phenotype, lymphopenia-induced memory cells also acquire functional characteristics similar to those of conventional antigen-driven $CD8^+$ memory T cells. Compared to naïve cells, both classes of memory cells respond to antigen stimulation with increased proliferation, enhanced cytotoxic effector function, and elevated effector cytokine production [139-141]. Studies have shown that HP memory cells are able to control infections, including control of bacterial infections [108, 148, 153]. Many of these early studies were performed using induced lymphopenia [108, 140, 141, 154].

1.3.2c. Virtual memory

Work by research teams led by Jameson and Kedl have demonstrated that Ag-specific memory $CD8^+$ T cells exist in unimmunized mice as a normal part of the T cell repertoire [137, 169, 188]. These cells were dubbed "virtual memory (VM) cells". VM cells are defined as memory phenotype, antigen-specific $CD8^+$ T cells that exist in the steady-state in unimmunized mice. Other groups subsequently reported similar observations. VM cells have been shown to exist in both conventional mice as well as in germ free animals. Using unimmunized host animals, which were germ-free and specific pathogen free, Haluszczak *et al* (2009) isolated antigen-specific $CD8^+$ T cells which displayed a phenotype consistent with

HP memory cells [137]. Gnotobiotic mice are raised under germ free conditions, and as such have limited exposure to environmental antigens, nonetheless, unprimed gnotobiotic mice possess a population of $CD8^+$ memory T cells [155]. Because these cells exist under gnotobiotic conditions, it has been suggested that they are not generated by conventional priming [156]. VM cells express phenotypic and functional similarity to antigen-driven memory cells, however they exist at vanishingly low frequencies making them challenging to isolate, characterize and study functionally [137, 157, 158]. Haluszczak *et al* (2009) suggests that this population is a novel arm of the immune system and plays an active role in the primary immune response [137].

Studies using *Il-4 receptor* α (*Il4r*) KO mice provided evidence that the absence of IL-4 reduces VM cells as well as other populations of $CD8^+$ memory T cells, but VM cells are not entirely dependent upon IL-4, as the population was not completely ablated. The authors suggested that in the absence of IL-4 VM cells are most likely using IL-7 and IL-15 to support lymphopenia-induced proliferation and maintenance, as suggested by other studies [159, 160]. Other groups have shown that IL-7 and IL-15 support the maintenance of memory $CD8^+$ cells which are characterized by $CD44^{hi}$ $CD122^{hi}$ [156].

Important work by Akue *et al* (2012) provided evidence that VM cells originate during a natural phase of neonatal lymphopenia which triggers lymphopenia-induced proliferation in the periphery [156]. After the neonatal period, this cell population is maintained through adulthood. It is also maintained during response to unrelated antigens. Time course studies in neonatal mice and

showed that VM cells arise in the periphery and not in the thymus. Other groups have shown that memory cells can home the thymus [161].

Figure 1.3: Summary of pathways that generate innate and antigen-induced CD8$^+$ memory T cells. Exogenous stimuli is indicated by red text, blue text indicates endogenous stimuli (adapted from [120]).

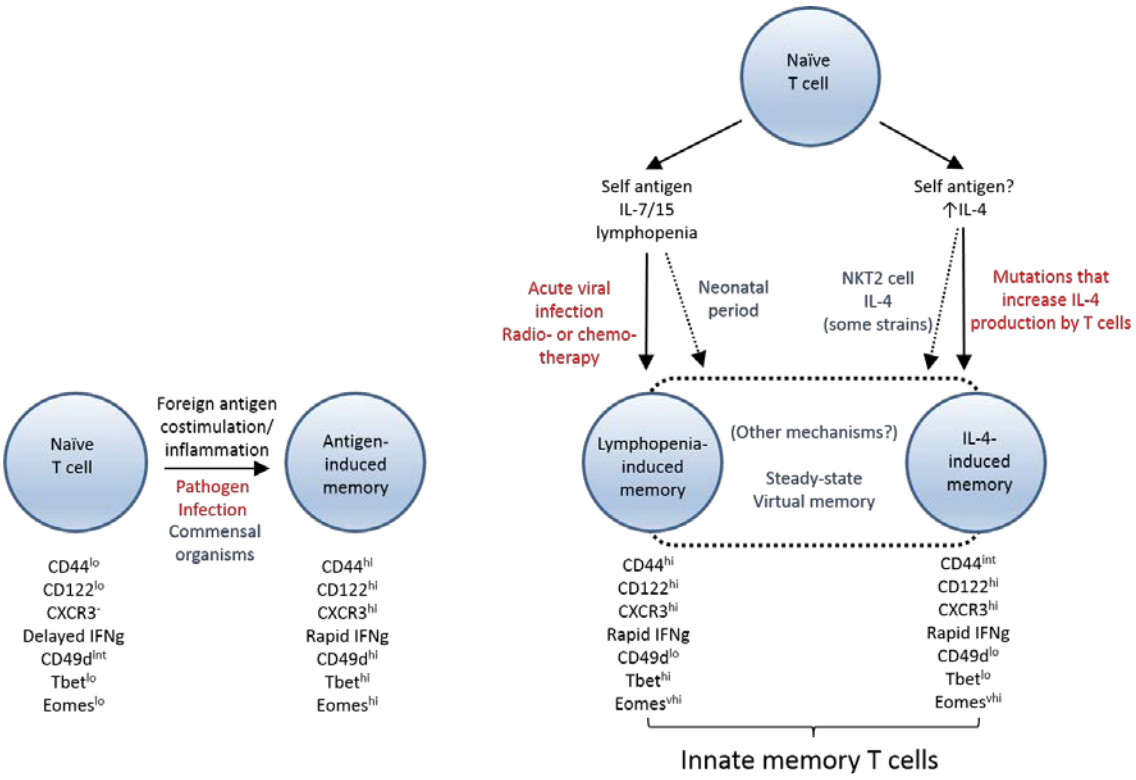
Naïve
T cell
Foreign antigen
costimulation/
inflammation
Pathogen
Infection
Commensal
organisms
Antigen-
induced
memory
CD44lo
CD122lo
CXCR3-
Delayed IFNg
CD49dint
Tbetlo
Eomeslo
CD44hi
CD122hi
CXCR3hi
Rapid IFNg
CD49dhi
Tbethi
Eomeshi
Naïve
T cell
Self antigen
IL-7/15
lymphopenia
Self antigen?
↑IL-4
Acute viral
infection
Radio- or chemo-
therapy
Neonatal
period
NKT2 cell
IL-4
(some strains)
Mutations that
increase IL-4
production by T cells
Lymphopenia-
induced
memory
(Other mechanisms?)
Steady-state
Virtual memory
IL-4-
induced
memory
CD44hi
CD122hi
CXCR3hi
Rapid IFNg
CD49dlo
Tbethi
Eomesvhi
CD44int
CD122hi
CXCR3hi
Rapid IFNg
CD49dlo
Tbetlo
Eomesvhi
Innate memory T cells

1.3.3. Use of memory CD8$^+$ T cells in ACT

Because memory CD8$^+$ T cells respond more quickly to their target antigen than do naïve CD8$^+$ T cells, and because memory CD8$^+$ T cells persist in the host, it would seem that they would be an attractive option for use in ACT. Some studies have compared the therapeutic efficacy and *in vivo* fate of T_{CM} to T_{EM} cells in animal models of ACT. The Restifo and Rosenberg labs demonstrated that T_{CM} conferred superior tumor protection compared with T_{EM} cells in mouse models [35, 53, 162]. Studies in primates by Berger *et al* (2008) support the initial observations in mouse that adoptively transferred central memory cells can persist [163]. They found that effector cells derived from CD8$^+$ central memory cells results in persistent T cell memory. In contrast, when effector cells were expanded from T_{EM} the cells did not lead to persistent memory [163]. Wang *et al* (2012), expanded these studies in human metastatic melanoma by isolating autologous tumor-specific T_{CM} cells [164]. These cells were then differentiated *ex vivo* into effector cells and transferred back into the patients. They found that the adoptively transferred cells targeted tumor, persisted over time, and regained the T_{CM} phenotype [164].

1.4. Hypothesis and Specific Aims

ACT provides a promising means to harness the immune system to combat tumors. Despite the potential of ACT as an effective cancer immunotherapy, studies in mice and humans have demonstrated that regression of tumor is most often followed by uncontrollable relapse [56, 57]. A significant obstacle that is thought to lead to failure of tumor control is T cell tolerance. Data from our lab

and others suggest that lower avidity TCRs are more resistant to tolerization by the tumor microenvironment. Meanwhile, other studies suggest that memory cells may be useful in ACT.

Our lab has generated a mouse model that harbors a Tg TCR that is expressed on $CD8^+$ T cells. The VLO model 1) is very low avidity 2) displays a memory phenotype and 3) is targeted to a tumor-specific antigen in a mouse model of melanoma. Given the unique features of these cells, we were curious to explore the phenotype of these cells in more detail and to test their efficacy when used in ACT.

Hypothesis: VLO cells develop in a unique manner resulting in their acquisition of a memory-like phenotype and innate-like function and may serve as model for non-antigen-induced memory cells.

My research aims are delineated below and addressed in subsequent chapters of this dissertation.

Aim 1: Investigate the phenotype of VLO cells and VLO mice to determine the class of memory that VLO most closely resembles.

Hypothesis: VLO cells acquire their memory phenotype through a non-antigen-induced pathway.

- Characterize the cellular phenotype of VLO cells by flow cytometry by exploring the expression of memory markers listed in Figure 1.3.
- Explore the phenotype of VLO mice by examining them for lymphopenia.

Aim 2: Explore the *in vitro* and *in vivo* function of VLO cells.

Hypothesis: VLO cells, because of their unique memory phenotype, will possess unique *in vitro* and *in vivo* function and will be more responsive to stimulation than naïve cells.

- Compare proliferation of VLO, LO and HI cells in response to antigen stimulation, and to cytokine stimulation.
- Compare IFNγ production of VLO, LO and HI cells in response to antigen stimulation, and to cytokine stimulation.
- Explore *in vivo* function by testing the ability of VLO, LO and HI cells to proliferate in response to lymphopenia.
- Test the ability of VLO, LO and HI cells to control a mouse model of melanoma.

Aim 3: Investigate the developmental requirements for the memory phenotype of VLO cells.

Hypothesis: VLO cells do not require their antigen, TRP-2, but do require cytokines to acquire their memory phenotype.

- Examine VLO memory phenotype when cells develop in the absence of TRP-2.
- Examine VLO memory phenotype when cells develop in the absence of IL-15 or IL-7.

Chapter 2: Methods

2.1. Mice

Mice were housed under specific pathogen-free conditions and were treated in accordance with National Institutes of Health guidelines under protocols approved by the Animal Care and Use Committee of the National Cancer Institute-Frederick facility (Frederick, MD).

2.1.1. Recipient mice: C57BL/6, B6.*Rag*$^{-/-}$, B6.*Rag*$^{-/-}$ Thy1.1^{+} and CD45.1^{+}

C57BL/6 mice (6–8 weeks of age) were obtained from Charles River Laboratories (Frederick, MD). B6.*Rag*$^{-/-}$ and B6.*Rag*$^{-/-}$ Thy1.1^{+} were bred as needed in our animal facility and were originally obtained from The Jackson Laboratory. CD45.1^{+} mice were purchased from The Jackson Laboratory. CD45.1^{+} mice were bred with B6.*Rag*$^{-/-}$ until they were homozygous for CD45.1 and lacked both alleles for *Rag*, thus generating the CD45.1^{+} *Rag*$^{-/-}$ line that was maintained in our facility.

2.1.2. TCR Tg mice: VLO, LO and HI

TCR Tg mouse strains 2A5 (VLO), 37B7 (LO), and 24H9 (HI) harbor TCR transgenes that recognize an H-2K^{b}-restricted epitope of TRP-2$_{180–188}$. These strains were generated by the Hurwitz lab using the methods that were described previously [102]. Each strain was breed onto a B6.*Rag*$^{-/-}$ background.

2.1.3. KO mice used for developmental studies: *Il-7*$^{-/-}$, *Il-15*$^{-/-}$ and *Dct*-Exon 1$^{-/-}$

C57BL/6-*Il-7*$^{-/-}$*Rag*$^{-/-}$ mice were a kind gift from Scott Durum's lab at the National Cancer Institute, Frederick MD. The mice were originally obtained from Charles Surh, (The Scripps Research Institute, La Jolla, CA). C57BL/6-*Il-15*$^{-/-}$ mice were a kind gift from Cristina Bergamaschi from George Pavlakis's laboratory at the National Cancer Institute, Frederick, MD. The mice were originally bought from Taconic Farms (Germantown, NY). *Dct*-Exon 1$^{-/-}$ were obtained from The Jackson Laboratory and were originally generated in Friedrich Beermann's lab [165].

2.1.4. Generation of *Dct*-Exons 2-6$^{-/-}$ mice

The *Dct* Exon 2-6 KO construct was generated by a commercial company, IDT (Coralville, IA). Electroporation of the gene construct into mouse embryonic stem cells (mESC) was performed by the Transgenic Mouse Model Laboratory (TMML) of the Laboratory Animal Services Program at the National Cancer Institute, Frederick, MD. I designed polymerase chain reaction (PCR) primers to screen for the presence of the recombined construct in the proper location in the genomic of prospective clones. I used pDRAW32 deoxyribonucleic acid (DNA) analysis software (www.acalone.com), and Primer3 (www.simgene.com) to design primers and the NCBI Primer-BLAST tool to confirm specificity of primers in the mouse genome (https://www.ncbi.nlm.nih.gov/tools/primer-blast/).

Genomic DNA from candidate mESC samples was purified using standard phenol chloroform extraction. Clones were screened by PCR using the primer pairs described in Table 2.1. Hot-Start Taq Blue Master Mix from Denville

Scientific (Holliston, MA) was used with the following conditions 5 minutes at 95 degrees Celsius (^{o}C), followed by 40 cycles of 1 minute at 95^{o}C, 1 minute at 55^{o}C and 7 minutes at 72^{o}C, followed by cooling and storage at 4^{o}C. PCR products were visualized by agarose gel electrophoresis. After screening approximately 350 mESC samples, four candidates were found that showed recombination. These cells were then transferred into blastocysts and inserted into pseudo-pregnant females by TMML. Ultimately two chimera lines were generated and transferred into our laboratory's mouse colony where we oversaw the breeding of chimeras and the intercrossing of pups. Pups were screened for slate coat color which is the phenotype expected for mice with a homozygous deletion of DCT. Tail clips were used to test for presence or absence of exons by PCR. Primer pair sequences are listed in Table 2.2. Hot-Start Taq Blue Master Mix from Denville Scientific (Holliston, MA) was used with the following conditions 5 minutes at 95^{o}C, followed by 30 cycles of 1 minute at 95^{o}C, 1 minute at 60^{o}C and 1 minute at 72^{o}C, followed by cooling and storage at 4^{o}C. All primers were purchased from Integrated DNA Technologies, Inc (Coralville, IA).

Table 2.1: Primers used to screen prospective clones for presence of homologous recombination of the DCT knockout construct.

Position	Forward Primer	Sequence (5' to 3')	Reverse Primer	Sequence (5' to 3')	Product Size (basepairs)
5' External	5-Arm-5F	GCA GCT CCA GGT GTG CCA CTT	Linker-R1	GTT AGC CAG AGG GCC GCT CT	4007
3' External	Neo-9F	AAG GGG CCA CCA AAG AAC GG	3-Arm-4R	GCC ACT TCG CAG CCA GAC GA	5286
3' Internal	Neo-4F	CTA AAG CGC ATG CTC CAG ACT GCC	3-Arm-In-2R	CTT CCG GGA GAG GCT CTG GCT	3883
5' Internal	5-Arm-In-F	CTA AAG CGC ATG CTC CAG ACT GCC	Linker-R1	GTT AGC CAG AGG GCC GCT CT	2907

Table 2.2: Primers used to screen mice to confirm deletion of *Dct* gene.

Position	Forward Primer	Sequence (5' to 3')	Reverse Primer	Sequence (5' to 3')	Product Size (basepairs)
Exon 1	DCT-Ex1-F	TCC CAA TTA AGA AGG CAT GG	DCT-Ex1-R	CCA GGG TCT GGT GTC TGT TT	294
Exon 2	DCT-Ex2-F	CCC GAC TGT AAT CGG AAG AA	DCT-Ex2-R	TTG CGT GGT GAT CAC GTA GT	299
Exon 3	DCT-Ex3-F	TAC CAT CTG TTG TGG CTG GA	DCT-Ex3-R	AAA AGC ATC CAC ACT GGG TC	100
Exon 4	DCT-Ex4-F	CAG TTT TCC TAT GGG AGG CA	DCT-Ex4-R	GGT AGG GTT GAT ACT CGC CA	166
Exon 5	DCT-Ex5-F	TGA GAC CCT TTC TCG CAG TT	DCT-Ex5-R	GTG TCT GCC AAA ACC TGG AT	179
Exon 6	DCT-Ex6-F	GTG GCA TAG CCT CTG CTT TC	DCT-Ex6-R	AGT CCA GTG TTC CGT CTG CT	135
Exon 7	DCT-Ex7-F	TCT TGC AGG TCC TCC ACT CT	DCT-Ex7-R	AAG TTG CTC TGC GGT TAG GA	201

2.1.5. Generation of bone marrow chimeras

B6.*Rag*$^{-/-}$ or CD45.1^{+} *Rag*$^{-/-}$ recipient mice were sub-lethally irradiated with 500 gray. 24 hours post-irradiation, recipient mice were reconstituted with bone marrow (BM) that was either 100% VLO BM, 100% WT BM or a 50/50 mix of VLO and WT BM. In all cases, BM was depleted of T cells using Miltenyi LD columns according to the manufacturer's instructions (Miltenyi Biotec, Inc, San Diego, CA) using Miltenyi microbeads directed against CD3, CD8, CD90.1 and CD90.2. At least 3 x 10^6 cells were then transferred via tail vein injection into prepared recipient mice which were allowed to engraft for at least 2 months before assessment and harvesting.

2.2. Generation of memory phenotype LO cells

2.2.1. *In vitro* method

Spleen and peripheral lymph nodes from one LO mouse were processed to generate a single cell suspension of 40 x 10^6 cells total. Media was Roswell Park Memorial Institute (RMPI) 1640 (Gibco) supplemented with 10% fetal bovine serum (FBS) (Invitrogen), 1 x Minimum Essential Media (MEM) vitamins (Gibco), 2 millimolar (mM) glutamine (Gibco) and 1:100 Penicillin-Streptomycin (Gibco). Cells were treated with media containing 2 micromolar (μM) TRP-2 peptide for two hours in the presence of 1:1000 β-mercaptoethanol (BioRad). IL-12 (10 nanograms/millimeter (ng/mL)) and IL-2 (20ng/mL) were added and cells were cultured for three days. The cells were washed, split and cultured in media containing IL-15 (20 ng/mL), 2 μM TRP-2 antigen and 1:1000 β-mercaptoethanol. Cells were harvested after 5 days. This method was developed in our lab based on modifications of the protocol found in Mueller *et al* (2008) [166].

2.2.2. *In vivo* method

Single cell suspension of LO cells were generated from the lymph nodes of LO mice. Cells (3 to 5 x 10^6) were adoptively transferred via tail vein injection into CD45.1$^+$ host animals. After 3 hours, the mice received a dendritic cell vaccine pulsed overnight with 20 μM TRP-2 peptide. After 10 days the recipient mice were harvested for spleen and lymph nodes to generate single cell suspensions which were labeled and sorted to isolate LO cells (CD45.1$^-$ CD8$^+$) which had acquired a memory phenotype *in vivo*.

2.3. Peptide, cytokines and antibodies

2.3.1. Peptide

All references in this dissertation to "TRP-2 peptide" refer to the TRP-$2_{180–188}$ (SVYDFFVWL) peptide was purchased from New England Peptide (Gardner, MA).

2.3.2. Cytokines

All cytokines were recombinant mouse and were reconstituted and handled according to manufacturer's instructions. IL-2 and thymic stromal lymphopoietin (TSLP) were sourced from R&D Systems, Inc, Minneapolis, MN. IL-7, IL-12 and IL-15 were bought from BioLegend, Inc, San Diego, CA. IL-18 was obtained from Medical and Biological Laboratories Co, Ltd.

2.3.3. Antibodies

All antibodies were bought from Biolegend, San Diego, CA, excepting anti-T-bet and anti-Eomes which came from eBioscience. Antibodies were used and

handled according to manufacturers' recommendations. Fixable Viability Dye eFluor 450 was purchased from eBioscience.

Table 2.3: Antibodies used for flow cytometry experiments.

Antibody	Clone	Isotype
CD45.1, anti-mouse	A20	Mouse IgG2a
CD4, anti-mouse	GK1.5	Rat IgG2b
CD183 (CXCR3), anti-human	G025H7	Mouse IgG1
CD45, anti-mouse	30-F11	Rat IgG2b
Ly-6C, anti-mouse	HK1.4	Rat IgG2c
CD3e, anti-mouse	145-2C11	Armenian Hamster IgG
CD8a, anti-mouse	53-6.7	Rat IgG2a
CD90.1 (Thy1.1), anti-rat	OX-7	Mouse IgG1
CD44, anti-mouse	IM7	Rat IgG2b
CD5, anti-mouse	53-7.3	Rat IgG2a
CD49d, anti-mouse	9C10	Rat IgG2a
CD122 (IL-2Rb), anti-mouse	5H4	Rat IgG2a
Tbet, anti-mouse	4B10	Mouse IgG1
Eomes, anti-mouse	Dan11mag	Rat IgG2a

2.4. Flow cytometry and cell sorting

Flow cytometry was performed according to standard practices at the Center for Cancer Research Frederick Flow Cytometry Core, Frederick, MD using the BD LSRII flow cytometer (BD Biosciences). Cell sorting was performed by the Flow Cytometry Core staff using a BD FACSAria III (BD Biosciences). Data was analyzed using FCS Express analysis software (De Novo Software, Glendale, CA).

2.5. *In vitro* assays

Media used in *in vitro* assays was Dulbecco's Modified Eagle's Medium (Gibco) supplemented with 10% FBS (Invitrogen), 1 x MEM vitamins (Gibco), 2 mM glutamine (Gibco) and 1:100 Penicillin-Streptomycin (Gibco) and 1:1000 β-mercaptoethanol (BioRad).

2.5.1. Proliferation assay

TCR Tg T cells, 2 x 10^4 per well in a 96-well plate, were cultured in the presence of indicated doses of TRP-2 peptide (0 to 10 μM) and 2 x 10^5 irradiated (3000 rad) WT splenocytes which acted as APCs. All cytokines, TSLP, IL-2, IL-7, IL-12, IL-15, IL-18 or combinations thereof, were used at 100 ng/mL final concentration and were used in the absence of APCs. At 60 hours, 1 microcurie (μCi) tritiated (^{3}H) thymidine (PerkinElmer) was added to each well and the cells were harvested at 68 hours using a Cell Harvester from Tomtec Life Sciences, Hamden, CT, USA. Radioactivity was measured in a Liquid Scintillation Counter (Trilux MicroBeta, Wallac). Proliferation was measured by the incorporation of radioactive thymidine indicated as counts per minute (CPM). Samples were studied in triplicate.

2.5.2. IFN-γ ELISPOT assay

IFNγ production was measured following manufacturer's instructions using Mouse IFN gamma enzyme-linked immunospot (ELISPOT) Ready-SET-Go!® from EBioscience. TCR Tg T cells, 5 x 10^3 per well, were cultured in the presence of indicated doses of TRP-2 peptide (0 to 10 uM) and 4 x 10^5 irradiated (3000 rad) WT splenocytes which acted as APCs. All cytokines, TSLP, IL-2, IL-7, IL-12, IL-15, IL-18 or combinations thereof, were used at 100 ng/mL final concentration and were used in the absence of APCs. T cells treated with cytokines were used at a dose of 2.5 x 10^3 per well. After incubation for 48 to 60 hours, plates were washed and processed as previously described [167].

2.6. *In vivo* experiments

2.6.1. CFSE dilution

Naïve $CD44^{lo}$ TCR Tg T cells were labeled with 5 μM 5,6-carboxyfluorescein-diacetate succinimidyl ester (CFSE) as described [103]. Labeled cells were adoptively transferred via tail vein injection into recipient B6.*Rag*$^{-/-}$ mice. After a four days, mice were euthanized and single cell suspensions were made from peripheral lymph nodes. These were analyzed for CFSE dilution, CD44, CD49d and CD3 expression on $CD8^+$ T cells.

2.6.2. Adoptive transfer of Tg T cells to treat subcutaneous B16 tumor

The TRP-2-expressing murine melanoma cell line, B16-BL6, was maintained in cell culture conditions as described [102]. B16-BL6 cells (1 x 10^5) were injected subcutaneously into C57BL/6 recipient mice. Three to six days after tumor injection, 2.0 x 10^6 antigen-specific HI or VLO $CD8^+$ T cells were adoptively transferred into host mice via tail vein injection. Three to 24 hours after T cell

transfer, mice were vaccinated subcutaneously with TRP-2 peptide-pulsed, BM-derived DC as described [102] using 20uM TRP-2 peptide. Tumor size was estimated by measuring perpendicular diameters using a caliper. Mice were euthanized when tumor area exceeded 400 mm^2. Tumor size was recorded as 400 mm^2 for any timepoints after death. Tumor-bearing mice that died with tumors less than 400 mm^2 were assigned the tumor size at the time of death.

2.6.3. Generation of dendritic cell vaccine

This method is described in detail in Zhu *et al* (2015) [103]. Briefly, red blood cell-depleted BM from WT mice was treated with media containing GM-CSF. After seven days, nonadherent cells were harvested and pulsed with TRP-$2_{180–188}$ (20 μM) overnight. The next day, nonadherent cells were washed and resuspended and used to vaccinate mice by injecting 5 x 10^5 cells subcutaneously.

2.7. Statistical analysis

2.7.1. Statistical analysis for *in vitro* studies and cell counts

Statistical analyses for differences between group means were performed by Single Factor Analysis of Variance (ANOVA). $P<0.05$ was considered statistically significant. Error bars were calculated for Standard Error. Microsoft Excel software was used to analyze the data.

2.7.2. Statistical analysis for tumor studies

Statistical analysis for tumor studies was conducted by Dr. Robert Leighty of the Data Management Services at the National Cancer Institute in Frederick, MD.

Logistic growth curves for four groups of volume data were calculated using the following model:

Let y_{ijk} be the volume on the kth day for the jth mouse in ith group. Let x_{ijk} be kth day for the jth mouse in the ith group. The model is

$$y_{ijk} = \frac{\phi_1}{1 + \exp[(\phi_2 - x_{ijk})/ \phi_3]}$$

Where ϕ_1 = Asym is the horizontal asymptote

ϕ_2 = xmid is thex value at which the response is $\phi_1/2$, and

ϕ_3 = scal is the scale parameter, the distance between the inflection point ϕ_2 and the point where the response is $\phi_1 /(1+e^{-1})$. The parameters ϕ_2 measures the speed with which the growth curve is increasing towards the asymptote. These parameters are compared between the four groups.

Chapter 3: Aim 1 - Phenotypic Characterization of VLO

Rationale: To characterize the phenotype of $CD8^+$ VLO cells and VLO mice.

Background: As described in the Introduction, HI, LO and VLO mice were developed by the Hurwitz lab as tools to study TCR avidity, and in particular how T cell avidity impacts efficacy of ACT. As the HI, LO and VLO Tg mouse lines were being characterized, it was noted that $CD8^+$ VLO cells displayed the unexpected and unusual feature of almost uniformly expressing high levels of CD44, indicating previous activation ("antigen experience") or possibly memory status. It was of interest to more fully characterize the phenotype of VLO cells and VLO mice.

The studies described in this chapter explore the phenotype of VLO cells by examining the expression pattern of cell surface markers and intracellular proteins using flow cytometry. The VLO mice themselves were interrogated phenotypically by comparing the cell count of peripheral lymph nodes to those of wild-type mice as well as the HI and LO strains. Mixed BM chimeras were generated using VLO and WT marrow transferred into *Rag*$^{-/-}$ recipients in an attempt to perturb the development of elevated CD44 expression on VLO cells.

3.1 Phenotypic analysis of VLO cells by flow cytometry

As a general strategy, single cell suspensions were generated from the lymph nodes of the indicated mice. Cells were labeled with fluorescently-conjugated antibodies and analyzed by flow cytometry. Appropriate isotype controls were used. Data is typically displayed as histograms which were generated from $CD8^+$ singlet lymphocytes, unless otherwise noted. The gating strategy to select this population is shown in Figure 3.1. Singlet cells were gated based on forward scatter height (FSC-H) and forward scatter area (FSC-A) (Figure 3.1A).

This population was further refined by selection of the lymphocyte population based on side scatter area (SSC-A) and FSC-A (Figure 3.1B). $CD8^+$ cells were then selected in Figure 3.1C.

Figure 3.1: Gating strategy used for phenotypic analysis by flow cytometry. Cells were isolated from the lymph nodes of mice, labeled for the indicated markers and analyzed by flow cytometry. (A) Single cells were selected based on FSC-H vs FSC-A. (B) The lymphocyte population was selected based on size and granularity (SSC-A vs FSC-A). (C) $CD8^+$ cells were further selected by gating on a positive signal after labeling with anti-CD8 antibody coupled with a fluorochrome.

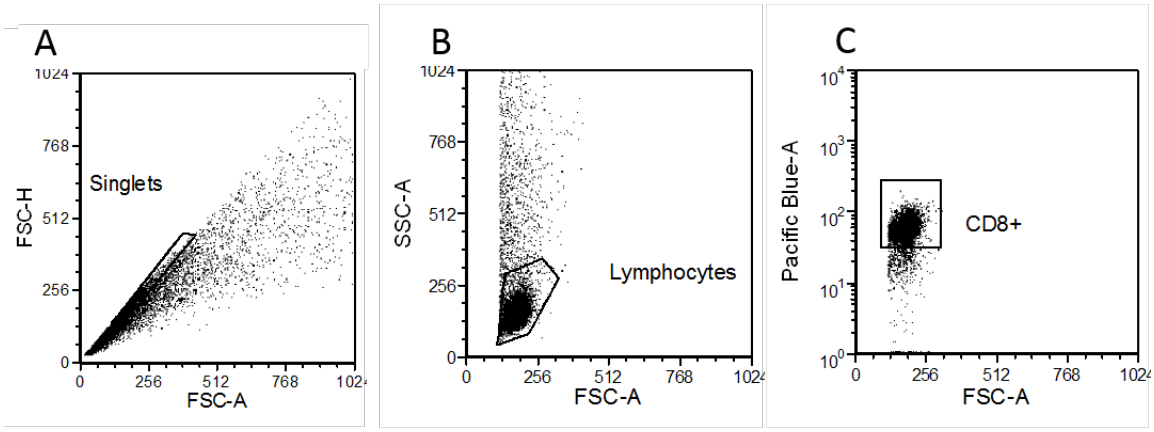
A
Singlets
FSC-H
FSC-A
B
Lymphocytes
SSC-A
FSC-A
C
CD8+
Pacific Blue-A
FSC-A

3.2 VLO cells express high levels of memory markers and low levels of CD49d on their surface

Based on the initial observation that VLO cells expressed high levels of CD44, it was hypothesized that they could be displaying an antigen-induced memory phenotype or an IMP (Figure 1.3). The first step in ascertaining the pathway that was triggering the phenotype was to characterize the cells in more detail. To this end, the expression of cell surface markers CD122, CXCR3, and CD49d was investigated along with intracellular expression of the transcription factors T-bet and Eomesodermin (Eomes). The differential expression of these proteins was expected to assist in determining which pathway directed the acquisition of VLO T cell phenotype.

As shown in Figure 3.2A, CD44 expression was elevated on the cell surface of VLO cells (red) compared to LO (green), HI (blue) and WT (black). Note that LO cells in green are almost uniformly naïve, expressing low or absent levels of CD44. WT cells in black and HI cells in blue express a range of CD44 expression indicative of a sub-population of memory T cells. CXCR3 (Figure 3.2B) and CD122 (Figure 3.2C) were examined and found to be elevated on VLO cells compared to $CD8^+$ T cells from other strains of mice further supporting the idea that VLO cells are memory cells. CD49d expression was down-regulated on VLO cells compared to the other cell populations (Figure 3.2D). Low levels of CD49d expression support the idea that VLO cells bear an innate memory phenotype and might originate from either a lymphopenia-induced pathway or an IL-4-induced pathway.

Figure 3.2: VLO cells express high levels of CD44 (A), CXCR3 (B), CD122 (C) and low levels of CD49d (D) on their cell surface compared to HI, LO and wild-type cells. Cells were isolated from the lymph nodes of the indicated mice, labeled for the indicated markers and analyzed by flow cytometry. Cells were gated on $CD8^+$ singlet lymphocytes before being analyzed for expression of indicated markers. This is representative data from more than three experiments.

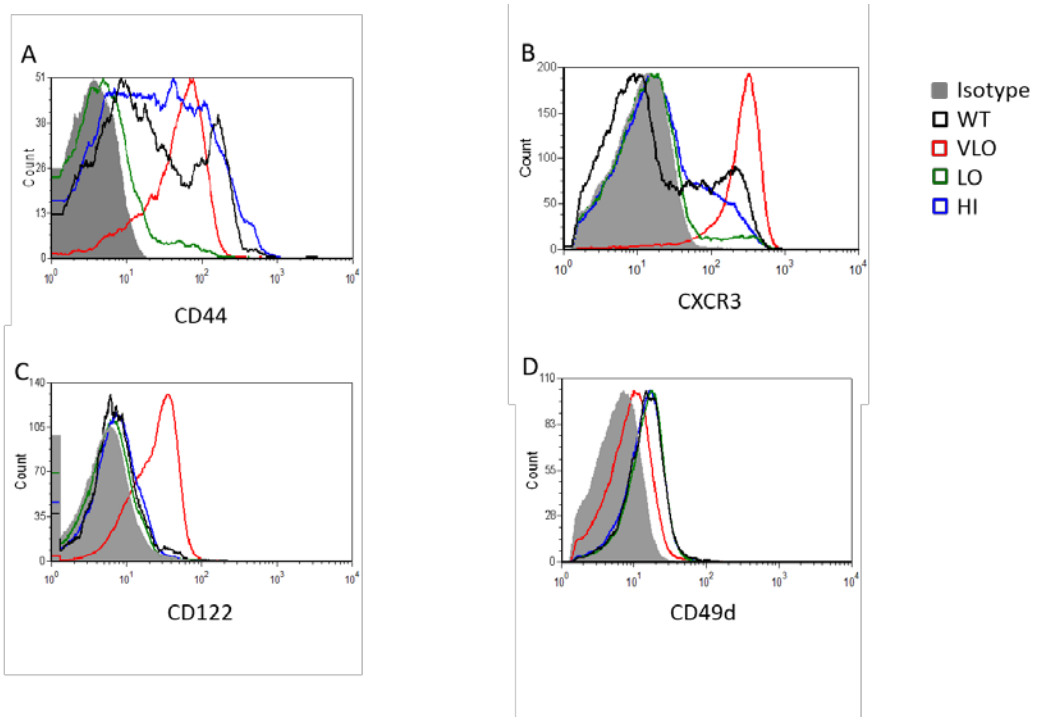
A
Count
CD44
B
Count
CXCR3
C
Count
CD122
D
Count
CD49d
Isotype
WT
VLO
LO
HI

3.3 VLO cells express high levels of the transcription factors Eomesodermin and T-bet

Lymphopenia-induced memory cells and IL-4-induced memory cells are phenotypically distinguished by their intracellular T-bet expression levels (Figure 1.3). High levels of T-bet correspond to lymphopenia-induced memory cells while low levels correspond to IL-4-induced memory. Eomesodermin is expressed at high levels in all classes of memory cells, with highest levels of expression seen in innate memory T cells. Expression of T-bet and Eomesodermin is described to be low in naïve cells. As shown in Figure 3.3A, T-bet is elevated in VLO cells compared to T cells isolated from other Tg mice which is consistent with a lymphopenia-induced memory phenotype. Eomesodermin is also upregulated in VLO cells (Figure 3.3B). Taken together, the pattern of expression of surface markers and transcription factors in VLO cells is consistent with what has been reported for lymphopenia-induced memory cells that fall under the broader category of innate memory T cells.

Innate memory T cells, whether they are generated via a lymphopenia-induced pathway or an IL-4 induced pathway have also been described as virtual memory cells [120]. This designation applies when innate memory T cells exist under steady-state conditions, and have not been triggered by merely transient events. In the case of VLO cells, we suggest that these qualify as VM cells because they exist in the steady-state conditions of the unmanipulated VLO mouse. VM cells normally exist in other Tg models and in WT animals at vanishingly low numbers and are notoriously challenging to study as a result of their low frequency

[120]. As a result, this mouse model may provide a rich source of VM T cells for subsequent study.

Figure 3.3: VLO cells express high levels of (A) T-bet and (B) Eomesodermin. Cells were isolated from the lymph nodes of the indicated mice, stained for the indicated markers and analyzed by flow cytometry. Cells were gated on $CD8^+$ singlet lymphocytes before being analyzed for expression of indicated markers. This is representative data from more than three experiments.

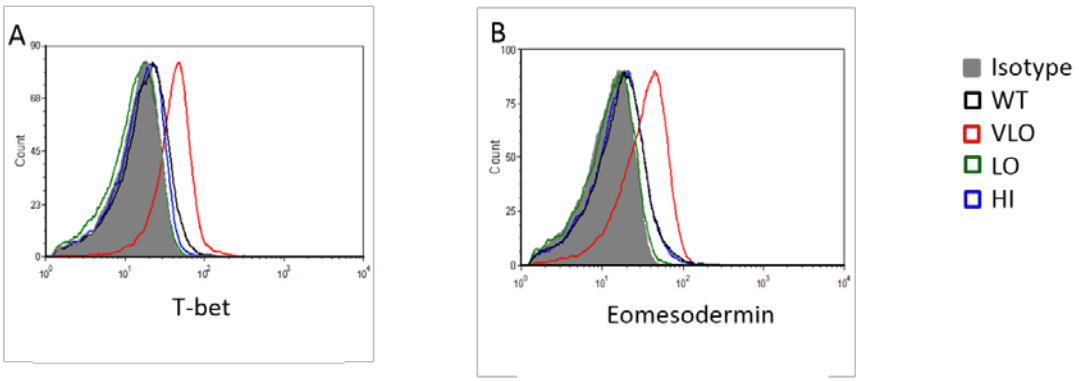
A
Count
T-bet
B
Count
Eomesodermin
Isotype
WT
VLO
LO
HI

3.4 VLO cells express higher levels of Ly6C and lower levels of CD3 on the cell surface

In addition to the proteins that distinguish lymphopenia-induced memory cells from other classes of memory cells, we also interrogated a variety of cell surface proteins with the intention of carefully phenotyping VLO cells. Two proteins that consistently showed differential expression compared to LO, HI and WT cells were Ly6C and CD3. VLO cells consistently express higher levels of Ly6C on their cell surface compared to LO, HI and WT cells (Figure 3.4A), although a sub-population of HI cells do express elevated levels of Ly6C. VLO cells consistently express lower levels of CD3 on their cell surface compared to LO, HI and WT cells (Figure 3.4B). Both phenotypes are consistent with previous engagement of TCR or antigen experienced cells.

Figure 3.4: VLO cells upregulate Ly6C (A) and downregulate CD3 (B) on the cell surface. Cells were isolated from the lymph nodes of the indicated mice, stained for the indicated markers and analyzed by flow cytometry. Cells were gated on $CD8^+$ singlet lymphocytes before being analyzed for expression of indicated markers. This is representative data from more than three experiments.

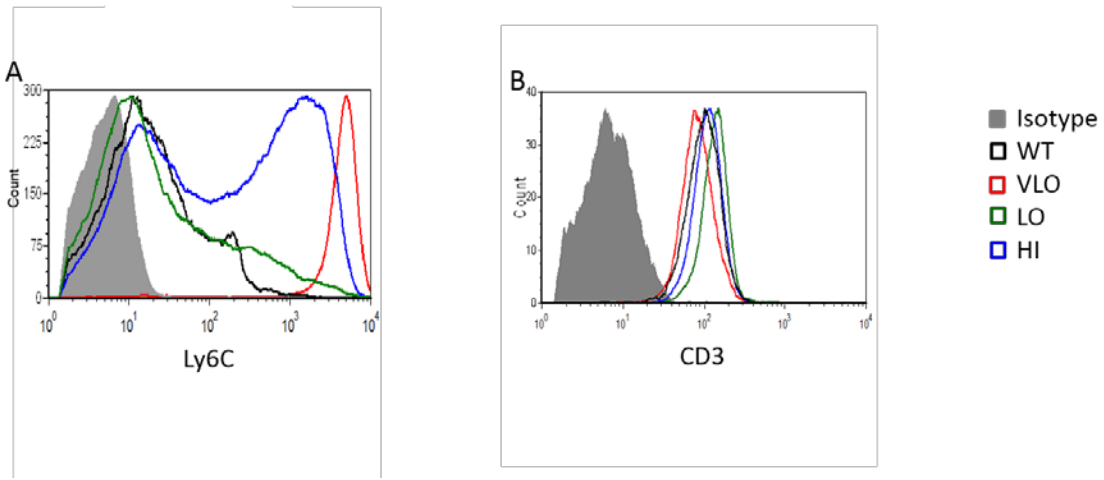
A
Count
Ly6C
B
Count
CD3
Isotype
WT
VLO
LO
HI

3.5 Severe lymphopenia of VLO mice compared to other TRP-2 Tg mice

Given that VLO cells express markers indicative of lymphopenia-induced memory we were interested in assessing their cell counts in lymph nodes as a measure of lymphopenia. Single cell suspensions were pooled from inguinal, axial, mesenteric and brachial lymph nodes and counted on a cell counter. At least four individual animals were tested in each group. As shown in Figure 3.5, VLO animals are severely lymphopenic with average cell counts of 4×10^6 compared to LO (13.6×10^6), HI (26.6×10^6) and WT (26.9×10^6). It is interesting to note that as avidity increases, so does cell count in the periphery. LO cell counts are greater than VLO, while HI animals display no evidence of lymphopenia with no statistical difference compared to WT. This is somewhat surprising, given that all three transgenic strains were crossed onto a *Rag*$^{-/-}$ background. The severe lymphopenia of VLO is a phenotype of the mouse strain, and supports the idea that VLO CD8$^+$ cells acquire their memory phenotype through a lymphopenia-induced pathway. It is possible that there is something unique about the VLO TCR that is contributing to this chronic lymphopenic state, given its specificity for a self-antigen, TRP-2.

Figure 3.5: VLO mice are severely lymphopenic compared to other TRP-2 Tg mice. Peripheral lymph nodes (inguinal, axial, mesenteric and brachial) were harvested and used to make single cell suspensions which were counted on a cell counter. Mice are all 6-10 weeks of age. Error bars were calculated by Standard Error. * Indicates $p<0.05$ calculated by Single Factor ANOVA.

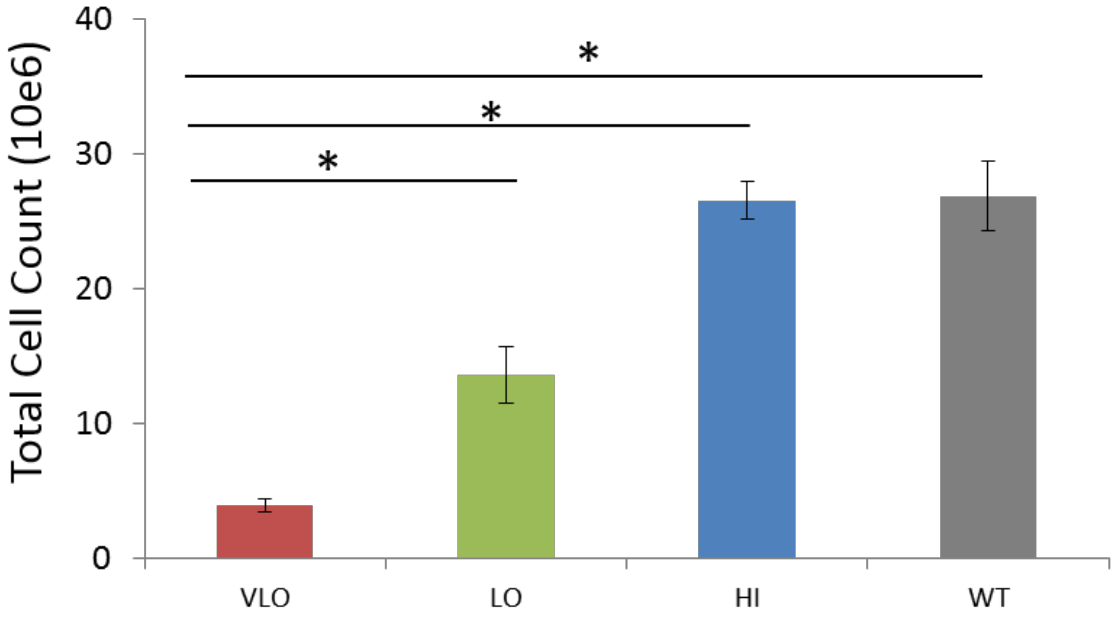
Total Cell Count (10e6)
40
30
20
10
0
*
*
*
VLO
LO
HI
WT

3.6 Generation of BM chimeras to investigate VLO lymphopenia

Given that the VLO mouse model exists in a state of chronic lymphopenia, and that phenotypic markers on VLO $CD8^+$ T cells indicate that the cells acquire their memory status as a result of lymphopenia, we were curious if the memory phenotype of the cells could be relieved if the cells developed in a lymphoreplete environment. To address this question, sub-lethally irradiated B6.*Rag*$^{-/-}$ recipient mice were reconstituted with BM that was either 100% VLO BM, 100% WT BM or a 50/50 mix of VLO and WT BM. This method is represented schematically in Figure 3.6A.

In all cases, BM was depleted of T cells using magnetic beads in order to provide an enhanced opportunity to allow T cells to develop from donor BM stem cells, rather than through mature T cells that might be circulating in the donor BM. As shown in Figure 3.6B, there exists approximately 4% of cells in the BM that are $CD8^+$ T cells. These cells were depleted using magnetic beads coupled with antibodies against CD8, CD3, Thy1.1 and Thy1.2 so that their frequency was reduced to less than 0.2%. T cell depleted marrows were then transferred into prepared recipient mice which were allowed to engraft for at least 2 months before assessment and harvesting.

Figure 3.6: BM chimeras were generated to investigate VLO lymphopenia. (A) Generation of chimeric mice. B6.*Rag*$^{-/-}$ mice were sublethally irradiated and reconstituted with BM from VLO mice, WT mice or a 50/50 mix of VLO and WT. Mice were allowed to engraft for at least 2 months before assessment. (B) Depletion of T cells from BM. In all cases, BM used for reconstitution was depleted of T cells prior to transfer using magnetic beads coupled to antibodies targeting CD3, CD8, Thy1.1 and Thy1.2.

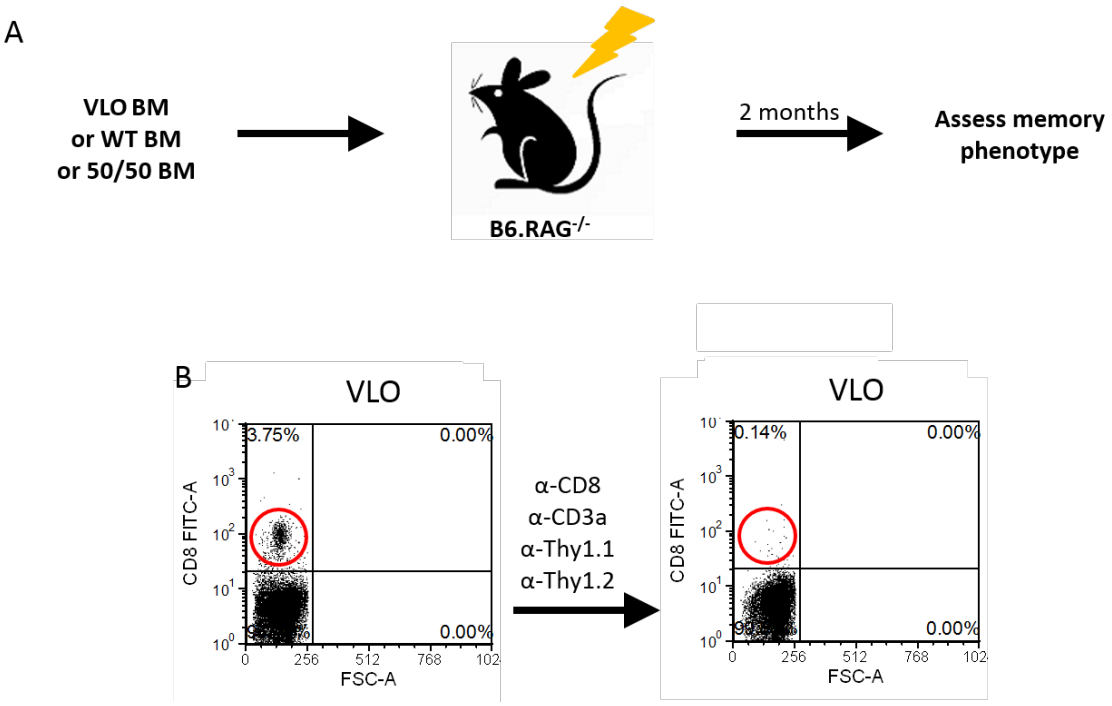
A
VLO BM
or WT BM
or 50/50 BM
B6.RAG-/-
2 months
Assess memory
phenotype
B
VLO
3.75%
0.00%
0.00%
CD8 FITC-A
FSC-A
α-CD8
α-CD3a
α-Thy1.1
α-Thy1.2
VLO
0.14%
0.00%
0.00%
CD8 FITC-A
FSC-A

3.7 Mixed BM chimerism relieves memory phenotype of VLO cells

Peripheral lymphocytes from engrafted B6.*Rag*$^{-/-}$ recipients were analyzed by flow cytometry for expression of CD8 and CD44. This experiment was performed more than 10 times and representative examples are shown in Figure 3.7. Data represented in Figures 3.7A and B were pre-gated on CD8 to make it easier to compare to data presented in Figure 3.7D. As shown in Figure 3.7A, recipient mice that received 100% VLO BM generated CD8$^+$ cells that are almost all CD44^{hi}, which is consistent with the phenotype observed in unmanipulated VLO mice (Figure 3.2A). Recipients that received 100% WT BM (Figure 3.7B) generate CD8$^+$ T cells which express a range of CD44 expression which is consistent with what is observed in unmanipulated WT mice (Figure 3.2A). Recipients which received mixed BM (50% WT and 50% VLO) are shown in Figures 3.7 C-D.

Cells from mixed BM recipients were gated on expression of CD8 and Thy1.1 in Figure 3.7C. VLO mice were bred to express Thy1.1 which is used as a congenic marker for CD8$^+$ T cells. WT mice do not express Thy1.1, but instead express Thy1.2. Thy1.1$^+$ cells are therefore necessarily VLO in origin. The CD8$^+$ Thy1.1$^+$ cell population in Figure 3.7C, the upper right quadrant circled in black, was necessarily VLO in origin and was further examined for expression of CD44 in Figure 3.7D. CD8$^+$ Thy1.1$^+$ VLO cells display a range of CD44 expression with a preferential dominance of CD44^{lo} cells, circled in red (Figure 3.7D). This is in sharp contrast to unmanipulated VLO mice (Figure 3.2A) and BM chimeras that received 100% VLO BM (Figure 3.7A) which generate greater than 95% of CD8$^+$ T cells as CD44^{hi}. These data suggest that CD8$^+$ VLO cells are not fundamentally limited in their ability to exist as naïve cells, because they are able to do so when

they develop in the presence of WT cells. These data suggest that $CD8^+$ VLO cells develop their memory phenotype in response to environmental cues, presumably from cytokine signals.

Because of the unique features of $CD8^+$ VLO cells, we wanted to learn more about how they might function which is explored in the next chapter. Importantly, BM chimeras generated from mixed BM from both VLO and WT mice provide a method of generating a source of $CD44^{lo}$ VLO cells for future studies. This cell population is present at such a low frequency in unmanipulated VLO mice that is essentially not accessible for studying. Thus, these chimeras present a tractable model for comparing responses of naïve T cells to VM T cells with identical antigenic specificity.

Figure 3.7: Mixed BM chimerism relieves memory phenotype of VLO cells. Peripheral lymphocytes from engrafted B6.*Rag*$^{-/-}$ recipients were analyzed by flow cytometry for expression of CD8 and CD44. This experiment was performed more than 10 times. Representative examples are shown. Lymphocytes analyzed in 3.7A and B were pre-gated on CD8 to make them comparable to 3.7D. (A) 100% VLO BM recipients expressed high levels of CD44 in almost all CD8^{+} cells, a pattern of expression which recapitulates what is observed in unmanipulated VLO mice. (B) 100% WT BM recipients generated CD8^{+} cells with a range of CD44 expression which is observed in unmanipulated WT mice. (C) Cells from mixed BM recipients were gated on expression of CD8 and Thy1.1. The CD8^{+} Thy1.1^{+} cell population, upper right quadrant circled in black, was necessarily VLO in origin and was further examined for expression of CD44 in 3.7D. (D) CD8^{+} Thy1.1^{+} VLO cells display a range of CD44 expression with a preferential dominance of CD44^{lo} cells, circled in red.

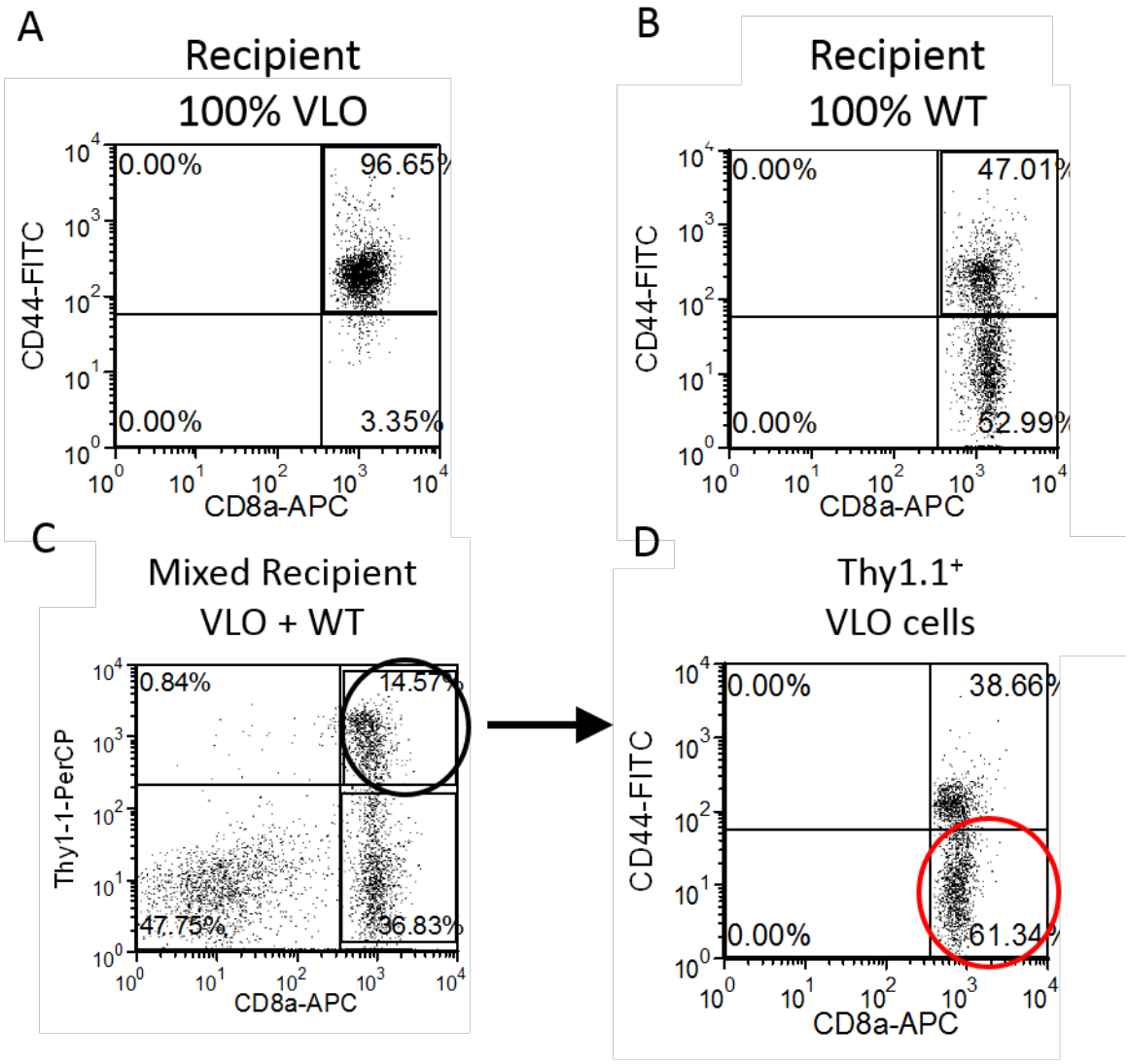
A
Recipient
100% VLO
0.00%
96.65%
0.00%
3.35%
CD44-FITC
CD8a-APC
B
Recipient
100% WT
0.00%
47.01%
0.00%
52.99%
CD44-FITC
CD8a-APC
C
Mixed Recipient
VLO + WT
0.84%
14.57%
47.75%
36.83%
Thy1-1-PerCP
CD8a-APC
D
Thy1.1+
VLO cells
0.00%
38.66%
0.00%
61.34%
CD44-FITC
CD8a-APC

Summary of Chapter 3: To more fully understand the nature of VLO mice and $CD8^+$ VLO cells, we undertook phenotypic characterization of the cells by flow cytometry. The data were consistent with a previously reported signature for innate memory cells that originated from a lymphopenia-induced pathway [120]. The lymphopenic status of VLO mice was compared to LO, HI and WT mice. VLO mice were observed to be in a state of severe and chronic lymphopenia. In an attempt to reverse the lymphopenia-induced memory status of $CD8^+$ VLO cells, we generated mixed BM chimeras derived from both WT and VLO BM. We observed that the memory status of $CD8^+$ VLO cells was relieved under these conditions resulting in the persistence of $CD44^{lo}$ $CD8^+$ VLO cells. Taken together, these data suggest that the memory status of $CD8^+$ VLO cells is not solely driven by an intrinsic factor of the cells themselves, but rather is triggered, at least in part, by an extrinsic factor of the environment in which the cells develop.

Chapter 4: Aim 2 - Functional Characterization of VLO

Rationale: To characterize the *in vitro* and *in vivo* function of $CD8^+$ VLO cells.

Background: Given that VLO cells display phenotypic features that are consistent with innate memory $CD8^+$ T cells, we were interested to explore their functional capacities. Innate memory $CD8^+$ T cells include at least three subclasses of cells: lymphopenia-induced memory cells, IL-4-induced memory cells, and steady-state VM cells. Historically, the study of the function of innate memory $CD8^+$ T cells has been challenged because of the difficulty of isolating these rare cell populations. This is especially true of steady-state VM cells [137, 168-172].

Innate memory $CD8^+$ T cells are functionally similar to classical antigen-induced memory cells. They: 1) produce IFNγ in response to inflammatory cytokines (IL-12/IL-18) [137], and 2) display potent effector function, such as controlling infections *in vivo* [137, 168]. Identifying functional differences between these cell types has been challenging, but Lee *et al* (2013) showed that VM cells respond differently to antigen *in vivo* compared to antigen-induced memory cells [168]. Specifically, the kinetics of INFγ production in response to antigen are slower in VM cells compared to antigen-induced memory cells [168].

To understand the function of VLO cells, HI, LO and VLO $CD8^+$ T cells were tested for their ability to proliferate or produce IFNγ in response to their cognate TRP-2 peptide, or to a panel of cytokines *in vitro*. $CD44^{lo}$ and $CD44^{hi}$ cells from each group were compared. $CD44^{lo}$ is a marker of naïve T cell status, while $CD44^{hi}$ is a marker for memory status and antigenic experience [173]. As discussed in Chapter 3, $CD8^+$ T cells from HI animals are a mixture of $CD44^{lo}$ and $CD44^{hi}$. The pattern of expression of memory markers on HI cells suggests that the $CD44^{hi}$ cells

from this group are antigen-induced memory cells. They display the pattern $CD44^{hi}$ $CD49d^{hi}$ and HI mice display spontaneous vitiligo-like depigmentation, indicative of autoimmune destruction of melanocytes by activated HI T cells. HI cells from lymph nodes were sorted to generate pure $CD44^{hi}$ and $CD44^{lo}$ cell populations. $CD8^{+}$ T cells from LO animals are almost exclusively $CD44^{lo}$ as seen in Figure 3.2. Lymph nodes from these animals were reduced to single cell suspensions and used directly in assays as a source of $CD44^{lo}$ LO cells. To generate $CD44^{hi}$ LO cells, two methods were employed. LO cells were stimulated *in vitro* as described in the Methods section to convert them to $CD44^{hi}$. Alternatively, LO cells were adoptively transferred into recipient mice, which then received DC pulsed with TRP-2 peptide. After a period of time, lymph nodes were isolated from these recipient animals and $CD44^{hi}$ LO cells were isolated by sorting. $CD8^{+}$ T cells from VLO animals are largely $CD44^{hi}$ as shown in Figure 3.2. In order to generate a $CD44^{lo}$ VLO cells, chimeras were generated using the method described in Chapter 3. Cells from the lymph nodes of chimeric animals and VLO animals were sorted to generate pure populations of VLO $CD44^{hi}$ or $CD44^{lo}$.

In addition to *in vitro* studies of VLO function, VLO cells were also tested *in vivo* to assess their rate of proliferation in response to lymphopenic conditions. $CD44^{lo}$ VLO, LO and HI cells were stained with CFSE and adoptively transferred into lymphopenic hosts to examine kinetics of proliferation. VLO cells were also used in an adoptive transfer model to assess their ability to control B16 melanoma tumor.

4.1. VLO cells proliferate less than HI or LO in response to higher doses of TRP-2 peptide

CD44^{lo} cells (Figure 4.1A) from each group were isolated as described and cultured in the presence of antigen and APCs. Proliferation was measured by the incorporation of radioactive thymidine. Naïve VLO cells proliferate less than HI and LO in response to 5 uM and 10 uM TRP-2 antigen treatment. This is an expected outcome given that proliferation is being driven by antigen and in this case proliferation corresponds to the avidity of the TCR of the given cell type. HI cells proliferate the most, LO cells proliferate to an intermediate level and VLO proliferate the least. At a lower dose of antigen, 2.5 uM, HI cells still proliferate the most, while the difference between LO and VLO is inverted. Focusing on the response of HI and LO to decreasing doses of antigen, we observe a stepwise decrease in proliferation as antigen dose is lowered. Proliferation corresponds to antigen dose in both groups. VLO proliferation decreases from the 10 uM treatment to the 5 µM treatment in a small but statistically significant manner. However, there is no statistical difference in proliferation between the 5 µM and 2.5 µM treatments for the VLO group. This suggests that VLO proliferation at this low threshold is not antigen specific and could be driven by other factors, such as cytokines being expressed by the VLO cells themselves, or by the ability of the VLO cells to respond to cytokines being expressed by the APCs that are present in the well. The ability of VLO to be more sensitive to cytokine signals may indicate that these cells are uniquely programmed to be more sensitive to cytokines than to antigen, which has been reported for innate memory cells [137].

CD44^{hi} cells (Figure 4.1B) from each group were similarly isolated and cultured in the presence of peptide and APCs. Proliferation was measured by the incorporation of radioactive thymidine. CD44^{hi} VLO cells proliferate less than HI and LO in response to all doses of TRP-2 peptide treatment. At the highest dose of antigen stimulation, 10 µM, HI and LO CD44^{hi} cells proliferate to a similar extent, while VLO cells proliferate at a very low level. At 5 µM and 2.5 µM TRP-2, the level of proliferation corresponds to the avidity of the receptor with HI proliferating the most, then LO, then VLO. The ability of CD44^{hi} VLO to proliferate in response to antigen is very small, raising the question of whether these cells are geared to responding to other signals, such as cytokines, instead of antigenic stimulation, or whether chronic stimulation *in vivo* has rendered them anergic to subsequent TCR ligation.

Figure 4.1: VLO cells proliferate less than HI and LO in response to TRP-2 peptide. (A) 2 x 10^4 $CD44^{lo}$ cells or (B) $CD44^{hi}$ cells from each group were cultured in the presence of indicated doses of TRP-2 antigen and 2 x 10^5 irradiated WT splenocytes per well in a 96 well plate. At 60 hours, 1 uM ^{3}H-thymidine was added to each well and cells were harvested at 68 hours. Proliferation was measured by the incorporation of radioactive thymidine indicated as CPM. VLO cells proliferated less than HI and LO in almost all conditions. Samples were tested in triplicate. This is representative data from three similar experiments. Error bars were calculated for Standard Error. * indicates $p<0.05$ calculated by Single Factor ANOVA.

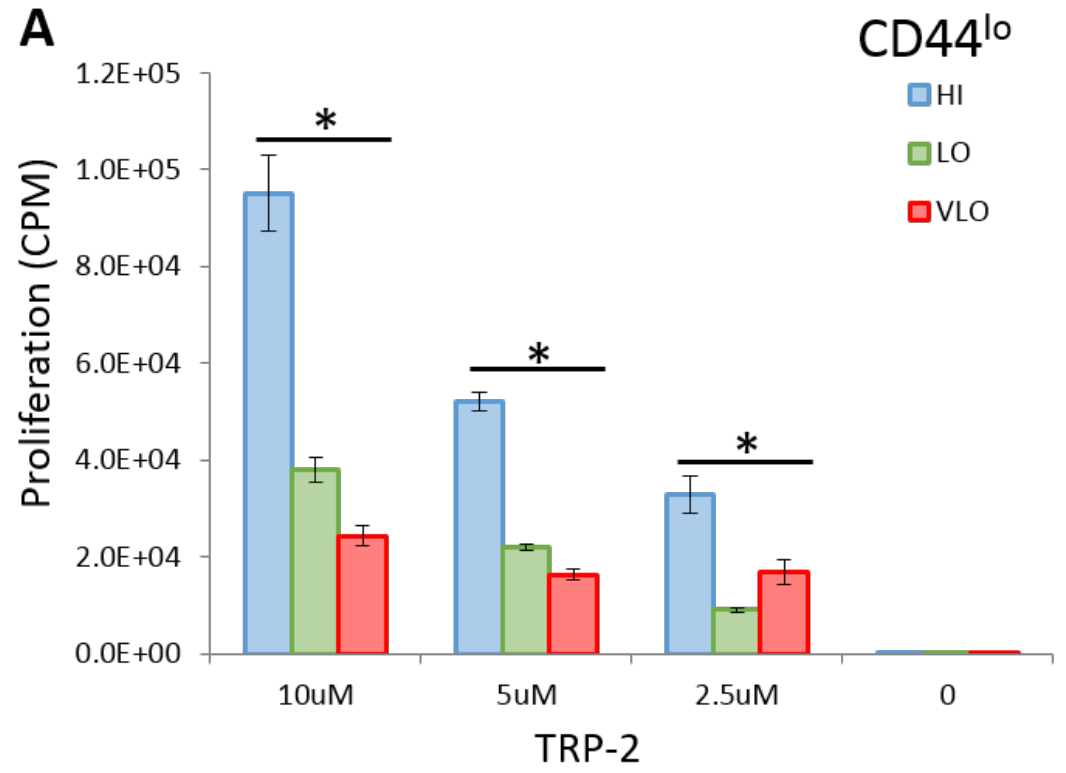
A
CD44lo
HI
LO
VLO
1.2E+05
1.0E+05
8.0E+04
6.0E+04
4.0E+04
2.0E+04
0.0E+00
Proliferation (CPM)
*
*
*
10uM
5uM
2.5uM
0
TRP-2

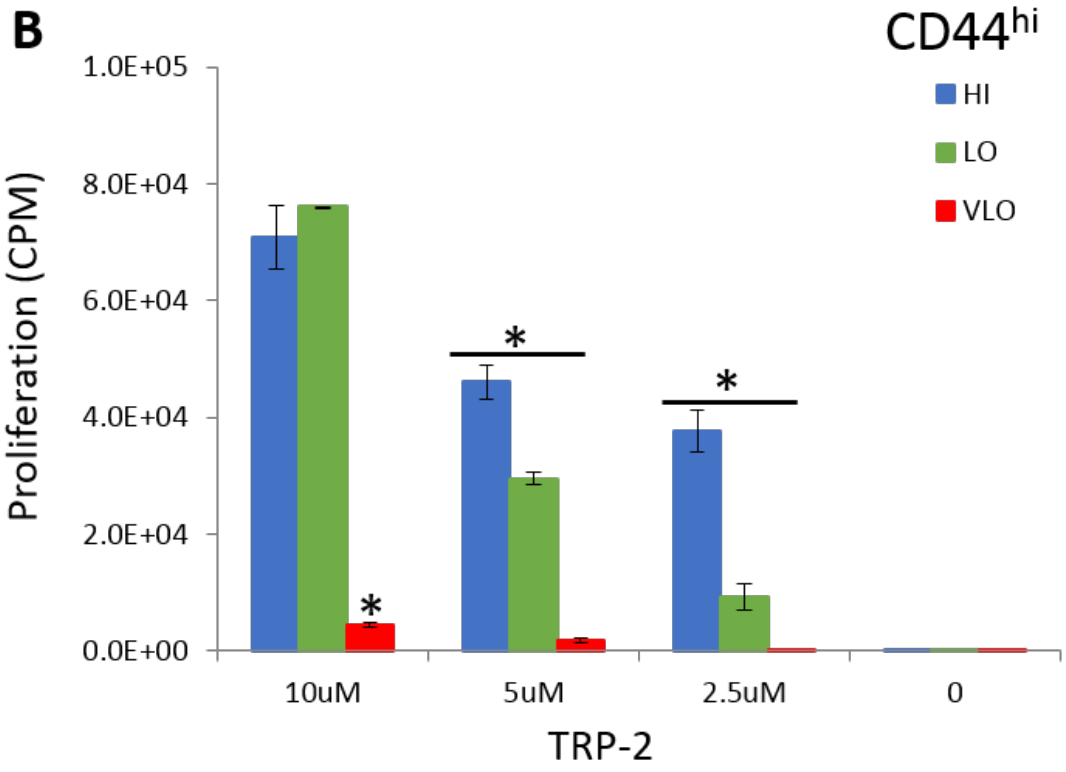
B
CD44hi
HI
LO
VLO
1.0E+05
8.0E+04
6.0E+04
4.0E+04
2.0E+04
0.0E+00
Proliferation (CPM)
*
*
*
10uM
5uM
2.5uM
0
TRP-2

4.2 VLO cells produce less IFNγ than HI and LO in response to TRP-2 peptide

To measure IFNγ production in response to antigen stimulation, HI, LO or VLO cells were cultured in the presence of TRP-2 peptide and irradiated APCs. IFNγ production was measured by ELISPOT. Naïve $CD44^{lo}$ VLO cells (Figure 4.2A) produced no IFNγ above baseline in response to TRP-2 peptide. In contrast both HI and LO cells secreted measurable IFNγ at both 10 µM and 5 µM doses of antigen. It is possible that higher levels of TRP-2 antigenic stimulation would result in IFNγ production by naïve VLO cells, although these levels of TRP-2 induced mild proliferation by VLO cells.

$CD44^{hi}$ VLO cells secreted measurable IFNγ in response to 10 µM TRP-2, with a decrease in IFNγ at 5 µM treatment (Figure 4.2B). There was no difference in IFNγ secretion between 5 µM and 2.5 µM TRP-2 treatment. This suggests that these cells may be responding to signals other than antigen that are present in the well. Both the HI cells and the LO cells produce IFNγ in response to antigen in a dose-dependent manner. In contrast to what we would have predicted the $CD44^{hi}$ LO cells secreted more IFNγ than the HI cells at all doses of antigen. We would have expected these cells to respond according to the avidity of their TCRs. It is possible that this difference is a result of how the $CD44^{hi}$ cells were generated. The HI cells acquired their memory phenotype *in vivo* and may be exhausted [174]. The LO cells were stimulated to acquire a $CD44^{hi}$ phenotype during *in vitro* culture. This culturing process may have activated the cells which resulted in their hyper-responsiveness to antigen stimulation.

Figure 4.2: VLO cells produce less IFNγ than HI and LO in response to TRP-2 peptide. (A) 5 x 10^3 $CD44^{lo}$ cells or (B) $CD44^{hi}$ cells from each group were cultured in the presence of indicated doses of TRP-2 antigen and 4 x 10^5 irradiated WT spleenocytes per well in a 96 well plate format using Ebioscience's Ready-SET-Go ELISPOT kit. The plate was harvested at 60 hours. VLO cells secreted less IFNγ than HI and LO in almost all conditions. Samples were tested in triplicate. This is representative data from three similar experiments. Error bars were calculated for Standard Error. * indicates $p<0.05$ calculated by Single Factor ANOVA.

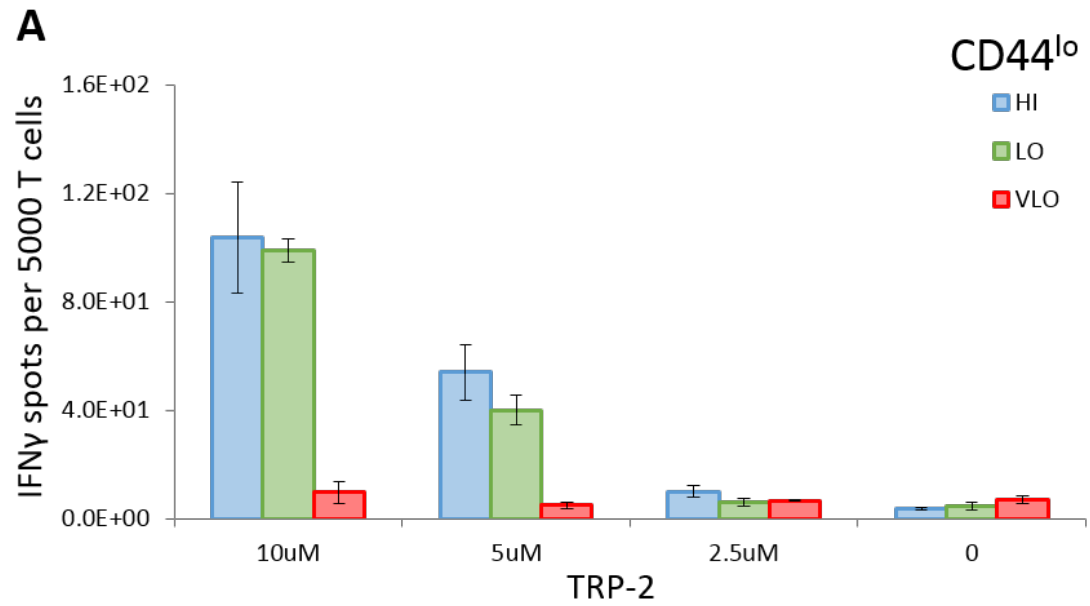
A
CD44lo
HI
LO
VLO
1.6E+02
1.2E+02
8.0E+01
4.0E+01
0.0E+00
IFNγ spots per 5000 T cells
10uM
5uM
2.5uM
0
TRP-2

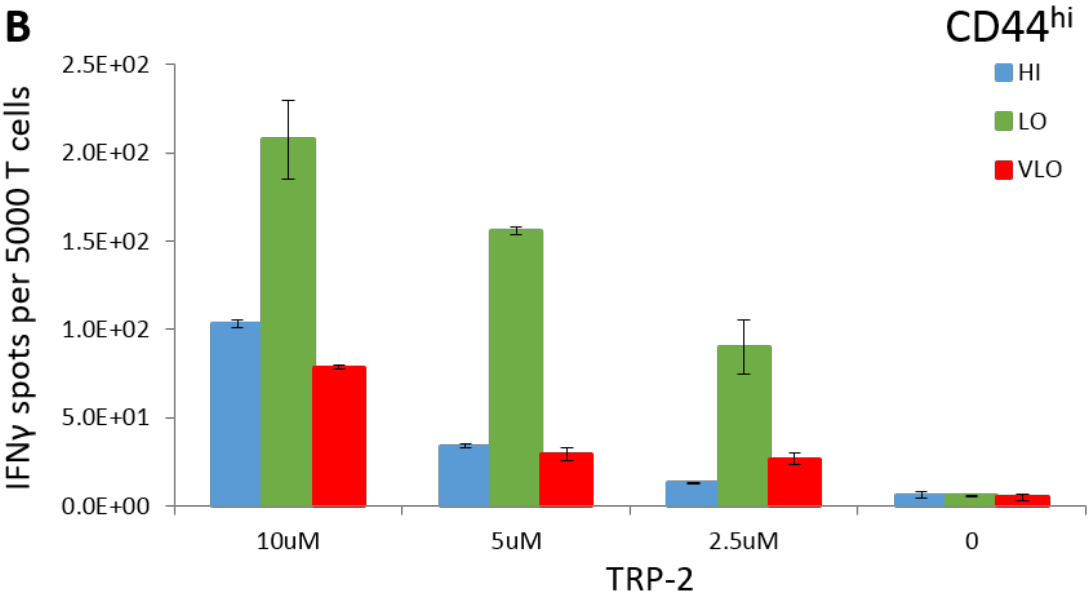
B
CD44hi
HI
LO
VLO
2.5E+02
2.0E+02
1.5E+02
1.0E+02
5.0E+01
0.0E+00
IFNγ spots per 5000 T cells
10uM
5uM
2.5uM
0
TRP-2

4.3. VLO cells proliferate more than HI and LO in response to proinflammatory cytokines in the absence of TCR stimulation

The response of VLO cells at low doses of TRP-2 antigen suggests that VLO cells may be uniquely poised to respond to cytokine cues, rather than to antigenic stimuli. With this in mind, we stimulated our cell populations with a panel of cytokines that have been reported to stimulate response from innate memory $CD8^+$ T cells [137]. Cells were incubated in the following conditions: IL-2 only, IL-12 only, IL-18 only, IL-2 with IL-12, IL-2 with IL-18, IL-12 with IL-18, IL-2 with IL-12 and IL-18, and finally no cytokine stimulation. No APCs were included in any of the conditions. VLO cells whether $CD44^{lo}$ or $CD44^{hi}$ proliferated significantly more than their LO and HI counterparts (Figure 4.3A and 4.3B). Maximal proliferation occurred in the presence of IL-2 with IL-18 for both naïve and memory VLO cells. Naïve LO and HI cells proliferated above background but were dramatically reduced compared to VLO. $CD44^{hi}$ VLO cells proliferated robustly in response to cytokine-only stimulation. Notably, VLO memory cells proliferate well in the presence of IL-2 alone or the combination of IL-2 with IL-12 or the combination of IL-2 with IL-18. In contrast, proliferation is suppressed in the presence of all three cytokines (IL-2 with IL-12 and IL-18). These data suggest that VLO cells, in a naïve or memory state are uniquely poised to respond to cytokine stimulation, consistent with what has been reported for the behavior of innate memory $CD8^+$ T cells [137].

In Figure 4.3C, the data from Figures 4.3A and 4.3B has been combined in order to compare VLO naïve with VLO memory. VLO memory cells proliferate much more than naïve cells, but this pattern of memory cells proliferating more

than naïve cells is expected and is true of traditional memory cells as well as innate memory cells [137].

Figure 4.3: VLO cells proliferate more than HI and LO in response to proinflammatory cytokines in the absence of TCR stimulation. (A) 2 x 10^4 $CD44^{lo}$ cells or (B) $CD44^{hi}$ cells from each group were cultured in the presence of indicated combinations of cytokines in a 96 well plate. All cytokines were at a dose of 100 ng/mL. No APCs were included. At 60 hours, 1 µM ^3H thymidine was added to each well and cells were harvested at 68 hours. Proliferation was measured by the incorporation of radioactive thymidine CPM. VLO cells proliferated more than HI and LO in almost all conditions. (C) $CD44^{hi}$ VLO cells proliferate more than $CD44^{lo}$ VLO in response to proinflammatory cytokines in the absence of TCR ligation. Data from Figures 4.3A and 4.3B were combined to illustrate the difference in proliferation between $CD44^{hi}$ and $CD44^{lo}$ groups. Samples were tested in triplicate. This is representative data from three similar experiments. Error bars were calculated for Standard Error. * indicates $p<0.05$ calculated by Single Factor ANOVA.

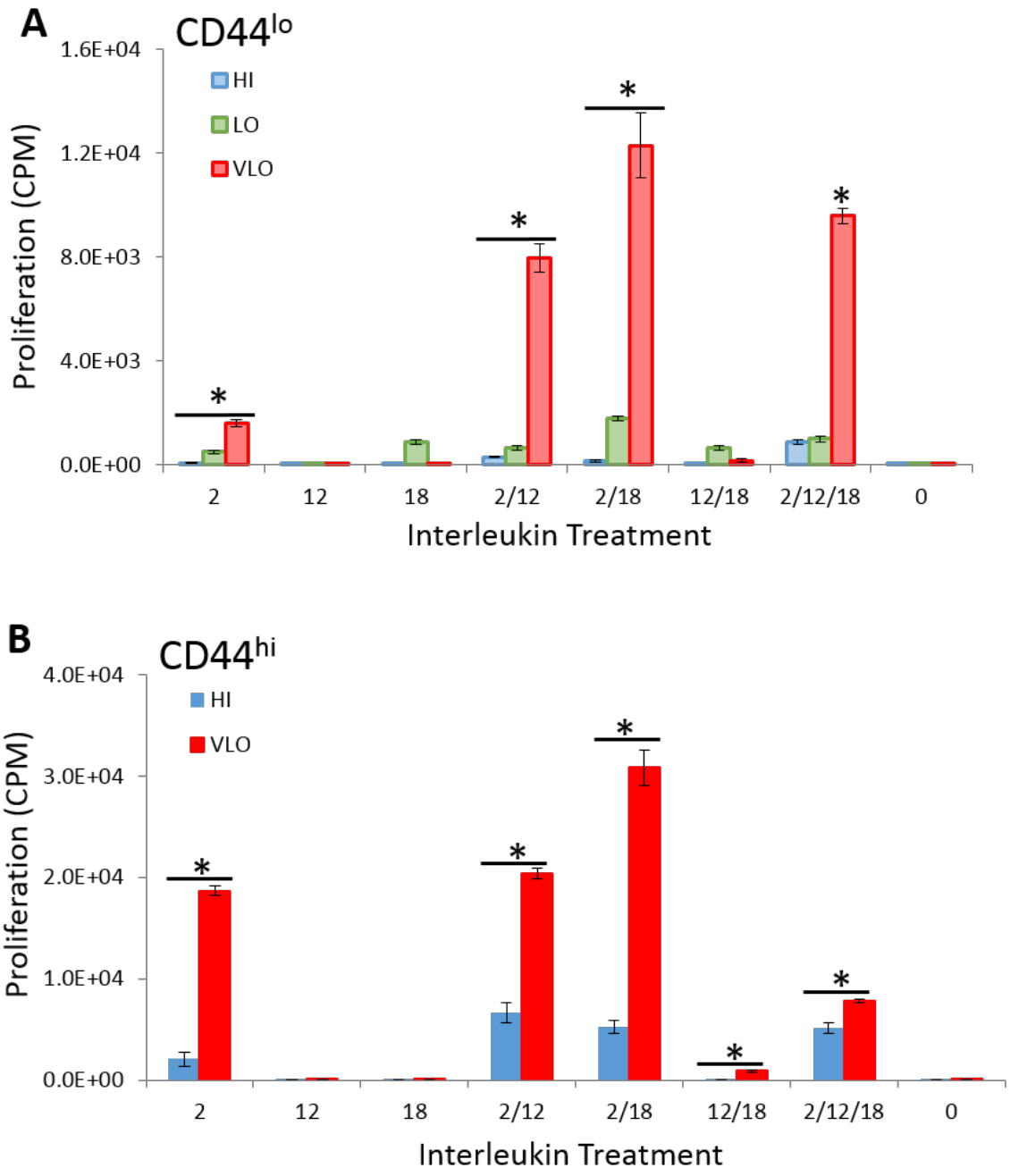
A
CD44lo
1.6E+04
1.2E+04
8.0E+03
4.0E+03
0.0E+00
HI
LO
VLO
Proliferation (CPM)
*
2
12
18
2/12
2/18
12/18
2/12/18
0
Interleukin Treatment
B
CD44hi
4.0E+04
3.0E+04
2.0E+04
1.0E+04
0.0E+00
HI
VLO
Proliferation (CPM)
*
2
12
18
2/12
2/18
12/18
2/12/18
0
Interleukin Treatment

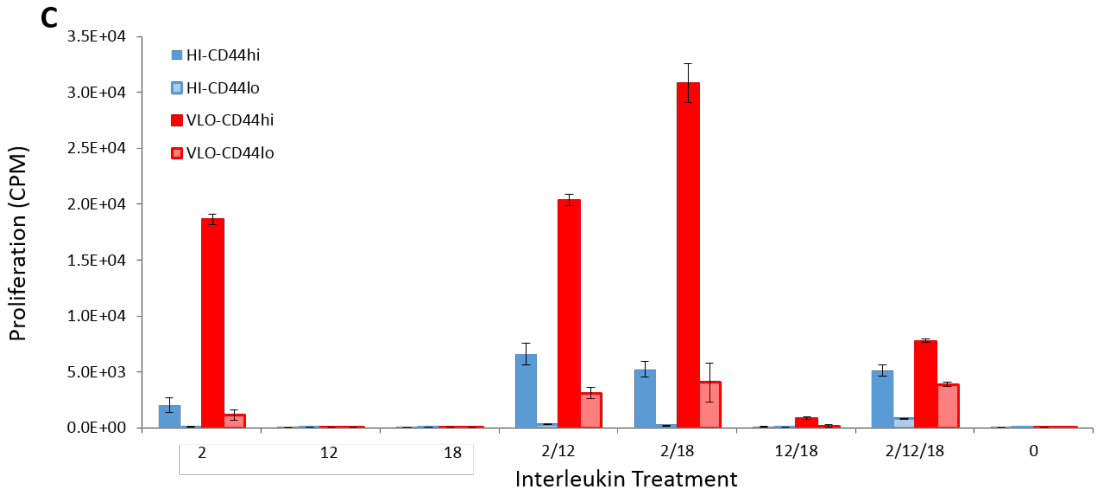
C
3.5E+04
3.0E+04
2.5E+04
2.0E+04
1.5E+04
1.0E+04
5.0E+03
0.0E+00
Proliferation (CPM)
HI-CD44hi
HI-CD44lo
VLO-CD44hi
VLO-CD44lo
2
12
18
2/12
2/18
12/18
2/12/18
0
Interleukin Treatment

4.4. VLO cells secrete more IFNγ than HI and LO in response to proinflammatory cytokines in the absence of TCR stimulation

Given the heightened sensitivity of VLO proliferation to cytokine stimulation, we were curious if other functions of VLO cells would be responsive to this treatment. With this in mind, we stimulated our cell populations with the same panel of cytokines and measured their ability to secrete IFNγ. As before, no APCs were included in any of the conditions. Naïve VLO cells secrete IFNγ in response to the combination of IL-2 with IL-12 and IL-18 cytokines. In contrast LO and HI cells secrete minimal levels (Figure 4.4A). A similar pattern is observed with $CD44^{hi}$ VLO cells which dominate LO and HI in their ability to produce IFNγ (Figure 4.4B). $CD44^{lo}$ and $CD44^{hi}$ groups are presented side-by-side in Figure 4.4C which illustrates the capacity of $CD44^{hi}$ VLO cells to produce robust IFNγ compared to naïve cells.

Taken together, the data suggest that the proliferative capacity of VLO cells is uncoupled from its ability to secrete IFNγ. Note that VLO cells respond to the triple combination of IL-2, IL-12 and IL-18 by producing large amounts of IFNγ (Figures 4.4A-B). In contrast, the same combination of cytokines limits proliferation when compared to IL-2 with IL-18, this is especially notable for $CD44^{hi}$ VLO cells (Figure 4.3B).

Figure 4.4: VLO cells secrete more IFNγ than HI and LO in response to proinflammatory cytokines in the absence of TCR stimulation. (A) 2.5 x 10^3 $CD44^{lo}$ cells or (B) $CD44^{hi}$ cells from each group were cultured in the presence of indicated combinations of cytokines in a 96 well plate. (C) $CD44^{hi}$ VLO cells proliferate more than $CD44^{lo}$ VLO in response to proinflammatory cytokines in the absence of TCR ligation. Data from Figures 4.4A and 4.4B were combined to illustrate the difference in IFNg production between $CD44^{hi}$ and $CD44^{lo}$ groups. All cytokines were at a dose of 100 ng/mL. No APCs were included. Samples were tested in triplicate. This is representative data from three similar experiments. Error bars were calculated for Standard Error. * indicates $p<0.05$ calculated by Single Factor ANOVA.

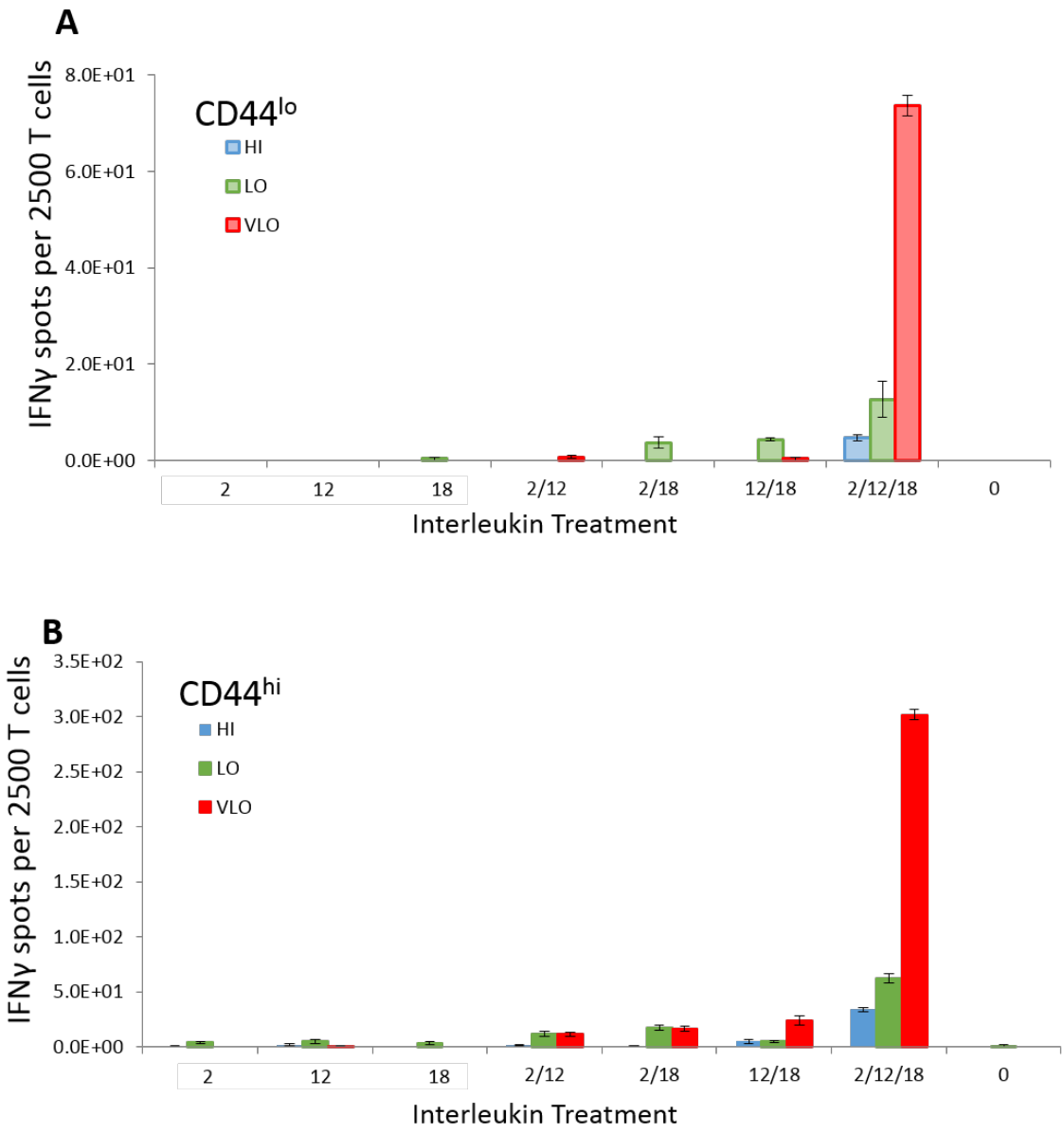
A
IFNγ spots per 2500 T cells
8.0E+01
6.0E+01
4.0E+01
2.0E+01
0.0E+00
CD44lo
HI
LO
VLO
2
12
18
2/12
2/18
12/18
2/12/18
0
Interleukin Treatment
B
IFNγ spots per 2500 T cells
3.5E+02
3.0E+02
2.5E+02
2.0E+02
1.5E+02
1.0E+02
5.0E+01
0.0E+00
CD44hi
HI
LO
VLO
2
12
18
2/12
2/18
12/18
2/12/18
0
Interleukin Treatment

C

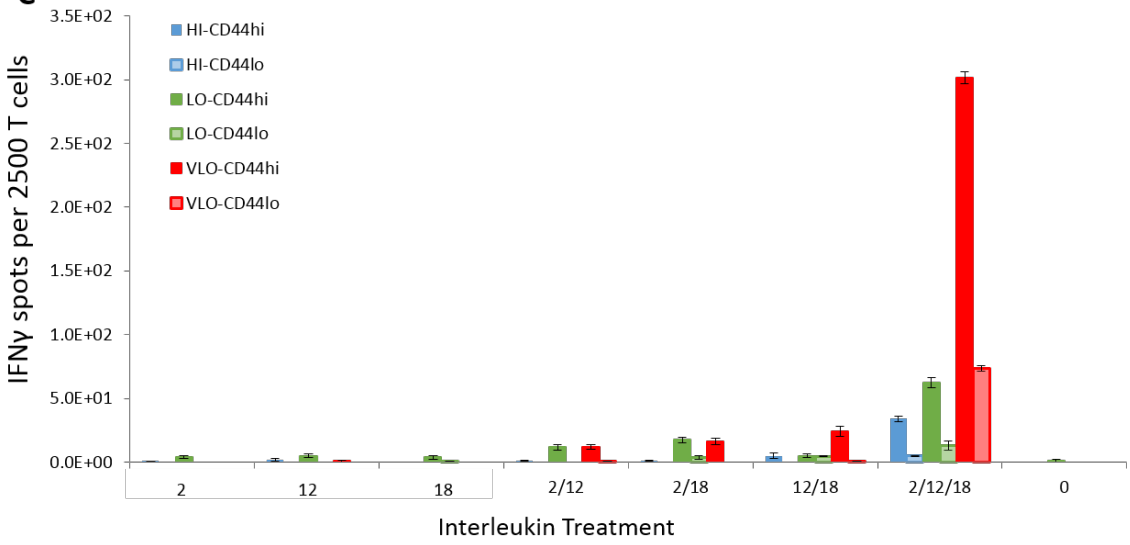
3.5E+02
3.0E+02
2.5E+02
2.0E+02
1.5E+02
1.0E+02
5.0E+01
0.0E+00
IFNγ spots per 2500 T cells
HI-CD44hi
HI-CD44lo
LO-CD44hi
LO-CD44lo
VLO-CD44hi
VLO-CD44lo
2
12
18
2/12
2/18
12/18
2/12/18
0
Interleukin Treatment

4.5. VLO undergo rapid homeostatic proliferation

Given that VLO cells respond to *in vitro* stimulation in a manner that is consistent with what has been reported for VM cells, we were curious to see if their behavior *in vivo* would also correspond to what has been described. In particular, we were interested in designing an experiment that would allow us to observe the rate of proliferation of VLO cells in a homeostatic setting. It has been reported that VM cells proliferate at a faster rate than other types of naïve cells when they encounter a homeostatic environment.

To address this question, naïve CD44^{lo} VLO cells were generated using the chimeric model that has been described in previous chapters. CD44^{lo} LO and HI cells were also isolated as previously described. Cells were stained with CFSE and adoptively transferred into B6.*Rag*$^{-/-}$ mice. After four days, CD8^{+} cells from single cell suspensions made from peripheral lymph nodes were analyzed for CFSE dilution, CD44, CD49d and CD3 expression (Figure 4.5). We were aware that B6.*Rag*$^{-/-}$ express TRP-2 which is the cognate antigen of all three cells types (HI, LO and VLO). Based on *in vitro* observations, we know that naive CD44^{lo} HI cells (Figure 4.1A) proliferate dramatically in response to cognate antigen, in contrast to LO and VLO naïve cells which proliferate much less. We expected the HI cells to proliferate in response to antigen and rapidly dilute CFSE. In contrast, we were expecting the LO and VLO cells to respond less dramatically to antigen and proliferate in response to homeostatic signals.

In Figure 4.5B-E, we see that HI cells (blue) indeed rapidly diluted CFSE and expressed high levels of CD44 and CD49d. The CD44 expression was most likely the result of antigen encounter and the CD49d expression is also indicative

of antigen experience. In contrast, LO cells (green) are slowly dividing and slowly diluting CFSE with minimal expression of CD44 and CD49d which is a hallmark of HP in response to lymphopenia. Traditional HP typically requires high levels of IL-7 and self-pMHC [160]. The VLO cells (red) show a different pattern of expression compared to both the HI and LO populations. VLO (red) is intermediate to HI (blue) and LO (green). Similarly, CD44 levels are intermediate for VLO cells (Figure 4.5C). CD49d levels on VLO cells (mean fluorescence intensity (MFI) = 11.6) are lower than both LO (MFI = 16.2) and HI (MFI = 34.5). This observation is noteworthy because Haluszczak and colleagues (2009) make a point that CD49d is lower on VM cells compared to homeostatic memory cells [137]. VLO cells which we posit are VM cells express less CD49d than do LO cells which we believe are displaying traditional HP. This pattern further supports the idea that VLO cells are VM cells.

A new observation for both HP and VM proliferation is the down-regulation of CD3 which has not been reported to our knowledge. We suggest that this is a natural reaction of the cell. This cell is essentially tuning down the responsiveness of its TCR by down-regulating CD3. This in turn allows the cell to upregulate components that allow it to be more responsive to cytokine signals that are driving its proliferation. An unresolved question regarding VM cells is what is driving their proliferation. Surh and Sprent (2008) have reviewed multiple mechanisms of HP including cytokine-induced proliferation (CIP) that is driven by high IL-2 and/or IL-15 or IL-4 [160]. This mechanism has been reported for VM cells and is characterized by a fast rate of proliferation. It is possible that VLO cells are driven by IL-15 or IL-4. It is also possible that the VLO cells are undergoing chronic

lymphopenia-induced proliferation which is driven by commensal antigens and is characterized by fast proliferation [160].

Figure 4.5: VLO undergo rapid homeostatic proliferation. $CD44^{lo}$ cells (1×10^6) from each population were stained with CFSE and adoptively transferred into *Rag*$^{-/-}$ mice. After 4 days, single cell suspensions were made from peripheral lymph nodes analyzed by flow cytometry. (A) Schematic diagram of experiment. (B) Dilution of CFSE. (C) Expression of CD44. (D) Expression of CD49d. (E). Expression of CD3. Two or three mice were tested per group in two separate experiments.

A

CFSE-labeled
HI CD44^{lo}
LO CD44^{lo}
VLO CD44^{lo}

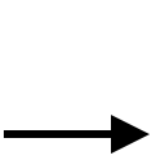

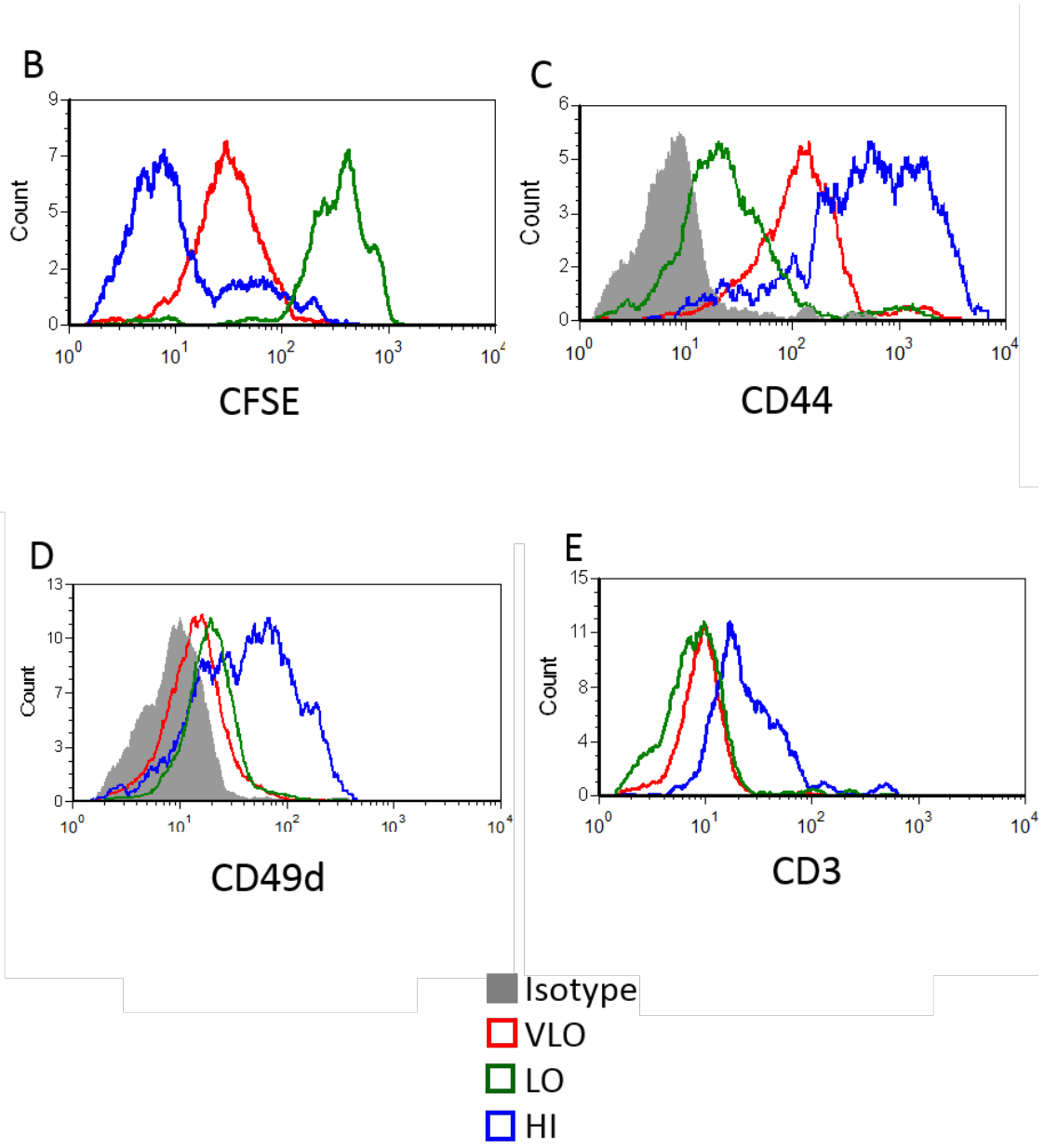
B
Count
CFSE
C
Count
CD44
D
Count
CD49d
E
Count
CD3
Isotype
VLO
LO
HI

4.6. VLO cells proliferate more than HI and LO in response to IL-15 in the absence of TCR stimulation

Based on the data observed thus far, we suspected that VLO cells have the capacity to exist as VM cells. Based on reports in the literature, we were curious if these cells proliferate in response to IL-7 or IL-15. Naïve VLO, LO and HI cells were treated with IL-15 or IL-7 or TSLP. IL-15 and IL-7 are common gamma chain cytokines, both signaling via Janus kinase 1 and Janus kinase 3 with signal transduction mediated via signal transducer and activator of transcription (STAT) 5. It has been reported that TSLP can substitute for IL-7 in some cases [175, 176]. The receptors for IL-7 and TSLP both utilize the IL-7Rα, signals through STAT5 [177-179]. Figure 4.6A provides a schematic summary of the similarities and differences for these signaling molecules.

VLO naïve cells proliferate better than LO or HI cells in the presence of IL-15, but these levels are very low and barely at the limit of detection for the assay. Counts are <2000cpm. There was no proliferation in response to IL-7 nor TSLP (Figure 4.6A). $CD44^{hi}$ HI, LO and VLO cells proliferate to some extent in response to IL-15, with VLO cell proliferation about 6-fold more than LO or HI cells (Figure 4.6B). The counts for LO and HI are barely at the level of detection for the assay, <1000 CPM.

Figure 4.6: VLO cells proliferate more than HI and LO in response to IL-15 in the absence of TCR stimulation. (A) 2 x 10^4 $CD44^{lo}$ cells or (B) $CD44^{hi}$ cells from each group were cultured in the presence of indicated combinations of cytokines in a 96 well plate. All cytokines were at a dose of 100ng/mL. No extraneous APCs were included. At 60 hours, 1uM ^3H thymidine was added to each well and cells were harvested at 68 hours. Proliferation was measured by the incorporation of radioactive thymidine indicated as CPM. VLO cells proliferated more than HI and LO in response to IL-15. Samples were tested in triplicate. This is representative data from three similar experiments. Error bars were calculated for Standard Error. * indicates $p<0.05$ calculated by Single Factor ANOVA.

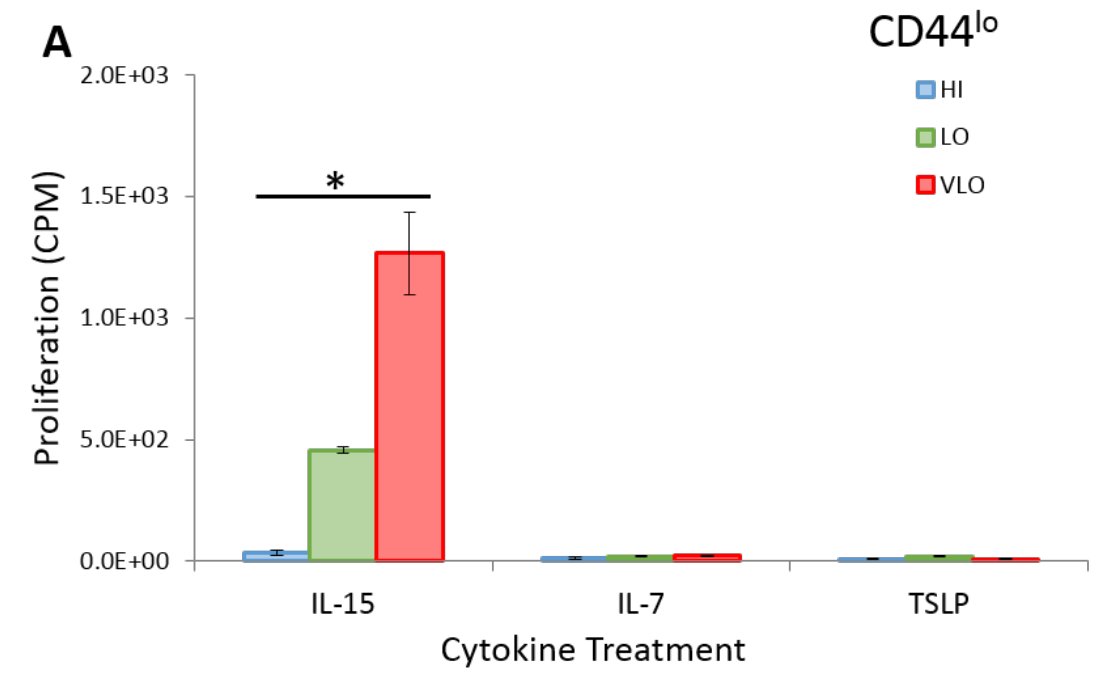
A
CD44lo
HI
LO
VLO
2.0E+03
1.5E+03
1.0E+03
5.0E+02
0.0E+00
Proliferation (CPM)
*
IL-15
IL-7
TSLP
Cytokine Treatment

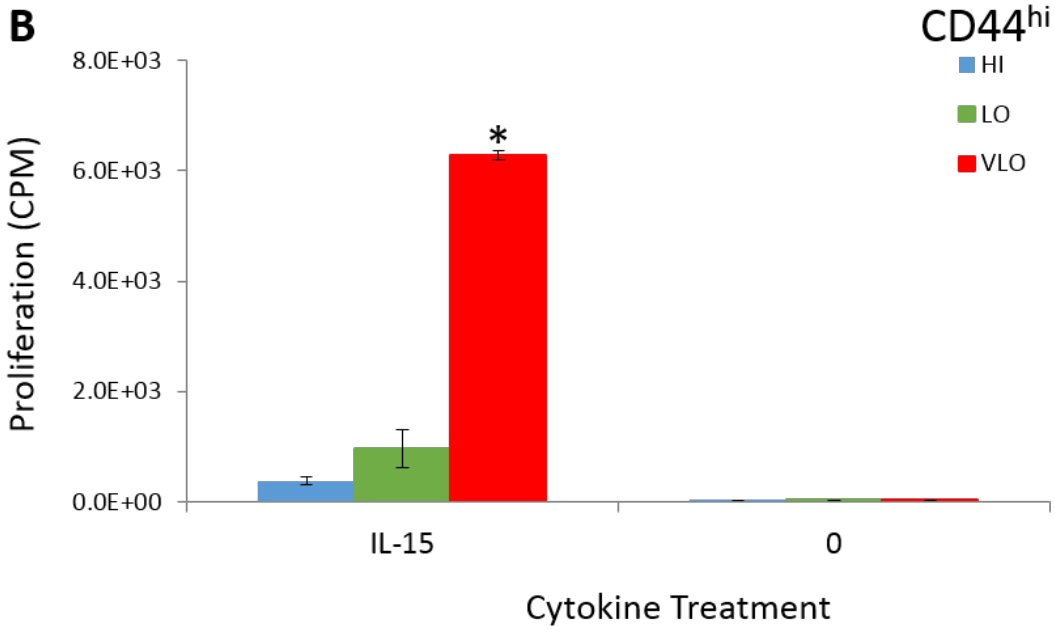
B
CD44hi
HI
LO
VLO
8.0E+03
6.0E+03
4.0E+03
2.0E+03
0.0E+00
Proliferation (CPM)
*
IL-15
0
Cytokine Treatment

4.7. IL-15 stimulated proliferation is not coupled with IFNγ production

Given the responsiveness of VLO to IL-15 in terms of proliferation, VLO, LO and HI cells were tested for their ability to produce IFNγ in response to IL-15 as described previously for other types of cytokine stimulation. None of the groups whether $CD44^{lo}$ or $CD44^{hi}$ produced IFNγ in response to IL-15 (Figure 4.7). This was the predicted result because it has not been reported that IL-15 triggers IFNγ production in $CD8^{+}$ T cells [180]. For VLO cells, unlike TCR-driven stimulation, proliferation and IFNγ production are uncoupled functions in response to IL-15. IL-15 triggered proliferation in these cells, but not IFNγ production.

Figure 4.7: IL-15 stimulated proliferation is not coupled with IFNγ production. (A) 2.5 x 10^3 $CD44^{lo}$ cells or (B) $CD44^{hi}$ cells (4.6B) from each group were cultured in the presence of 100 ng/mL of IL-15 in a 96 well plate. No extraneous APCs were included. Samples were tested in triplicate. None of the groups secreted IFNγ in response to IL-15 above background levels. This is representative data from three similar experiments.

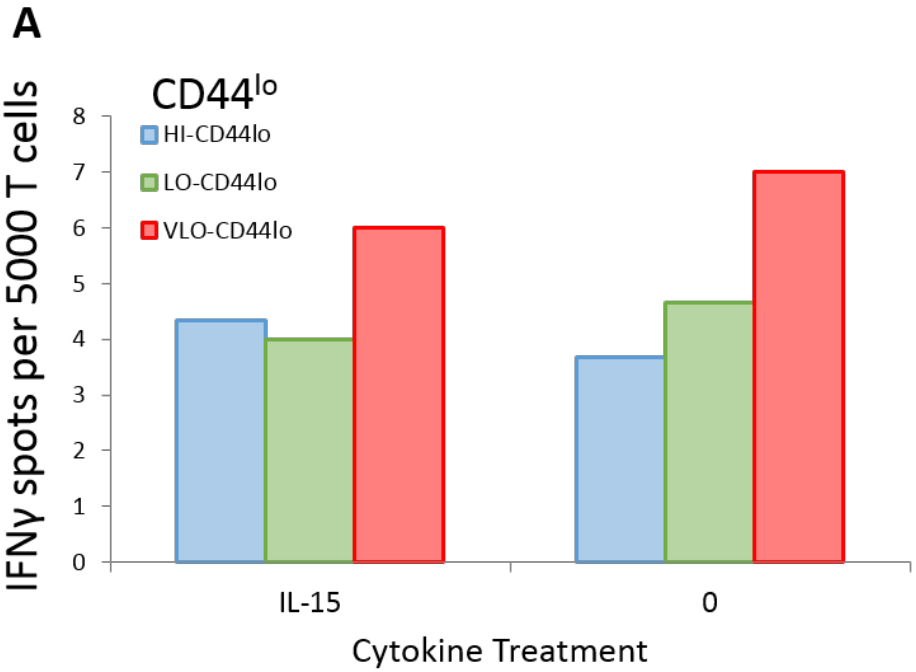
A
CD44lo
HI-CD44lo
LO-CD44lo
VLO-CD44lo
IFNγ spots per 5000 T cells
0
1
2
3
4
5
6
7
8
IL-15
0
Cytokine Treatment

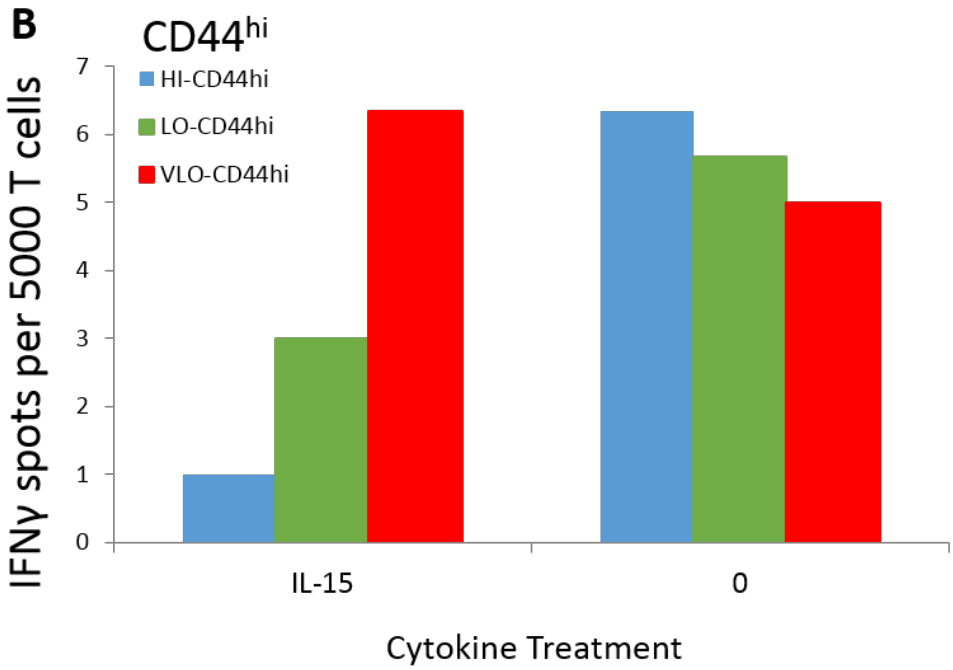
B
CD44hi
HI-CD44hi
LO-CD44hi
VLO-CD44hi
IFNγ spots per 5000 T cells
0
1
2
3
4
5
6
7
IL-15
0
Cytokine Treatment

4.8. VLO cells do not efficiently control B16 melanoma tumor in an adoptive transfer model

VLO cells were engineered to recognize TRP-2, a tumor antigen in the B16 mouse model of melanoma. As shown by the data in Aim 2, VLO $CD44^+$ cells respond to TRP-2 antigen stimulation *in vitro* by producing IFNγ, and also have the unique ability to respond to pro-inflammatory cytokines. We were interested to examine whether these cells are able to control tumor growth *in vivo*. The characteristics of the ideal T cell to use in adoptive therapy in both animals and humans is constantly being clarified. Several studies have compared the memory status of $CD8^+$ T cells used in adoptive therapy, [53, 105, 181], however no group has been able to examine innate memory T cells for use in tumor therapy because of the scarcity of this cell population. The VLO model provides a valuable source of innate memory T cells to use to examine this question.

The experimental design is described schematically in Figure 4.8A. Briefly, host animals were injected with B16 cells subcutaneously. Animals were divided into four groups of five mice each: untreated, dendritic cell vaccine only (DCv20), VLO with dendritic cell vaccine (VLO+DCv20), or HI with dendritic cell vaccine (HI+DCv20). Three to six days after tumor injection, animals received adoptively transferred VLO cells, or HI cells by intravenous injection. Within 24 hours after T cell transfer, animals were given a dendritic cell vaccine (DCv20) which was generated as described in the Methods Section.

The untreated group was used as a control with which to compare all other groups. The group that received DCv20 was used as a control to monitor the effects of the DC vaccine alone. HI+DCv20 was included as a positive control because our

lab had previously observed that this controlled B16 tumor growth in mice. VLO+DCv20 was the experimental group of interest. Tumor growth was measured over time. This experiment was repeated four times and the results of one representative experiment are shown in Figure 4.8. Figure 4.8C lists the tumor incidence for each group represented in Figure 4.8B. Data was combined from all four tumor experiments and analyzed via a logistic growth model. Significance between groups was tested and is shown in Table 4.1.

Figure 4.8: VLO cells do not efficiently control B16 melanoma tumor in an adoptive transfer model. (A) Schematic of experimental design of tumor studies. CD45.1 host animals were injected subcutaneously with B16 cells. After three to six days, designated animals received adoptively transferred VLO cells, or HI cells by intravenous injection. Dendritic cell vaccine (DCv) was administered intravenously within 24 hours after T cell transfer. Tumors were measured until they reached the size of 400 mm^2. (B) Animals were divided into four groups of five mice each: untreated, dendritic cell vaccine only (DCv), VLO with dendritic cell vaccine (VLO + DCv), or HI with dendritic cell vaccine (HI + DCv). Tumor growth was measured over time. This is representative data from four similar experiments. Error bars were calculated for Standard Error. (C) Tumor incidence indicates how many animals per group grew tumor from subcutaneously injected B16 cells in this representative experiment.

A

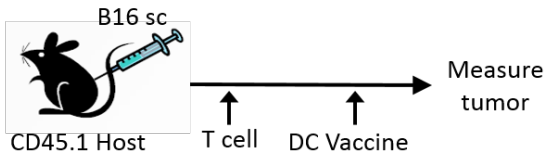
B16 sc
CD45.1 Host
T cell
DC Vaccine
Measure tumor

B

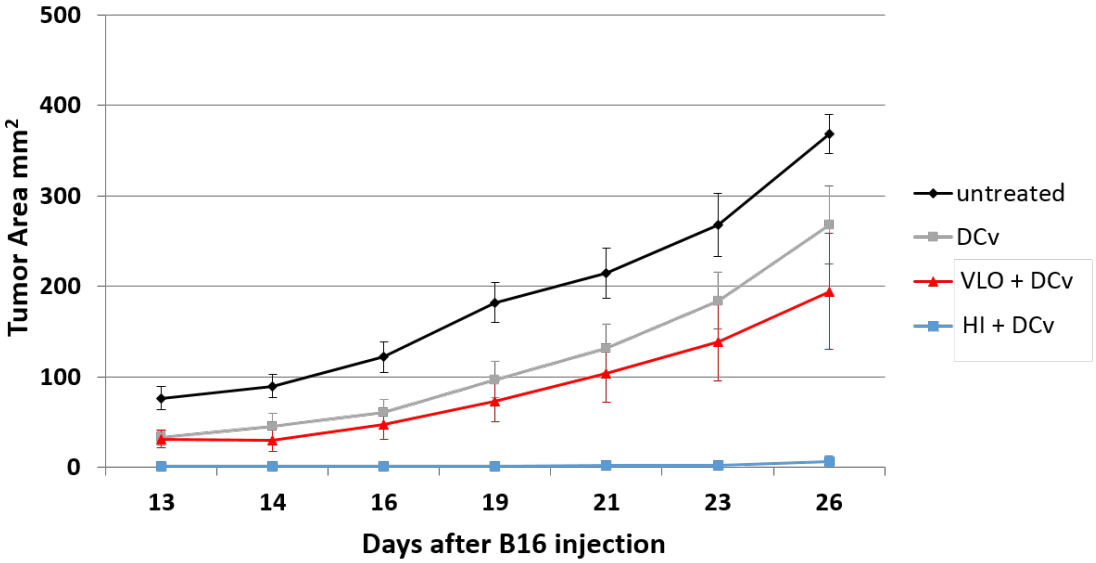
500
400
300
200
100
0
Tumor Area mm2
13
14
16
19
21
23
26
Days after B16 injection
untreated
DCv
VLO + DCv
HI + DCv

C

Group	Tumor Incidence
Untreated	5/5
DCv	5/5
VLO + DCv	4/5
HI + DCv	1/5

Table 4.1: Observed differences in xmid parameters and p values for the pairwise xmid contrasts. Logistic growth curves for the four groups were calculates using a statistical model which is explained in the Methods Section. There is a significant difference between all the pairs of groups except DC_v and VLO.

Group 1	Group 2	Xmid difference	p value
Untreated	DC_v	-2.6809	0.0041
Untreated	HI	-11.8216	<0.0001
Untreated	VLO	-2.7639	0.0032
DC_v	HI	-9.8124	<0.0001
DC_v	VLO	-0.7728	0.2204
HI	VLO	8.2381	<0.0001

As predicted, HI+DCv20 controlled tumor growth compared to the untreated group ($p<0.0001$) as well as DCv20 ($p<0.0001$). The experimental group of interest, VLO+DCv20, controlled tumor growth compared to the untreated group ($p=0.0032$), however it did not control tumor growth compared to DCv20 ($p=0.2204$) indicating that the observed tumor control by VLO+DCv20 was driven largely by the presence of the dendritic cell vaccine itself. In two of the four tumor studies, treatment with VLO+DCv20 resulted in the apparent complete regression of tumor in one animal out of five in the group. In contrast, tumor regression was never observed in either the untreated group or the DCv20 group. This suggests that VLO may have the potential to control tumor growth. Exploration of the requirements to bolster VLO anti-tumor efficacy require further work. Interpretation of these findings should also consider the possibility that the low affinity of the VLO TCR restricts the ability of these cells to control tumor growth, such that the innate memory status may actually improve the tumor control by these cells.

Summary of Chapter 4: In order to more fully understand the functional capabilities of VLO cells, we undertook a systematic study of their response to antigen and cytokines *in vitro* by measuring their proliferation and production of IFNγ. We observed that VLO cells proliferate weakly and produce moderately low levels of IFNγ in response to antigen-driven stimulation, but seem poised to respond to cytokine stimulation. In contrast, VLO cells whether $CD44^{lo}$ or $CD44^{hi}$ respond dramatically to pro-inflammatory cytokines by proliferating robustly and expressing high levels of IFNγ in comparison to LO and HI cells. An *in vivo* study examining the response of these cells to a lymphopenic environment revealed that

VLO cells proliferate more rapidly than LO cells, which themselves behave in a manner consistent with traditional HP. In contrast, VLO cells also display higher levels of CD44 and lower levels of CD49d, which are all consistent with a VM phenotype. In order to explore which cytokines might be triggering proliferation in VLO cells, we tested their ability to proliferate in response to cytokines that are thought to guide HP, specifically IL-7 and IL-15. VLO cells did not respond to IL-7, but proliferated in response to IL-15. The cells did not produce IFNγ in response to IL-15, suggesting that IL-15 serves mainly to induce proliferation. It has been suggested by Jameson and others that VM cells might provide an advantage in controlling cancer [120]. This idea has been difficult to test because of the low frequency of this cell type. The VLO mouse model provides a unique opportunity to explore this question. When VLO cells where tested in an adoptive transfer model for treatment of B16 melanoma, they did not statistically control tumor any better than a control, vaccine-only group. Taken all together these data support the idea that VLO cells behave consistently with what has been reported about VM cells. We suggest that VLO cells and the VLO mouse are a useful model to study the behavior and development of VM cells. The next chapter will explore what features are required for development of VLO cells (Chapter 5).

Chapter 5: Aim 3 - Investigation of the Developmental Requirements for the Memory Phenotype of VLO Cells

Rationale: To investigate the molecular requirements for acquisition of memory phenotype by VLO cells using mouse models.

Background: Based on the data presented thus far we concluded that VLO cells display an IMP which is most likely acquired through lymphopenia-induced proliferation as discussed in Chapter 3 (Aim 1). The *in vitro* function and *in vivo* proliferation of VLO cells is similar to what has been described in the literature for innate memory $CD8^+$ T cells as shown in Chapter 4 (Aim 2). Despite these unique features, these cells do not control tumors well, at least under the conditions in which they were tested in Chapter 5 (Aim 2).

We were curious to explore the developmental requirements of the memory phenotype of VLO cells. These cells behave in a manner that is consistent with what has been reported for steady-state VM cells (reviewed by [120]). VM cells occur at vanishingly low frequencies and require extensive efforts to study. If VLO mice are able to serve as a source of VM cells, then this model would allow the investigation of questions that were not able to be addressed previously.

5.1. VLO retain memory phenotype when developing in the absence of TRP-2 antigen

A critical defining feature of innate memory cells is that their lymphopenia-induced proliferation is not induced by stimulation of the TCR by the cognate antigen. To investigate this, we crossed VLO mice onto a $Dct^{-/-}$ background. As mentioned previously, the *Dct* gene encodes dopachrome tautomerase, an enzyme involved in the synthesis of melanin pigment which impacts coat color in mice

[182]. DCT is also known as tyrosinase-related protein 2, abbreviated as TRP-2 [183]. Historically, the DCT designation is used when the enzymatic function of the protein is being referenced, while the TRP-2 designation is used when the antigenic properties of the protein are being discussed. The terms are used interchangeably in this dissertation.

In 2004, Freidrich Beerman's team reported the creation of a *Dct* KO mouse with a diluted coat color phenotype caused by reduced melanin content [184]. In this model, *Dct* was knocked out by removing Exon 1 of *Dct*, resulting in loss of transcript and protein production [184]. The KO strategy for this model is represented schematically in Figure 5.1A. As we were interested in exploring the role of the cognate antigen of the VLO TCR, TRP-$2_{180\text{-}188}$, we bred VLO mice with *Dct*-Exon1$^{-/-}$ mice, ultimately generating a mouse that was *Dct*-Exon1$^{-/-}$, *Rag*$^{-/-}$ and carrying the VLO transgene.

CD8^{+} T cells from VLO *Dct*-Exon1$^{-/-}$ were examined phenotypically for CD44, CD49d, CXCR3, Ly6C and CD3 by flow cytometry. As shown in Figure 5.1B, they displayed the same level of expression of these markers as VLO cells that had developed in the presence of TRP-2. There was no observable difference in the expression of any of the proteins examined. These data support the idea that VLO cells fall into the category of innate memory cells because cognate antigen stimulation of the TCR is not required to induce their memory phenotype. When TRP-2 is absent, the memory phenotype persists, indicating that DCT is not required for the memory phenotype of VLO cells.

Given that the epitope of DCT that is recognized by the VLO TCR, TRP-$2_{180\text{-}188}$, is encoded in Exon 2 of the *Dct* gene, and that a predicted transcript variant of

mouse *Dct* has been annotated in GenBank (NCBI Reference Sequence: XM_006518510.3) with a start codon downstream of *Dct* Exon 1, we wanted to have complete confidence that no TRP-2 antigen was present. In order to account for this possibility, we engineered a new *Dct* KO model that fully deleted exons 2-6 (Figure 5.2).

Figure 5.1: VLO retain memory phenotype when developing in the absence of TRP-2 antigen (*Dct* Exon 1-/-). (A) The intact *Dct* gene is represented schematically with Exons 1 (E1) through 7 (E7) and large intronic regions represented in yellow. Beerman's *Dct* KO model is shown with the insertion of the neomycin (Neo) resistance gene in place of Exon 1. (B) $CD8^+$ T cells from the lymph nodes of VLO mice (red) and VLO *Dct*-$Exon1^{-/-}$ mice (purple) were analyzed by flow cytometry for expression of CD44, CD3, CD49d, CXCR3 and Ly6C. This is no difference in the level of expression of these proteins in the presence or absence of the TRP-2 antigen.

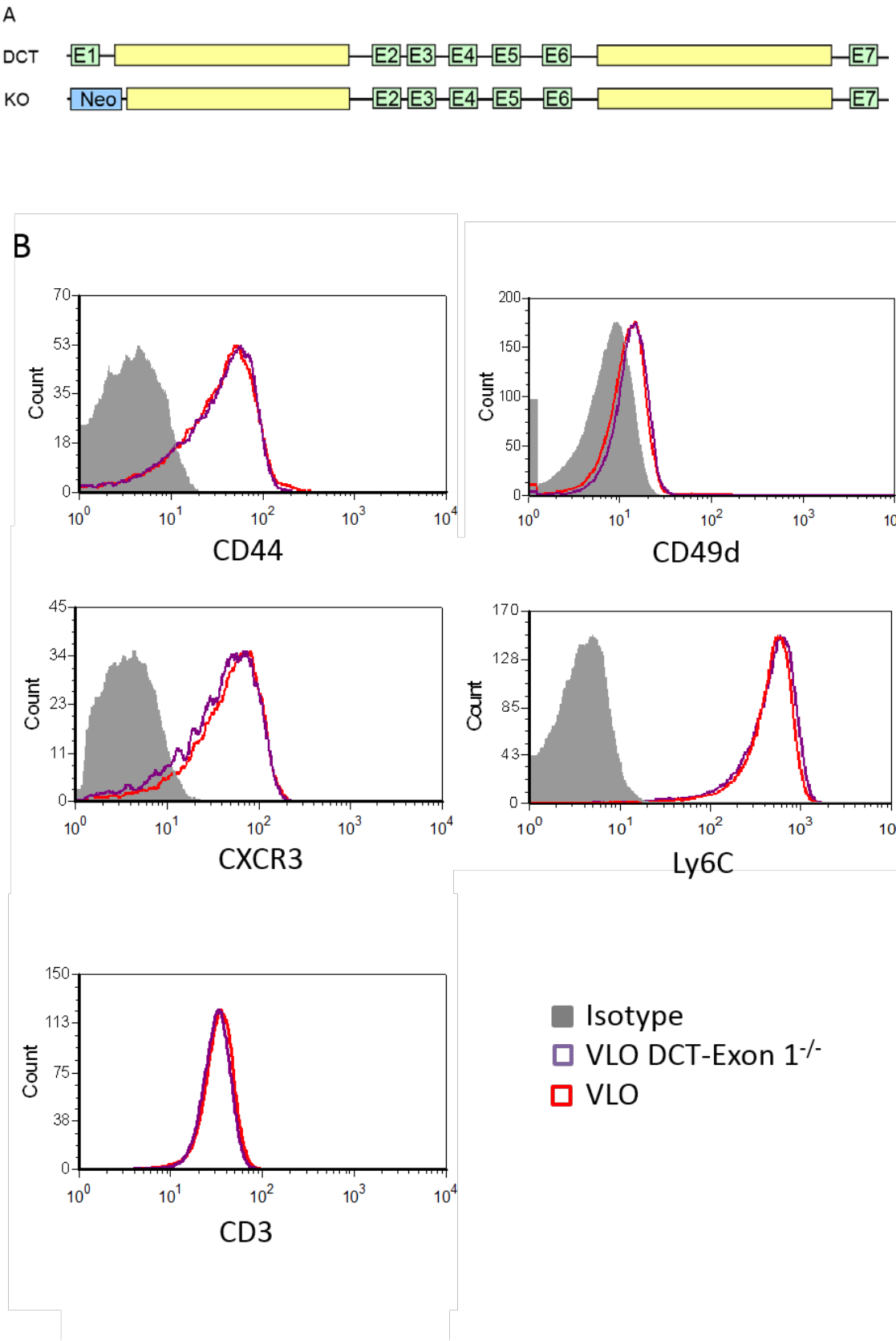
A
DCT
E1
E2
E3
E4
E5
E6
E7
KO
Neo
B
Count
CD44
CD49d
CXCR3
Ly6C
CD3
Isotype
VLO DCT-Exon 1-/-
VLO

5.2. Generation of DCT KO mouse model by deleting Exons 2 through 6

The *Dct* Exon 2-6 KO construct was generated by a commercial company, IDT (Coralville, IA). Electroporation of the gene construct into mESC was performed by the TMML of the Laboratory Animal Services Program at the National Cancer Institute, Frederick, MD. I performed the initial screening of mESC clones by southern blotting which proved to be inefficient. To create a high-throughput screening process, a PCR-based screening method was developed. This screening strategy allowed rapid and efficient screening of clones without the use of radioactivity. Primer sequences and PCR conditions are described in detail in Methods, Chapter 2. Figure 5.2A provides a schematic diagram of the intact *Dct* gene with 7 exons (E1-E7) in green with large intronic regions shown in yellow. A schematic of the KO construct is shown representing deletion of exons 2 through 6 with insertion of a Neo gene. Primers used for screening prospective clones are represented by blue arrows. Multiple primer sets were initially tested to ensure optimal screening strategy. Clones were screened using the primer sets described in the Methods section. Figure 5.2B provides an example of screening the genomic 5' arm of the *Dct* gene with primers 5-Arm-In-F and Linker-R1. "HR" indicates a band of the appropriate size, 2907 basepairs (bp), that is indicative of homologous recombination. "+" is a positive control using the cloning construct. "WT" is genomic DNA from a wild-type mouse that is negative for homologous recombination. Data from other primer sets are not shown for the sake of brevity.

After screening approximately 350 mESC samples, four candidates were found that showed recombination. These cells were then transferred into

blastocysts and inserted into pseudo-pregnant females by TMML. Two chimeric lines were generated and transferred into our laboratory's mouse colony where we oversaw the breeding of chimeras and the intercrossing of pups. Pups were screened for slate coat color which is the phenotype expected for mice with a homozygous deletion of *Dct* (Figure 5.2C). Tail clips were used to test for presence or absence of exons by PCR (Figure 5.2D). PCR conditions and primer sequences are detailed in Methods. Once the *Dct*-Exon 2-6$^{-/-}$ KO mouse line was fully established and characterized genetically and phenotypically, the KO mice were then bred onto a *Rag*$^{-/-}$ background with VLO transgene. The resulting mouse was named "CHAIRY".

Figure 5.2: Generation of *Dct* KO mouse model by deleting Exons 2 through 6. (A) The intact *Dct* gene is shown schematically with 7 exons (E1-E7) in green with large intronic regions shown in yellow. Our lab designed a new KO model which involved deleting exons 2 through 6 with insertion of a Neo gene. Primers used for screening prospective clones are represented by blue arrows. (B) Agarose gel showing the results screening mESC candidate clones for homologous recombination. In this example, the 5' arm is being interrogated with primers 5-Arm-In-F and Linker-R1. "HR" indicates a band of the appropriate size, 2907 bp, that is indicative of homologous recombination. "+" is a positive control using the cloning construct. "WT" is genomic DNA from a wild-type mouse that is negative for homologous recombination. (C) Chimeric mice were generated and interbreed producing pups that were white (W), slate (S), or black (B). Slate phenotype is expected for *Dct* KO mice. (D) Pups were screened by PCR for the presence of Exons 1 through 7. Black pups retain all exons of *Dct* in their genome, whereas slate pups retain only Exons 1 and 7 and lack exons 2 through 6 and are KOs for *Dct*. White pups are albino and are a byproduct of generating chimeric mice.

A

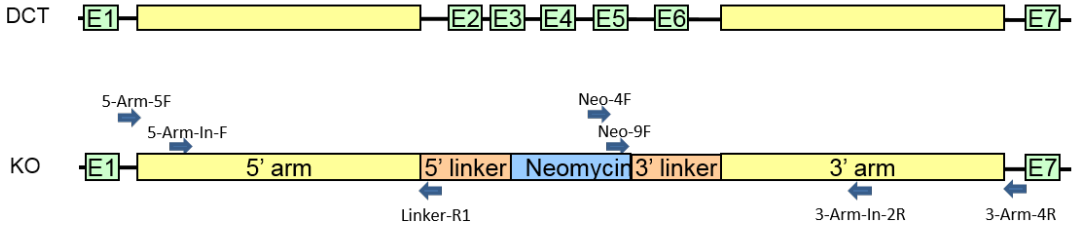
DCT
E1
E2
E3
E4
E5
E6
E7
5-Arm-5F
5-Arm-In-F
Neo-4F
Neo-9F
KO
E1
5' arm
5' linker
Neomycin
3' linker
3' arm
E7
Linker-R1
3-Arm-In-2R
3-Arm-4R

B

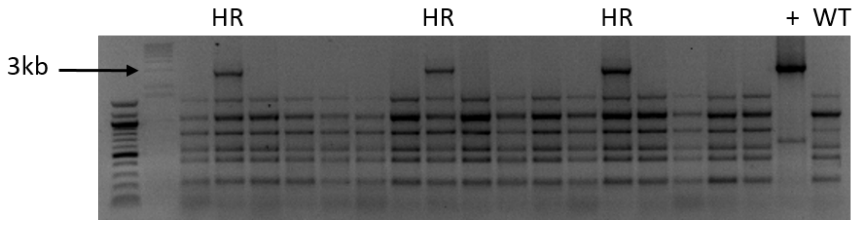
HR
HR
HR
+ WT
3kb

C

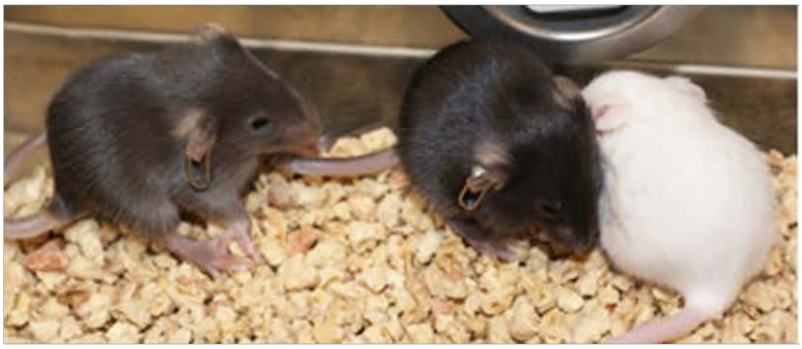

D

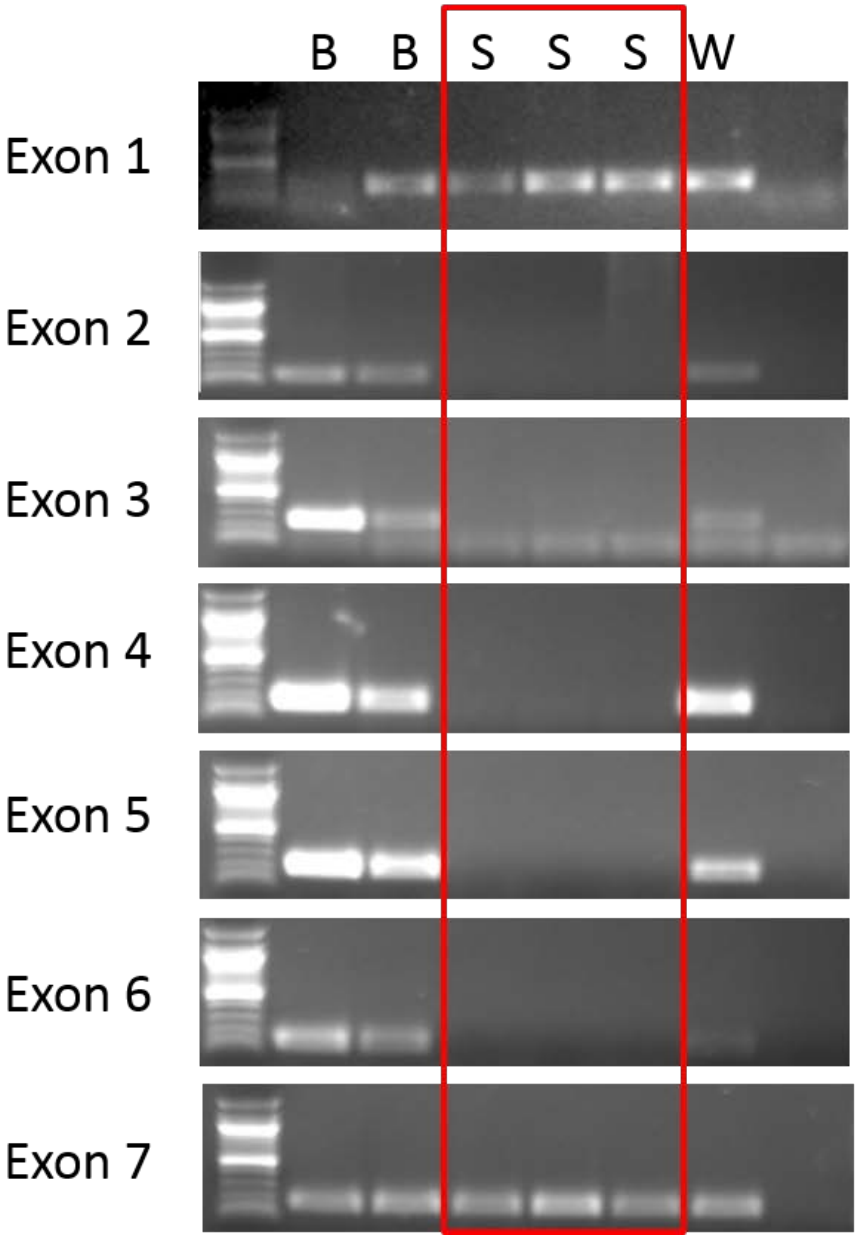

5.3. VLO *Dct*-Exon 2-6$^{-/-}$ retain memory phenotype while alleviating lymphopenia in the periphery

CD8^{+} T cells from the lymph nodes of CHAIRY mice were tested for phenotype by flow cytometry and compared with VLO cells (Figure 5.3A). No difference in expression of CD44, CD49d or Eomes was detected. Similarly, there was no difference in Ly6C, CD122, and CXCR3 expression (data not shown). These data support the original observation in the VLO *Dct*-Exon 1$^{-/-}$ mice (Figure 5.1B) that VLO cells do not require cognate antigen stimulation of the TCR to induce their memory phenotype. When TRP-2 protein is absent, the memory phenotype is retained, thus supporting the idea that VLO cells can be characterized in the category of innate memory cells.

Total cell counts generated from the peripheral lymph nodes of VLO and CHAIRY mice were compared (Figure 5.3B). Peripheral lymph nodes from 6 CHAIRY mice, and 16 VLO mice, aged 6 to 10 weeks, were collected and converted to single cell suspensions as described. Average cells counts were for VLO were 4 x 10^6 compared to 7 x 10^6 for CHAIRY. In contrast, there was no statistical difference in cell count in the thymi of VLO (140 x 10^6), and CHAIRY mice (120 x 10^6). These data suggest that direct TCR stimulation by the cognate antigen, TRP-2, may play a role in triggering the extreme lymphopenia observed in VLO mice. In the absence of the antigen, such as in CHAIRY mice, the lymphopenia is less severe with an increase in cell numbers in the periphery. Lymphopenia is not completely alleviated in the CHAIRY mice indicating that there are multiple factors driving lymphopenia in these mice. This is consistent with our evolving hypothesis that lymphopenia is being caused, at least in part, by deletion or abortive

proliferation driven by cognate antigen in the periphery. The observation that peripheral cell counts are increased in the absence of antigen in CHAIRY mice also supports the idea that the VLO TCR is indeed sensitive to the TRP-2 antigen.

Further evidence supporting the idea that the VLO TCR is sensitive to TRP-2 is seen in the decreased expression of T-bet in $CD8^+$ CHAIRY cells compared to VLO (Figure 5.3A). T-bet expression is triggered by TCR stimulation [185] which may lead to higher levels of T-bet expression in VLO cells compared to CHAIRY which exist in an environment devoid of TRP-2 antigen. Despite lack of antigen, T-bet expression is not completely eliminated in CHAIRY mice. Regulation of T-bet expression is complex, and is known to be induced by IL-15 [186]. We hypothesized that the maintenance of T-bet expression and memory phenotype in VLO cells may be driven in part by IL-15 or simply by homeostatic expansion.

Figure 5.3: VLO *Dct*-Exon 2-6-/- retain memory phenotype while alleviating lymphopenia in the periphery. *Dct*-KO-Exon 2-6$^{-/-}$ mice were crossed to generate a mouse that was *Dct*-Exon 2-6$^{-/-}$, *Rag*$^{-/-}$ and harbored the VLO transgene. The resulting mouse is referred to as the CHAIRY model. CD8^{+} cells from the lymph nodes of CHAIRY mice (purple) were compared to those from VLO mice (red) using flow cytometry. There was no difference found in expression of CD44, CD49d, nor Eomes. T-bet was downregulated in CHAIRY cells. (B) Total cell counts generated from the peripheral lymph nodes of VLO and CHAIRY mice were compared. CHAIRY mice had significantly more total cells in the periphery. In contrast, there was no difference in cell count in the thymi of VLO and CHAIRY mice. All mice in this study were 6-10 weeks of age. Error bars were calculated by Standard Error. * Indicates $p<0.05$ calculated by Single Factor ANOVA.

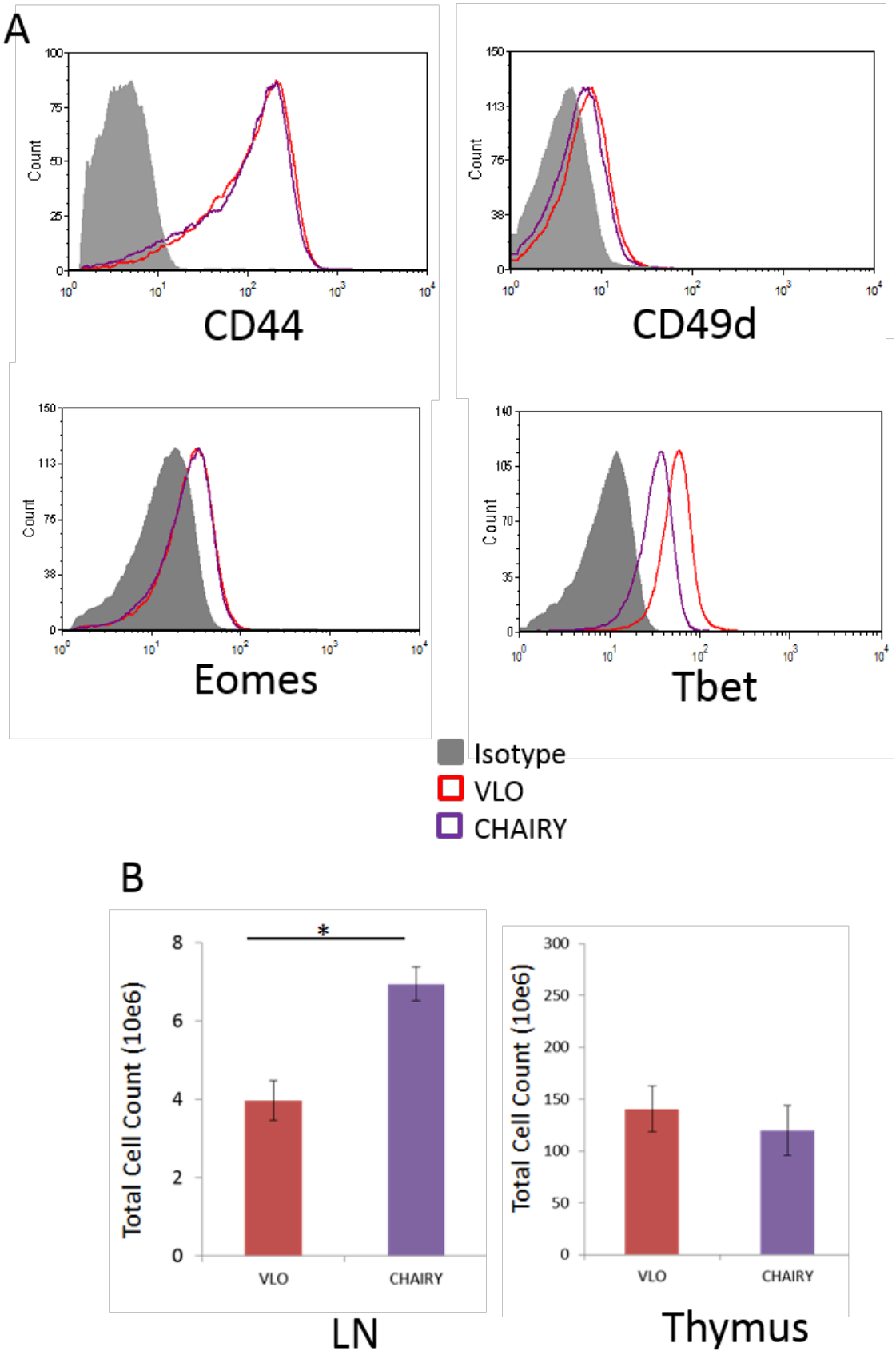
A
Count
CD44
CD49d
Eomes
Tbet
Isotype
VLO
CHAIRY
B
Total Cell Count (10e6)
*
VLO
CHAIRY
LN
Thymus

5.4 VLO develop in the absence of IL-15 and retain memory phenotype

Current understanding of memory phenotype $CD8^+$ T cells, suggests that IL-15 is critical for the development and maintenance of these cells [134, 169, 187, 188]. To investigate of the role of IL-15 in the development of the memory phenotype of VLO cells, VLO mice were breed onto *Il-15*$^{-/-}$ background, generating a mouse model that was *Il-15*$^{-/-}$, *Rag*$^{-/-}$ and possessed the VLO transgene. The resulting mouse was named "FAIRY".

$CD8^+$ cells from the lymph nodes of FAIRY mice were compared to those from VLO mice by flow cytometry (Figure 5.4A). There was no difference found in expression of CD49d, T-bet or Eomes. Similarly, there was no difference in Ly6C, CD122, and CXCR3 (data not shown). CD44 expression was slightly down-regulated in FAIRY mice. IL-15 has been reported to regulate expression of CD44, so this observation was not surprising [189].

Total cell counts generated from the peripheral lymph nodes of VLO and FAIRY mice were compared (Figure 5.4B). Peripheral lymph nodes from 2 FAIRY mice, and 16 VLO mice, aged 6 to 10 weeks, were collected and converted to single cell suspensions as described. There was no statistical difference in cells counts from the lymph nodes. VLO counts were 4×10^6 compared to 2.8×10^6 for FAIRY. There was no statistical difference in cell count in the thymi of VLO (140×10^6), and FAIRY mice (213×10^6). Statistical analysis is at a disadvantage for this study because only two FAIRY mice were available for analysis. It is possible that with higher numbers of animals the apparent trend of decreased numbers of FAIRY cells in the periphery might reach statistical significance. Nonetheless, the

memory phenotype of FAIRY cells allows us to conclude IL-15 is not required for memory development.

Figure 5.4: VLO cells develop in the absence of IL-15 and retain their memory phenotype. VLO mice were breed with *Il-15*$^{-/-}$ mice to generate a mouse model (FAIRY) that harbored the VLO transgene and lacked both *Rag* and *Il-15*. (A) CD8^{+} cells from the lymph nodes of FAIRY mice (orange) were compared to those from VLO mice (red) by flow cytometry. There was no difference found in expression of CD49d, Eomes and T-bet. CD44 was slightly downregulated in FAIRY mice. (B) Total cell counts generated from the peripheral lymph nodes of VLO and FAIRY mice were compared. FAIRY mice had no statistical difference in peripheral lymph nodes (LN) nor in the thymus compared to VLO mice as calculated by Single Factor ANOVA. Error bars were calculated by Standard Error.

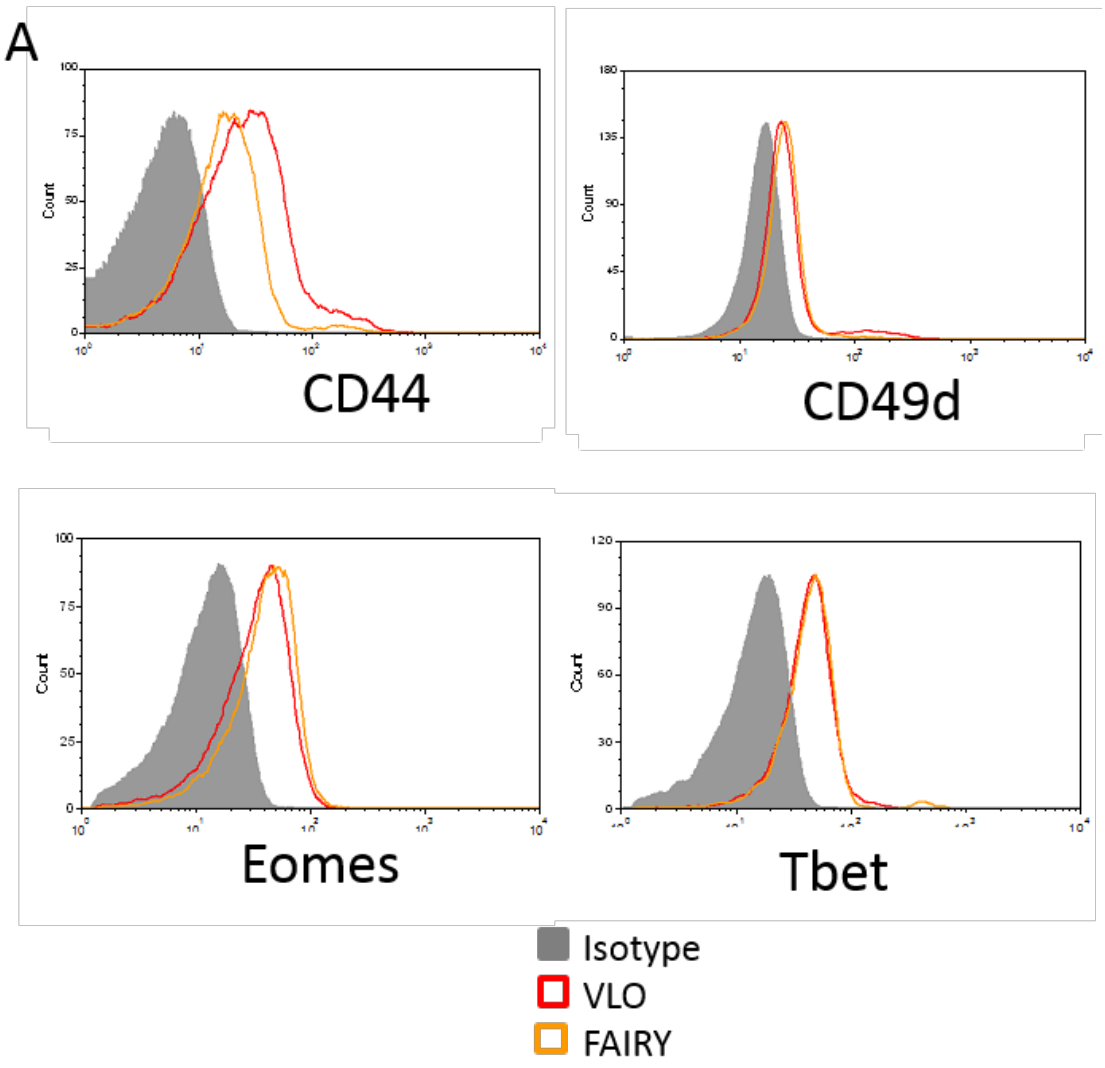
A
Count
CD44
CD49d
Eomes
Tbet
Isotype
VLO
FAIRY

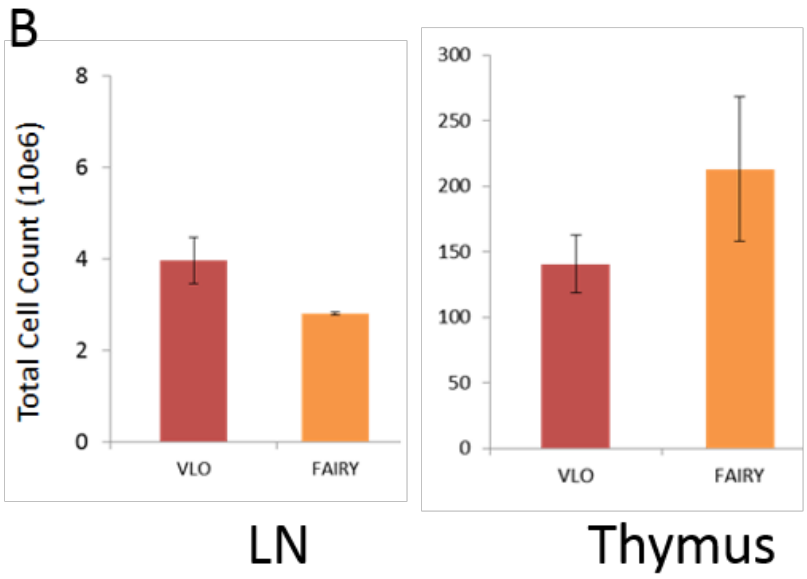
B
Total Cell Count (10e6)
VLO
FAIRY
LN
Thymus

5.5. VLO develop in the absence of IL-7 in contrast to HI

IL-7 is known to have overlapping functions with IL-15 [160] and is accepted to have a critical function in the HP and survival of T cells [190]. We were interested to examine the role IL-7 for the development of VLO cells. In order to explore this question, a series of BM chimeras were generated. VLO or HI BM was depleted of T cells and then adoptively transferred into sublethally-irradiated *Il-7*$^{-/-}$*Rag*$^{-/-}$ mice or congenic B6.*Rag*$^{-/-}$ mice. Mice were allowed to complete hematopoietic reconstitution and after two months were assessed for T cell phenotype. Figure 5.5A provides a schematic of the experimental design.

VLO cells that developed in a B6.*Rag*$^{-/-}$ background acquired a phenotype that is typical of what is observed in unmanipulated VLO mice. CD8^{+} T cells were predominantly CD44^{hi} CD49^{lo} as seen in the first panel of Figure 5.5B. In the second panel of the same figure, HI marrow was used to reconstitute *Il-7*$^{-/-}$*Rag*$^{-/-}$ mice. This chimera was generated as a control with the expectation that the development of HI cells would be severely impaired in the absence of IL-7 as IL-7 in the thymus provides a survival signal during T cell development and mice lacking IL-7 or its receptor show severe impairment of T cell development [191-193]. As expected, CD8^{+} HI T cells were almost undetectable in the periphery of these chimeras, presumably because they failed to develop through the thymus.

In sharp contrast to the HI chimera, VLO marrow that was used to reconstitute *Il-7*$^{-/-}$*Rag*$^{-/-}$ mice (third panel), permitted the development of CD8^{+} T cells in the periphery. The cells were predominantly CD44^{hi}, however they displayed a range of CD49d expression with 64% of the cells CD49d^{lo} and 36% expressing mid to high levels of CD49d. The fact that any T cells developed in the

absence of IL-7 was surprising. It is possible that these T cells originated from residual mature T cells derived from the transferred BM, as these cells would not require thymic development. However, the transferred marrow was largely depleted of adult T cells, and the HI marrow was equivalently depleted, and did not reconstitute T cells in the periphery. We suspect that VLO cells are receiving signals to bypass the requirement of IL-7 signaling. However, it remains possible that the VLO BM was capable of supplying a small but sufficient amount of IL-7 to support development of this phenotype. To more fully explore this question, VLO mice were crossed onto the *Il7*$^{-/-}$*Rag*$^{-/-}$ background and breed to homozygosity, generating "SAIRY" mice.

Figure 5.5: VLO develop in the absence of IL-7 in contrast to HI cells. (A) The experimental design is shown schematically. BM from either VLO or HI mice was depleted of CD8 cells before being adoptively transferred into irradiated recipient mice that were either *Rag*$^{-/-}$ or *Il-7*$^{-/-}$*Rag*$^{-/-}$. After two months, phenotype was assessed. (B) CD8^{+} cells from peripheral lymph nodes were analyzed by flow cytometry for CD44 and CD49d. *Rag*$^{-/-}$ mice reconstituted with VLO BM generated CD8^{+} cells expressing elevated cells of CD44 and low levels CD49d. *Il-7*$^{-/-}$*Rag*$^{-/-}$ recipients reconstituted with HI BM did not produce detectable CD8^{+} T cells. In contrast, when *Il-7*$^{-/-}$*Rag*$^{-/-}$ recipients were reconstituted with VLO BM, CD8^{+} T cells were produced with a CD44^{hi} phenotype.

A

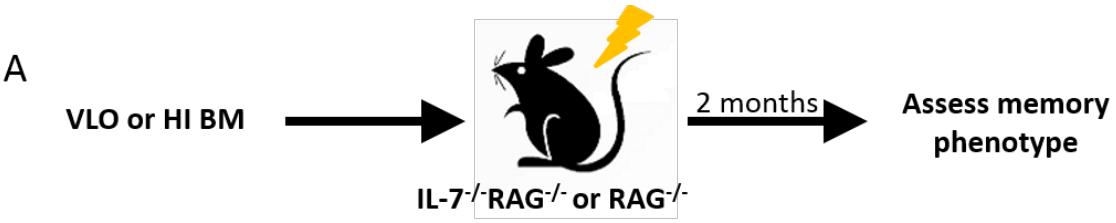
VLO or HI BM
2 months
Assess memory phenotype
IL-7-/-RAG-/- or RAG-/-

B

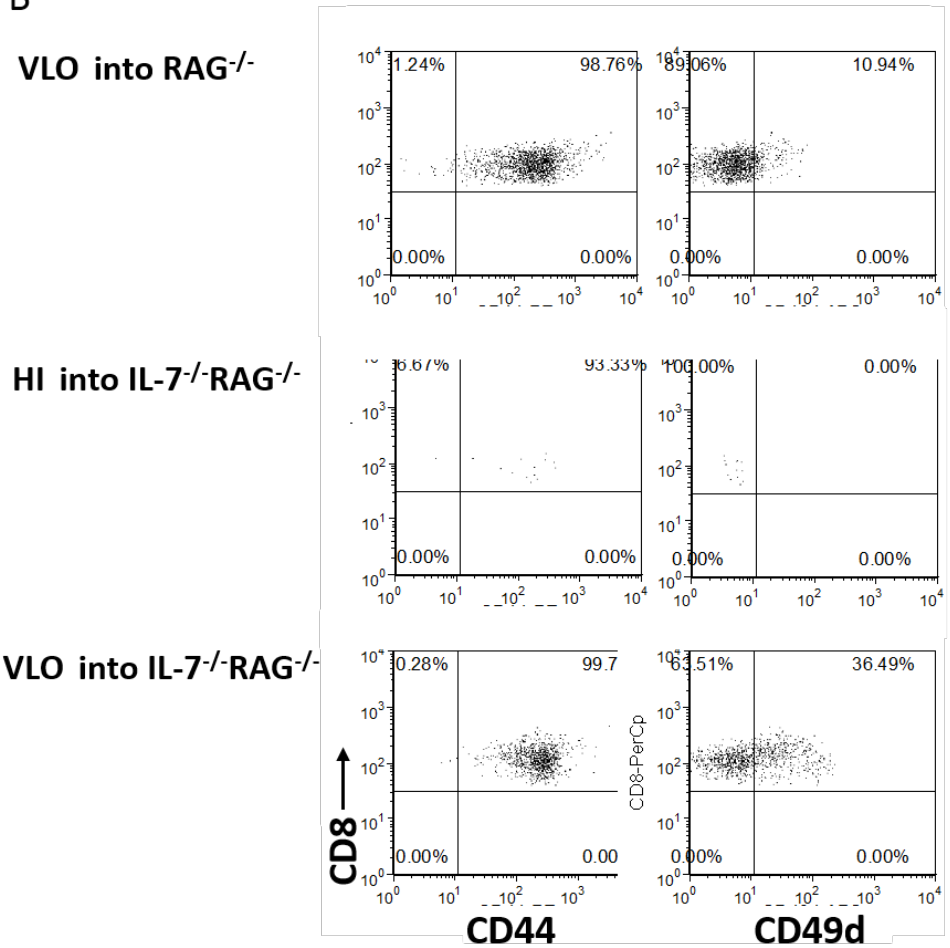
VLO into RAG-/-
HI into IL-7-/-RAG-/-
VLO into IL-7-/-RAG-/-
1.24%
98.76%
89.06%
10.94%
0.00%
0.00%
0.00%
0.00%
16.67%
93.33%
100.00%
0.00%
0.00%
0.00%
0.00%
0.00%
0.28%
99.7
63.51%
36.49%
0.00%
0.00
0.00%
0.00%
CD8
CD8-PerCp
CD44
CD49d

5.6. VLO retain memory phenotype and lymphopenia in the absence of IL-7

$CD8^+$ T cells from the lymph nodes of SAIRY mice were compared to those from VLO mice by flow cytometry (Figure 5.6A). There was no difference found in expression of CD44, and Eomes. Similarly, there was no difference in Ly6C, CD122, and CXCR3 (data not shown). The SAIRY mice also retain elevated CD5 on single positive $CD8^+$ cells in the thymus (data not shown). CD49d was slightly upregulated and T-bet was noticeably down-regulated compared to the VLO population. These findings support the idea that IL-7 is, in part, supporting the IMP of VLO cells, but remarkably is not absolutely required for the development of VLO cells through the thymus into the periphery.

Total cell counts generated from the peripheral lymph nodes of VLO and SAIRY mice were compared (Figure 5.6B). Lymph nodes cells from 4 SAIRY mice, and 16 VLO mice, aged 6 to 10 weeks, were compared. There was no statistical difference in cells counts from the lymph nodes. VLO counts were 4×10^6 compared to 2.9×10^6 for SAIRY. The cellular content of the thymi of SAIRY mice (13×10^6) was severely reduced compared to VLO (140×10^6). This finding was expected given the tiny thymic size that is typical of *Il-7*$^{-/-}$ mice.

Figure 5.6: VLO cells develop in the absence of IL-7 and retain their memory phenotype. VLO mice were breed with *Il-7*$^{-/-}$ mice to generate a mouse model (SAIRY) that harbored the VLO transgene and lacked both RAG and IL-7. (A) CD8^{+} cells from the lymph nodes of SAIRY mice (aqua) were compared to those from VLO mice (red) by flow cytometry. There was no difference found in expression of CD44, CD49d, and Eomes. T-bet is downregulated in SAIRY mice. (B) Total cell counts generated from the peripheral lymph nodes of VLO and SAIRY mice were compared. SARY mice had no statistical difference in peripheral lymph nodes (LN) compared to VLO mice, but were severely reduced in thymic size. Error bars were calculated by Standard Error. * Indicates $p<0.05$ calculated by Single Factor ANOVA.

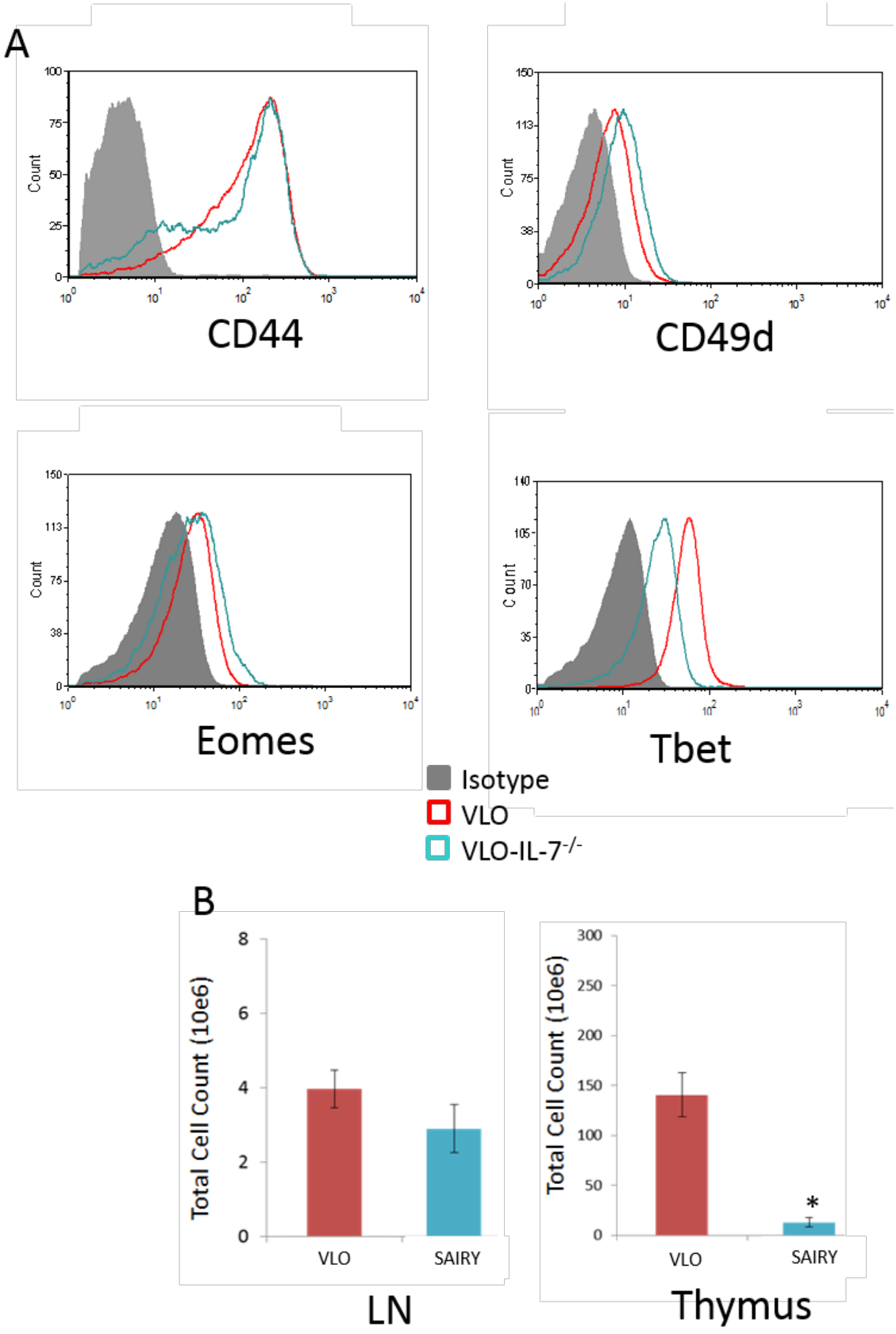
A
Count
CD44
CD49d
Eomes
Tbet
Isotype
VLO
VLO-IL-7-/-
B
Total Cell Count (10e6)
VLO
SAIRY
LN
Thymus
*

5.7. Lymphopenia of VLO mice worsens with age in the absence of IL-7

Lymphopenia was followed in VLO and SAIRY mice as they aged (Figure 5.7). Peripheral cell counts from lymph nodes were assessed at 6-8 weeks of age and in mice over 14 weeks of age (Figure 5.7A). There is no difference between SAIRY and VLO groups at age 6-8weeks, suggesting that IL-7 may not be required for the development of the cells as shown previously in Figure 5.6B. As SAIRY mice age, the peripheral lymph node cell populations significantly decrease suggesting that IL-7 plays a role in maintaining VLO cell homeostasis and/or survival. In addition to assessing lymphopenia in the periphery, thymic cell counts were also recorded. Thymic size is drastically reduced in the absence of IL-7, however there is no further reduction in thymic cell number as mice age (Figure 5.7B).

Figure 5.7: VLO lymphopenia worsens with age in the absence of IL-7. (A) Peripheral lymph nodes of VLO mice and SAIRY mice were harvested from mice aged 6-8 weeks (wk) or older than 14 weeks. VLO mice maintain the same level of lymphopenia as they age (red). As SAIRY mice age, peripheral cell populations significantly decrease (aqua). Error bars were calculated by Standard Error. * Indicates $p<0.05$ calculated by Single Factor ANOVA (B) SAIRY mice have a severely reduced thymic compartment compared to VLO mice in both age groups tested. There is no detectable reduction in relative thymic cell count for either SAIRY or VLO as they age.

A

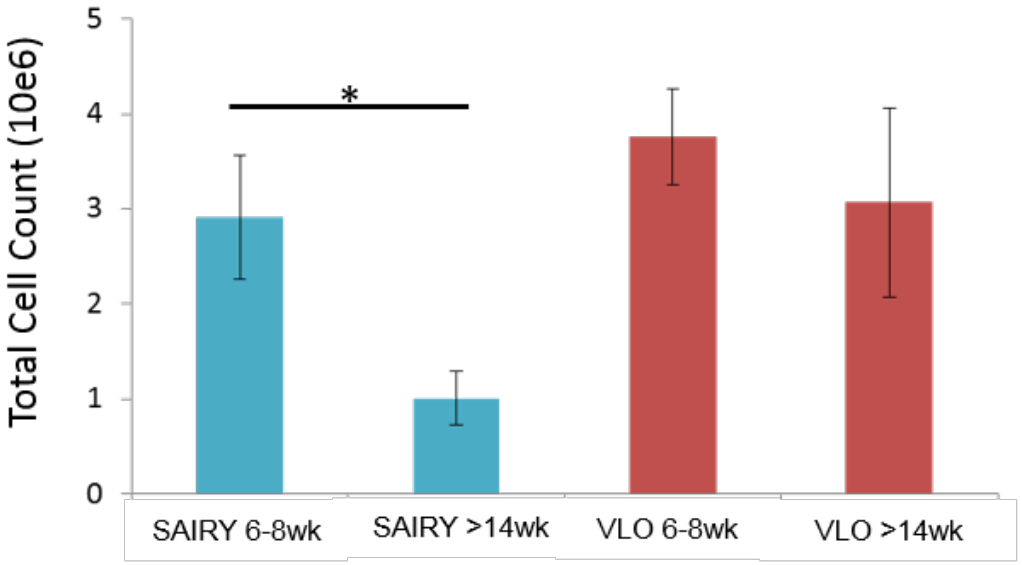
Total Cell Count (10e6)
5
4
3
2
1
0
*
SAIRY 6-8wk
SAIRY >14wk
VLO 6-8wk
VLO >14wk

LN

B

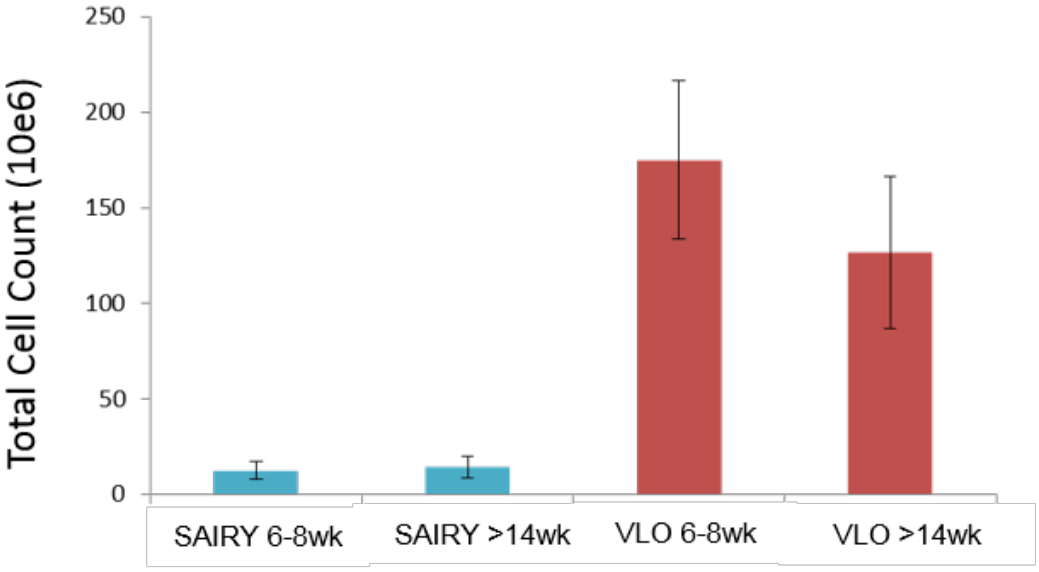
Total Cell Count (10e6)
250
200
150
100
50
0
SAIRY 6-8wk
SAIRY >14wk
VLO 6-8wk
VLO >14wk

Thymus

Summary of Chapter 5: To more fully understand the molecular requirements of acquisition of memory phenotype by VLO cells we used multiple mouse models to examine the contribution of cognate antigen, IL-7 and IL-15. VLO cells that developed in the absence of TRP-2 antigen in the VLO-*Dct*-Exon1$^{-/-}$ model retained the memory phenotype seen in VLO cells developing in the presence of TRP-2. Our lab generated a new *Dct* KO mouse strain to ensure that no TRP-2$_{180\text{-}188}$ epitope (contained within Exon 2) was present. We deleted Exons 2 through 6 in this model. VLO cells developing in the background of this model, again retained their memory phenotype, but also had increased cell numbers in the periphery suggesting that cognate antigen plays a role in negative selection of VLO cells in the periphery. T-bet was slightly down-regulated in this population as well, which may indicate that antigenic stimulation of the VLO TCR contributes to high levels of T-bet seen in VLO cells. VLO cells did not require IL-15 for their development, nor memory phenotype. VLO cells were able to develop in the absence of IL-7 in contrast to HI cells which did not develop without IL-7. VLO memory phenotype and peripheral lymphopenia were maintained in the absence of IL-7. Thymic size was greatly reduced in the absence of IL-7, but this is expected. Lymphopenia of VLO mice worsened with age in the absence of IL-7 suggesting that IL-7 plays a role in the homeostatic maintenance and/or survival of these cells.

Chapter 6: Discussion

6.1 VLO phenotype is consistent with virtual memory cells

VM cells are defined as antigen-specific $CD8^+$ T cells with a memory-like phenotype existing within an antigen-inexperienced host [137]. VM cells express high levels of expression of CD44, along with other markers associated with T cell memory [137]. The distinguishing feature between VM cells and true antigen experienced memory cells is down regulation of CD49d on the VM cells [137]. This cell type has been observed in normal non-lymphopenic mice, as well as in *Rag*$^{-/-}$ animals and gnotobiotic animals [137]. A key distinguishing feature of VM cells is that they exist in the steady-state which means the cells exist in the absence of manipulation to induce lymphopenia in the host animal. According to work by the lab of Jameson, VM cells can be found in germ-free mice in similar numbers as those found in specific pathogen-free animals [137]. This suggested to their team that the memory phenotype of the cells is generated by HP, rather than being triggered by antigens from the microbiome or the environment [137]. However, VM cells exist at vanishingly low frequencies with only about 100 to 1000 cells for any given epitope identified by tetramer binding [137, 156]. VM cells are therefore challenging to isolate, characterize, and study functionally. We suggest the VLO mouse is a useful model to study the behavior and development of VM cells because the phenotype and function of VLO cells is consistent with what has been reported for VM cells.

One of the essential features of VM cells is the requirement that the mice are antigen-inexperienced. The original VLO mouse was generated on a C57BL/6 background. These mice express TRP-2 in their coat, which suggests that the mice

are antigen-experienced. To ensure that VLO cells were indeed VM cells, we tested their phenotype in the absence of TRP-2 in two separate *Dct* KO backgrounds. In both cases, VLO cells retained their distinctive memory phenotype which is highly supportive of our conclusion that VLO cells fit the criteria for VM cells. The possibility remains that the VLO TCR cross-reacts with a different self-antigen which drives the memory phenotype.

We have shown that VLO cells display a memory phenotype in the periphery with low levels of expression of CD49d and high levels of other memory markers consistent with what has been reported for VM cells. In addition, Sosinowski *et al* (2012) reported that VM cells express very high levels of CD122 [169]. We found this to be true for VLO cells as well. We observed that VLO cells express high levels of Ly6C. Elevated levels of Ly6C have been reported for memory CD8 cells, but the levels of Ly6C on VLO cells is well beyond what was detected on WT cells, which calls for further investigation.

VLO animals exist in a state of chronic lymphopenia for reasons that are not yet fully understood. It is possible that VLO cells are negatively selected or deleted in the periphery limiting their number. In support of this idea, we observed alleviation of lymphopenia when VLO cells developed in the absence of TRP-2 antigen, presumably as a result of decreased negative selection in the periphery. It is also possible that cell number in the periphery is a result of low thymic output. The thymic compartment of these animals looks normal with thymic cell number equivalent to WT, and percentages of double negative, double positive and single positive cells similar to WT (data not shown). We conclude that VLO cells acquire memory phenotype in the periphery after thymic egress which is consistent with

what has been reported for VM cells [156]. Regardless of the cause of lymphopenia in VLO animals, it is their normal state and can therefore be considered "steady-state" because it occurs without manipulation. This supports our conclusion that VLO cells fit the criteria of VM cells.

The T cells of the HI, LO, and VLO models recognize the same ligand, but with different avidity. VLO and LO mice are both lymphopenic compared to HI and WT mice. Despite this, $CD8^+$ T cells from LO mice display a naïve phenotype while VLO mice display a VM phenotype. The lymphopenia of VLO mice is more severe than that of LO mice, suggesting that there may be something unique about the VLO TCR that is contributing to the severe lymphopenia and memory phenotype of VLO cells. As a result of these observations, we tested whether the VM phenotype of VLO cells was inherent to the cells themselves or if it was a feature of the lymphopenic environment in which the cells developed. By employing a BM chimera generated from a mix of WT and VLO marrow, we showed that VLO cells are not fundamentally limited in their ability to exist as $CD44^{lo}$ naïve cells as long as they develop in the presence of WT cells. From these data, we conclude that VLO cells acquire their VM phenotype as a result of the lymphopenic environment in which they develop. When the lymphopenic pressure is reduced in the presence of WT cells, a majority of VLO cells (>60%) are able to develop and sustain a naïve phenotype. The remaining ~40% of VLO cells in the mixed chimera retain a $CD44^{hi}$ phenotype. It would be interesting to investigate this population further to discern whether other VM memory markers are retained, in particular CD49d status would be interesting to know. Alternatively, the presence of WT cells may influence the VM phenotype independent of

lymphopenia; for example, the cytokines or growth factors that drive the VM phenotype could be consumed by WT cells.

It was reported by Lee *et al* (2013) that the frequency of VM cells increases with age with high avidity TCRs preferentially maintained in the VM population [168]. The presence of these high avidity TCRs was correlated to infection control in aged animals [168]. In our model, VLO cells are very low avidity for TRP-2. There is no published data that indicates that low avidity TCRs cannot develop into VM cells, but it seems that based on the current knowledge of VM cells, this VLO model would be somewhat unusual in this regard. There is some evidence that suggests that VLO may recapitulate high avidity signaling through its TCR. VLO single positive CD8 cells in the thymus display upregulation of CD5 (data not shown) which is indicative of strong signaling through the TCR which is usually taken as a sign of high avidity. It is possible that the VLO TCR is cross-reacting to another antigen with high affinity, or this could be another hint that the VLO TCR possesses some unusual signaling mechanism that would require further investigation. We also observed downregulation of CD3, TCR-β, and CD8 (data not shown) on VLO cells, again suggesting tuning of the VLO TCR possibly in response to strong signaling. Down-regulation of TCR components may explain in part why VLO cells respond poorly to antigen with dampened proliferation and IFNγ production compared to LO and HI cells. There is conflicting evidence in the literature regarding how VM cells respond to their cognate antigen. Some reports provide evidence that VM cells respond as robustly as their antigen-driven memory counterparts, while other reports indicate that VM cells respond weakly to antigen [137, 153, 168, 194]. Lee *et al* (2013) suggests that these differences may be a result

of the pathways used for homeostatic memory generation [168]. They concluded that artificially induced conditions to create severe lymphopenia do not result in the production of VM cells with the same functions as naturally occurring VM cells which are thought to respond weakly to cognate antigen [168]. These conclusions reveal the value of the VLO model with its naturally occurring lymphopenia and production of VM VLO cells with weak response to antigenic stimulation.

6.2 VLO cells develop independently of IL-15, and IL-7

Previous reports concerning the development of VM cells indicate that VM cells slowly fill the T-cell compartment after birth during a period of neonatal lymphopenia [156]. VM cell development depends on IL-15 to the extent that the absence of IL-15 in the host causes loss of VM cells [169]. In contrast to this report, VLO cells develop in the absence of IL-15, retain their memory phenotype, and show no difference in cellularity in the periphery or in the thymus compared to intact VLO mice. This observation was curious to us, and suggests that alternate mechanisms of VM development exist that allow IL-15 to be dispensable.

IL-7 and IL-15 can, in some circumstances, substitute for each other. Tan *et al* (2002) reported that in the absence of IL-15, memory $CD8^+$ T cells can utilize IL-7 for HP [195]. With this in mind, we also examined the development of VLO cells in the absence of IL-7. VLO cells developed in the absence of IL-7, retained their memory phenotype, and showed no difference in cellularity in the periphery compared to intact VLO mice. We did observe that IL-7 is required for the long term maintenance and survival of VLO cells. T-bet expression was decreased in

the absence of IL-7, and the cellularity of the thymus was severely reduced to levels similar to what has been reported for the parental *Il-7*$^{-/-}$ mouse [193].

IL-7 is considered to have a crucial non-redundant role in directing T cell development. However, even in parental *Il-7*$^{-/-}$ mice T cell development is not completely ablated [193]. There is still a very small fraction of T cells that develop in the absence of IL-7 [193]. We thought perhaps that VLO cells were simply representative of the developmental escape seen in the *Il-7*$^{-/-}$ model. To test this idea, we compared the development of VLO cells with HI cells using *Il-7*$^{-/-}$ BM chimeras. As shown, development of HI cells is almost completely ablated in the absence of IL-7 to the point where T cells are virtually undetectable. This leads us to conclude the VLO cells, and possibly, VM cells, have an unique capacity to utilize alternative cytokines in the absence of IL-7. Tan *et al* (2002) showed that the double KO of *Il-7*$^{-/-}$ *Il-15*$^{-/-}$ leads to failure of HP [195]. It would be interesting to examine the development of VLO cells in this type of double KO.

IL-4 is thought to play a role in the development of VM cells. Kurzweil *et al* (2014) provided evidence that an increase in peripheral IL-4 expression causes expansion of VM cells [196]. The reverse experiment, examining VM cells in an *Il-4r* deficient model was conducted by Akue *et al* (2012) showed that VM cells were reduced, but not eliminated in the absence of IL-4 signaling [156]. In the VLO model, serum levels of IL-4 were tested by enzyme-linked immunosorbent assay, but not signal was detected, suggesting that levels were below the limit of detection of the assay (data not shown). However, IL-4R (CD124) is upregulated on VLO cells (data not shown) suggesting that they may be more sensitive to IL-4 in their environment. It would be interesting to continue delving into the role that IL-4

might play in the development and maintenance of these cells, especially in the light of the fact that the VM phenotype develops independently of IL-7, and IL-15.

6.3 VLO cells respond robustly to proinflammatory cytokines

$CD8^+$ memory cells, whether antigen-induced memory, HP memory, or VM display enhanced response to stimulation compared to naïve cells [137, 148, 153, 194, 197]. The most functionally dramatic responses of VLO cells were in response to proinflammatory cytokines. VLO cells whether $CD44^{lo}$ naïve or $CD44^{hi}$ memory proliferate and secrete IFNγ more robustly when stimulated by proinflammatory cytokines in the absence of TCR stimulation. The combination of IL-2 with IL-18 yielded the highest levels of proliferation for both naïve and memory VLO cells compared to their LO and HI counterparts. VLO memory cell proliferation and IFNγ production greatly exceeded that achieved by naïve VLO cells. The cocktail of IL-2 with IL-12 and IL-18 induced the greatest amount of IFNγ secretion in both naïve and memory VLO cells, with memory cells producing more about six-times as much as naïve cells. These data are consistent with what has been previously reported for VM cells [137]. Production of IFNγ in response to IL-12 and IL-18 is described in the literature as an "innate-like function" [137, 198, 199]. The ability of VM cells to respond to proinflammatory cytokines in the absence of TCR ligation suggests to us and others that VM cells may act as a bridge between the innate and adaptive arms of the immune system [137, 168]. As discussed by Haluszczak *et al* (2009), the role of VM $CD8^+$ cells may be especially relevant in situations where the naïve T cell pool is low [137].

In addition to increased proliferation and IFNγ production in response to IL-12 and IL-18, VLO cells also differentially proliferate in response to IL-15, but

not IL-7, nor TSLP *in vitro*. IL-15 is a proinflammatory cytokine [200]. Again we observe the same pattern in which VLO proliferation significantly exceeds the responses of LO and HI cells which naïve cells or memory cells are being interrogated. We also observed that VLO memory cells proliferate more robustly compared to naïve VLO cells in response to IL-15. This may be due to increased expression of the receptor for this cytokine or possibly enhanced downstream signaling. IL-15 is know to promote proliferation and survival of memory CD8 T cells [201-203]. IL-15 normally signals through a trimeric receptor complex which consists of the IL-15Rα chain which trans-presents IL-15 to CD122 and the common γ chain. The dimer of CD122 and common γ also acts as a receptor for IL-2. IL-15Rα is typically expressed on monocytes and NK cells, but T cells can also express this receptor subunit [192, 204, 205]. The VLO proliferation assays were conducted in the absence of APCs which would traditionally trans-present IL-15 to the T cells. Cis-presentation of IL-15 has been reported for NK cells [206], and IL-15Rα has been reported on T cells, so it is possible that VLO cells are cis-presenting IL-15 to themselves. It is also possible that IL-15 levels in the cultures (100 ng/mL) are so high that they overcome the need for IL-15Rα. Regardless of the molecular mechanism of IL-15 signaling in VLO cells, the data show that VLO cells are more responsive to IL-15 than LO or HI cells. IL-15-induced proliferation of VLO cells is uncoupled from IFNγ secretion.

6.4 Treatment of tumors via adoptive transfer of VLO cells requires optimization

Multiple reports have provided evidence that VM cells are able to provide antigen-specific protection against pathogen infection [168]. It has also been

shown that memory cells can have a more potent anti-tumor reaction than naïve cells [105, 181, 207-210]. Until now, it has not been possible to determine if VM cells could be directed toward an anti-tumor response. In two of our four tumor studies, adoptive transfer of VLO cells with a TRP-2-pulsed dendritic cell vaccine resulted in the complete regression of tumor in 20% of the animals treated. These data suggest that VLO cells, and therefore VM cells, may have the potential to control tumor growth.

Given that VLO cells are poised to respond to a lymphopenic environment through rapid HP, it would be worthwhile to repeat these tumor studies and add in a lymphodepletion treatment prior to ACT. This would create a lymphopenic environment that may allow enhanced reactivity of the VLO cells, granting VLO cells access to IL-15 which we predict would trigger VLO proliferation in the host. Lymphodepletion is the standard of care with human ACT protocols [53, 211, 212]. Mouse models of ACT have shown that lymphodepletion increases the efficacy of ACT by removal of homeostatic cytokine sinks [35]. Gattinoni *et al* showed that IL-7 and IL-15 were required for supporting anti-tumor activity of transferred T cells in this model [35].

6.5 Overall summary

VM cells have been intensely challenging to study because of the low frequency at which they occur in mice, especially for cells of a defined antigenic specificity. Based on the results presented in this dissertation, we propose that the VLO mouse can serve as a model for VM cells. We described the phenotype, function and developmental requirements of VLO cells which coincide with what has been previously described by other groups for VM cells. In particular, we

observed that the memory signature of VLO mice is consistent with what has been reported for VM cells. Likewise, VLO cells display innate-like functions by responding robustly to proinflammatory cytokines, but not strongly to cognate antigen. *In vivo* studies demonstrated with naïve VLO cells are specially poised to respond to lymphopenia, and proliferate rapidly. Use of VLO cells in an ACT to treat melanoma in mice provided hints that these cells could be manipulated to reduce or eliminate tumor burden, but more extensive studies are required. Finally, we examined the developmental requirements of VLO cells and found surprisingly that they are able to develop and acquire their memory phenotype in the absence of IL-7 or the absence of IL-15. The VLO model opens up multiple avenues of investigation that were previously almost impossible to investigate for VM cells.

6.6 Future studies

A variety of questions related to VM cells remain to be investigated. Lee *et al* (2013) provided evidence that the cell cycle status of VM cells is uniquely poised in the advanced G1 status [168]. As such, it would be interesting to determine whether VLO cells recapitulated this finding. In the same paper, Lee *et al* showed that after VM cells are stimulated by antigen *in vivo*, they preferentially differentiate toward a central memory phenotype [168]. This study could easily be repeated with VLO cells, especially because the cognate antigen is already defined. In addition, it would be of interest to explore TCR signaling patterns of VLO cells, which we suspect would be different from LO and HI cells. Given the ability of VLO cells to respond dramatically to cytokines in the absence of TCR ligation, we would predict that these cells are already poised to preferentially respond to non-

antigenic signals. This idea is supported by our observations that the CD3, CD8, and TCR-β are all downregulated on VLO cells. We also propose examining telomere length of VLO cells, as well as epigenetic and genetic profiles in order to more carefully characterize this unique cell type. Recent studies have shown that memory cells use different metabolic pathways [213]. With this in mind we are interested in comparing the metabolic profiles of VLO, LO and HI cells when they are in either a naïve or memory state.

It was reported that antigen-driven memory cells can circulate beyond the normal boundaries of secondary lymph structures, and traffic to peripheral tissue especially during inflammation [137]. The trafficking patterns of VM cells are virtually unexplored and could be tracked in the VLO model. It is thought that memory T cells home to the BM, but it is unknown if VM cells are sequestered or enriched in that region. We observed that T cells account for approximately 3-4% of VLO BM, but more detailed analysis of the cells and their memory state are warranted.

Previous studies of VM cells have suggested that CD4 help is required for their function. It possible that our tumor studies could be enhanced by the addition of CD4 help as well. Our lab previously reported that, compared to LO cells, HI cells were preferentially "helped" by $CD4^+$ T cells [103]. Multiple studies of memory phenotype $CD8^+$ T cells have suggested that memory cell can have a suppressive function inhibiting T cell responses for both $CD4^+$ and $CD8^+$ T cells [214-218]. It would be interesting to explore this possibility with VLO cells. Developmentally, examining VLO cells in the context of an *Il-7*$^{-/-}$ *Il-15*$^{-/-}$ double KO would be very compelling. Likewise, it would be helpful to examine the

development of VLO cell in an *Il-4*$^{-/-}$ background. The VLO mouse model could provide a means to investigate these and other questions related to CD8^{+} VM cells.

Chapter 7: Bibliography

1. Decker, W.K. and A. Safdar, *Bioimmunoadjuvants for the treatment of neoplastic and infectious disease: Coley's legacy revisited.* Cytokine Growth Factor Rev, 2009. **20**(4): p. 271-81.
2. Coley, W.B., *The Treatment of Inoperable Sarcoma by Bacterial Toxins (the Mixed Toxins of the Streptococcus erysipelas and the Bacillus prodigiosus).* Proc R Soc Med, 1910. **3**(Surg Sect): p. 1-48.
3. Herr, H.W. and A. Morales, *History of bacillus Calmette-Guerin and bladder cancer: an immunotherapy success story.* J Urol, 2008. **179**(1): p. 53-6.
4. Burnet, M., *Cancer; a biological approach. I. The processes of control.* Br Med J, 1957. **1**(5022): p. 779-86.
5. Morales, A., D. Eidinger, and A.W. Bruce, *Intracavitary Bacillus Calmette-Guerin in the treatment of superficial bladder tumors. 1976.* J Urol, 2002. **167**(2 Pt 2): p. 891-3; discussion 893-5.
6. Xie, J., et al., *Differential Adverse Event Profiles Associated with BCG as a Preventive Tuberculosis Vaccine or Therapeutic Bladder Cancer Vaccine Identified by Comparative Ontology-Based VAERS and Literature Meta-Analysis.* PLoS One, 2016. **11**(10): p. e0164792.
7. Bindon, C., et al., *Clearance rates and systemic effects of intravenously administered interleukin 2 (IL-2) containing preparations in human subjects.* Br J Cancer, 1983. **47**(1): p. 123-33.
8. Kirkwood, J.M., et al., *Comparison of intramuscular and intravenous recombinant alpha-2 interferon in melanoma and other cancers.* Ann Intern Med, 1985. **103**(1): p. 32-6.
9. Stenehjem, D.D., et al., *Extension of overall survival beyond objective responses in patients with metastatic renal cell carcinoma treated with high-dose interleukin-2.* Cancer Immunol Immunother, 2016. **65**(8): p. 941-9.
10. Xu, D.H., et al., *Unveil the mysterious mask of cytokine-based immunotherapy for melanoma.* Cancer Lett, 2017. **394**: p. 43-51.
11. Dunn, G.P., L.J. Old, and R.D. Schreiber, *The three Es of cancer immunoediting.* Annu Rev Immunol, 2004. **22**: p. 329-60.
12. Hanahan, D. and R.A. Weinberg, *Hallmarks of cancer: the next generation.* Cell, 2011. **144**(5): p. 646-74.
13. Couzin-Frankel, J., *Breakthrough of the year 2013. Cancer immunotherapy.* Science, 2013. **342**(6165): p. 1432-3.
14. Baxevanis, C.N., S.A. Perez, and M. Papamichail, *Cancer immunotherapy.* Crit Rev Clin Lab Sci, 2009. **46**(4): p. 167-89.
15. Becker, Y., *Molecular immunological approaches to biotherapy of human cancers--a review, hypothesis and implications.* Anticancer Res, 2006. **26**(2A): p. 1113-34.
16. Borghaei, H., M.R. Smith, and K.S. Campbell, *Immunotherapy of cancer.* Eur J Pharmacol, 2009. **625**(1-3): p. 41-54.
17. Cheng, M., et al., *NK cell-based immunotherapy for malignant diseases.* Cell Mol Immunol, 2013. **10**(3): p. 230-52.
18. Hayakawa, M., et al., *Treatment of advanced renal cell carcinoma using regional arterial administration of lymphokine-activated killer cells in combination with low doses of rIL-2.* Urol Int, 1994. **53**(3): p. 117-24.
19. Sharma, P. and J.P. Allison, *Immune checkpoint targeting in cancer therapy: toward combination strategies with curative potential.* Cell, 2015. **161**(2): p. 205-14.

20. Sutlu, T. and E. Alici, *Natural killer cell-based immunotherapy in cancer: current insights and future prospects.* J Intern Med, 2009. **266**(2): p. 154-81.
21. Topalian, S.L., G.J. Weiner, and D.M. Pardoll, *Cancer immunotherapy comes of age.* J Clin Oncol, 2011. **29**(36): p. 4828-36.
22. Anassi, E. and U.A. Ndefo, *Sipuleucel-T (provenge) injection: the first immunotherapy agent (vaccine) for hormone-refractory prostate cancer.* P T, 2011. **36**(4): p. 197-202.
23. Hinrichs, C.S. and N.P. Restifo, *Reassessing target antigens for adoptive T-cell therapy.* Nat Biotechnol, 2013. **31**(11): p. 999-1008.
24. Exley, M.A., et al., *Adoptive Transfer of Invariant NKT Cells as Immunotherapy for Advanced Melanoma: a Phase 1 Clinical Trial.* Clin Cancer Res, 2017.
25. Wei, X.X., L. Fong, and E.J. Small, *Prostate Cancer Immunotherapy with Sipuleucel-T: Current Standards and Future Directions.* Expert Rev Vaccines, 2015. **14**(12): p. 1529-41.
26. Higano, C.S., et al., *Integrated data from 2 randomized, double-blind, placebo-controlled, phase 3 trials of active cellular immunotherapy with sipuleucel-T in advanced prostate cancer.* Cancer, 2009. **115**(16): p. 3670-9.
27. Kantoff, P.W., et al., *Sipuleucel-T immunotherapy for castration-resistant prostate cancer.* N Engl J Med, 2010. **363**(5): p. 411-22.
28. Hinrichs, C.S. and S.A. Rosenberg, *Exploiting the curative potential of adoptive T-cell therapy for cancer.* Immunol Rev, 2014. **257**(1): p. 56-71.
29. Tran, E., et al., *Cancer immunotherapy based on mutation-specific CD4+ T cells in a patient with epithelial cancer.* Science, 2014. **344**(6184): p. 641-5.
30. Farkona, S., E.P. Diamandis, and I.M. Blasutig, *Cancer immunotherapy: the beginning of the end of cancer?* BMC Med, 2016. **14**: p. 73.
31. Rosenberg, S.A. and N.P. Restifo, *Adoptive cell transfer as personalized immunotherapy for human cancer.* Science, 2015. **348**(6230): p. 62-8.
32. Brentjens, R.J., et al., *CD19-targeted T cells rapidly induce molecular remissions in adults with chemotherapy-refractory acute lymphoblastic leukemia.* Sci Transl Med, 2013. **5**(177): p. 177ra38.
33. Rosenberg, S.A., et al., *Durable complete responses in heavily pretreated patients with metastatic melanoma using T-cell transfer immunotherapy.* Clin Cancer Res, 2011. **17**(13): p. 4550-7.
34. Yao, X., et al., *Levels of peripheral CD4(+)FoxP3(+) regulatory T cells are negatively associated with clinical response to adoptive immunotherapy of human cancer.* Blood, 2012. **119**(24): p. 5688-96.
35. Gattinoni, L., et al., *Removal of homeostatic cytokine sinks by lymphodepletion enhances the efficacy of adoptively transferred tumor-specific CD8+ T cells.* J Exp Med, 2005. **202**(7): p. 907-12.
36. Dudley, M.E., et al., *Adoptive cell therapy for patients with metastatic melanoma: evaluation of intensive myeloablative chemoradiation preparative regimens.* J Clin Oncol, 2008. **26**(32): p. 5233-9.
37. Wrzesinski, C., et al., *Increased intensity lymphodepletion enhances tumor treatment efficacy of adoptively transferred tumor-specific T cells.* J Immunother, 2010. **33**(1): p. 1-7.
38. Martin-Liberal, J., et al., *The expanding role of immunotherapy.* Cancer Treat Rev, 2017. **54**: p. 74-86.
39. Cartellieri, M., et al., *Chimeric antigen receptor-engineered T cells for immunotherapy of cancer.* J Biomed Biotechnol, 2010. **2010**: p. 956304.

40. Eshhar, Z., T. Waks, and G. Gross, *The emergence of T-bodies/CAR T cells.* Cancer J, 2014. **20**(2): p. 123-6.
41. Jackson, H.J., S. Rafiq, and R.J. Brentjens, *Driving CAR T-cells forward.* Nat Rev Clin Oncol, 2016. **13**(6): p. 370-83.
42. Davila, M.L., et al., *Efficacy and toxicity management of 19-28z CAR T cell therapy in B cell acute lymphoblastic leukemia.* Sci Transl Med, 2014. **6**(224): p. 224ra25.
43. Ritchie, D.S., et al., *Persistence and efficacy of second generation CAR T cell against the LeY antigen in acute myeloid leukemia.* Mol Ther, 2013. **21**(11): p. 2122-9.
44. Morgan, R.A., et al., *Cancer regression in patients after transfer of genetically engineered lymphocytes.* Science, 2006. **314**(5796): p. 126-9.
45. Johnson, L.A., et al., *Gene therapy with human and mouse T-cell receptors mediates cancer regression and targets normal tissues expressing cognate antigen.* Blood, 2009. **114**(3): p. 535-46.
46. Robbins, P.F., et al., *A pilot trial using lymphocytes genetically engineered with an NY-ESO-1-reactive T-cell receptor: long-term follow-up and correlates with response.* Clin Cancer Res, 2015. **21**(5): p. 1019-27.
47. Robbins, P.F., et al., *Tumor regression in patients with metastatic synovial cell sarcoma and melanoma using genetically engineered lymphocytes reactive with NY-ESO-1.* J Clin Oncol, 2011. **29**(7): p. 917-24.
48. Bendle, G.M., et al., *Lethal graft-versus-host disease in mouse models of T cell receptor gene therapy.* Nat Med, 2010. **16**(5): p. 565-70, 1p following 570.
49. Ikeda, H., *T-cell adoptive immunotherapy using tumor-infiltrating T cells and genetically engineered TCR-T cells.* Int Immunol, 2016. **28**(7): p. 349-53.
50. Cohen, C.J., et al., *Enhanced antitumor activity of T cells engineered to express T-cell receptors with a second disulfide bond.* Cancer Res, 2007. **67**(8): p. 3898-903.
51. Cohen, C.J., et al., *Enhanced antitumor activity of murine-human hybrid T-cell receptor (TCR) in human lymphocytes is associated with improved pairing and TCR/CD3 stability.* Cancer Res, 2006. **66**(17): p. 8878-86.
52. Okamoto, S., et al., *Improved expression and reactivity of transduced tumor-specific TCRs in human lymphocytes by specific silencing of endogenous TCR.* Cancer Res, 2009. **69**(23): p. 9003-11.
53. Klebanoff, C.A., et al., *Central memory self/tumor-reactive CD8+ T cells confer superior antitumor immunity compared with effector memory T cells.* Proc Natl Acad Sci U S A, 2005. **102**(27): p. 9571-6.
54. Sommermeyer, D., et al., *Chimeric antigen receptor-modified T cells derived from defined CD8+ and CD4+ subsets confer superior antitumor reactivity in vivo.* Leukemia, 2016. **30**(2): p. 492-500.
55. Klebanoff, C.A., et al., *Memory T cell-driven differentiation of naive cells impairs adoptive immunotherapy.* J Clin Invest, 2016. **126**(1): p. 318-34.
56. Kaluza, K.M., et al., *Adoptive T cell therapy promotes the emergence of genomically altered tumor escape variants.* Int J Cancer, 2012. **131**(4): p. 844-54.
57. Straetemans, T., et al., *Recurrence of melanoma following T cell treatment: continued antigen expression in a tumor that evades T cell recruitment.* Mol Ther, 2015. **23**(2): p. 396-406.
58. Murphy, K. and C. Weaver, *Janeway's immunobiology*. 9th edition. ed. 2016, New York, NY: Garland Science/Taylor & Francis Group, LLC. xx, 904 pages.
59. Nurieva, R., J. Wang, and A. Sahoo, *T-cell tolerance in cancer.* Immunotherapy, 2013. **5**(5): p. 513-31.

60. Paulson, K.G., et al., *Downregulation of MHC-I expression is prevalent but reversible in Merkel cell carcinoma.* Cancer Immunol Res, 2014. **2**(11): p. 1071-9.
61. Salih, H.R., et al., *The role of leukemia-derived B7-H1 (PD-L1) in tumor-T-cell interactions in humans.* Exp Hematol, 2006. **34**(7): p. 888-94.
62. Agaugue, S., E.D. Carosella, and N. Rouas-Freiss, *Role of HLA-G in tumor escape through expansion of myeloid-derived suppressor cells and cytokinic balance in favor of Th2 versus Th1/Th17.* Blood, 2011. **117**(26): p. 7021-31.
63. Liu, F.T. and G.A. Rabinovich, *Galectins as modulators of tumour progression.* Nat Rev Cancer, 2005. **5**(1): p. 29-41.
64. Yamamoto, R., et al., *PD-1-PD-1 ligand interaction contributes to immunosuppressive microenvironment of Hodgkin lymphoma.* Blood, 2008. **111**(6): p. 3220-4.
65. Hinz, S., et al., *Bcl-XL protects pancreatic adenocarcinoma cells against CD95- and TRAIL-receptor-mediated apoptosis.* Oncogene, 2000. **19**(48): p. 5477-86.
66. Takahashi, H., et al., *FAS death domain deletions and cellular FADD-like interleukin 1beta converting enzyme inhibitory protein (long) overexpression: alternative mechanisms for deregulating the extrinsic apoptotic pathway in diffuse large B-cell lymphoma subtypes.* Clin Cancer Res, 2006. **12**(11 Pt 1): p. 3265-71.
67. Saff, R.R., et al., *Activation-induced cell death limits effector function of CD4 tumor-specific T cells.* J Immunol, 2004. **172**(11): p. 6598-606.
68. Shin, M.S., et al., *Mutations of tumor necrosis factor-related apoptosis-inducing ligand receptor 1 (TRAIL-R1) and receptor 2 (TRAIL-R2) genes in metastatic breast cancers.* Cancer Res, 2001. **61**(13): p. 4942-6.
69. Gabrilovich, D.I., et al., *Production of vascular endothelial growth factor by human tumors inhibits the functional maturation of dendritic cells.* Nat Med, 1996. **2**(10): p. 1096-103.
70. Gerlini, G., et al., *Metastatic melanoma secreted IL-10 down-regulates CD1 molecules on dendritic cells in metastatic tumor lesions.* Am J Pathol, 2004. **165**(6): p. 1853-63.
71. Li, M.O., et al., *Transforming growth factor-beta regulation of immune responses.* Annu Rev Immunol, 2006. **24**: p. 99-146.
72. Shields, J.D., et al., *Induction of lymphoidlike stroma and immune escape by tumors that express the chemokine CCL21.* Science, 2010. **328**(5979): p. 749-52.
73. Uyttenhove, C., et al., *Evidence for a tumoral immune resistance mechanism based on tryptophan degradation by indoleamine 2,3-dioxygenase.* Nat Med, 2003. **9**(10): p. 1269-74.
74. Banerjee, A., A. Vasanthakumar, and G. Grigoriadis, *Modulating T regulatory cells in cancer: how close are we?* Immunol Cell Biol, 2013. **91**(5): p. 340-9.
75. Chung, C.D., et al., *Galectin-1 induces partial TCR zeta-chain phosphorylation and antagonizes processive TCR signal transduction.* J Immunol, 2000. **165**(7): p. 3722-9.
76. Cawthon, A.G., H. Lu, and M.A. Alexander-Miller, *Peptide requirement for CTL activation reflects the sensitivity to CD3 engagement: correlation with CD8alphabeta versus CD8alphaalpha expression.* J Immunol, 2001. **167**(5): p. 2577-84.
77. Schamel, W.W., et al., *Coexistence of multivalent and monovalent TCRs explains high sensitivity and wide range of response.* J Exp Med, 2005. **202**(4): p. 493-503.
78. Stone, J.D., A.S. Chervin, and D.M. Kranz, *T-cell receptor binding affinities and kinetics: impact on T-cell activity and specificity.* Immunology, 2009. **126**(2): p. 165-76.
79. Vigano, S., et al., *Functional avidity: a measure to predict the efficacy of effector T cells?* Clin Dev Immunol, 2012. **2012**: p. 153863.
80. Hebeisen, M., et al., *Identifying Individual T Cell Receptors of Optimal Avidity for Tumor Antigens.* Front Immunol, 2015. **6**: p. 582.

81. Viola, A. and A. Lanzavecchia, *T cell activation determined by T cell receptor number and tunable thresholds.* Science, 1996. **273**(5271): p. 104-6.
82. Alexander-Miller, M.A., G.R. Leggatt, and J.A. Berzofsky, *Selective expansion of high- or low-avidity cytotoxic T lymphocytes and efficacy for adoptive immunotherapy.* Proc Natl Acad Sci U S A, 1996. **93**(9): p. 4102-7.
83. Borbulevych, O.Y., et al., *TCRs used in cancer gene therapy cross-react with MART-1/Melan-A tumor antigens via distinct mechanisms.* J Immunol, 2011. **187**(5): p. 2453-63.
84. Bullock, T.N., et al., *Manipulation of avidity to improve effectiveness of adoptively transferred CD8(+) T cells for melanoma immunotherapy in human MHC class I-transgenic mice.* J Immunol, 2001. **167**(10): p. 5824-31.
85. Dutoit, V., et al., *Heterogeneous T-cell response to MAGE-A10(254-262): high avidity-specific cytolytic T lymphocytes show superior antitumor activity.* Cancer Res, 2001. **61**(15): p. 5850-6.
86. McCormack, P.L., *Pertuzumab: a review of its use for first-line combination treatment of HER2-positive metastatic breast cancer.* Drugs, 2013. **73**(13): p. 1491-502.
87. Parkhurst, M.R., et al., *T cells targeting carcinoembryonic antigen can mediate regression of metastatic colorectal cancer but induce severe transient colitis.* Mol Ther, 2011. **19**(3): p. 620-6.
88. Zeh, H.J., 3rd, et al., *High avidity CTLs for two self-antigens demonstrate superior in vitro and in vivo antitumor efficacy.* J Immunol, 1999. **162**(2): p. 989-94.
89. Hurwitz, A.A., et al., *T cell avidity and tumor immunity: problems and solutions.* Cancer Microenviron, 2014. **7**(1-2): p. 1-9.
90. Irving, M., et al., *Interplay between T cell receptor binding kinetics and the level of cognate peptide presented by major histocompatibility complexes governs CD8+ T cell responsiveness.* J Biol Chem, 2012. **287**(27): p. 23068-78.
91. Zhong, S., et al., *T-cell receptor affinity and avidity defines antitumor response and autoimmunity in T-cell immunotherapy.* Proc Natl Acad Sci U S A, 2013. **110**(17): p. 6973-8.
92. Janicki, C.N., et al., *Loss of CTL function among high-avidity tumor-specific CD8+ T cells following tumor infiltration.* Cancer Res, 2008. **68**(8): p. 2993-3000.
93. Shafer-Weaver, K.A., et al., *Cutting Edge: Tumor-specific CD8+ T cells infiltrating prostatic tumors are induced to become suppressor cells.* J Immunol, 2009. **183**(8): p. 4848-52.
94. Filaci, G., et al., *CD8+ CD28- T regulatory lymphocytes inhibiting T cell proliferative and cytotoxic functions infiltrate human cancers.* J Immunol, 2007. **179**(7): p. 4323-34.
95. Filaci, G., et al., *Nonantigen specific CD8+ T suppressor lymphocytes originate from CD8+CD28- T cells and inhibit both T-cell proliferation and CTL function.* Hum Immunol, 2004. **65**(2): p. 142-56.
96. Kiniwa, Y., et al., *CD8+ Foxp3+ regulatory T cells mediate immunosuppression in prostate cancer.* Clin Cancer Res, 2007. **13**(23): p. 6947-58.
97. Meloni, F., et al., *Foxp3 expressing CD4+ CD25+ and CD8+CD28- T regulatory cells in the peripheral blood of patients with lung cancer and pleural mesothelioma.* Hum Immunol, 2006. **67**(1-2): p. 1-12.
98. Onyema, O.O., et al., *Shifts in subsets of CD8+ T-cells as evidence of immunosenescence in patients with cancers affecting the lungs: an observational case-control study.* BMC Cancer, 2015. **15**: p. 1016.
99. Tsukishiro, T., A.D. Donnenberg, and T.L. Whiteside, *Rapid turnover of the CD8(+)CD28(-) T-cell subset of effector cells in the circulation of patients with head and neck cancer.* Cancer Immunol Immunother, 2003. **52**(10): p. 599-607.

100. Parkhurst, M.R., et al., *Identification of a shared HLA-A*0201-restricted T-cell epitope from the melanoma antigen tyrosinase-related protein 2 (TRP2).* Cancer Res, 1998. **58**(21): p. 4895-901.
101. Currier, J.R. and M.A. Robinson, *Spectratype/immunoscope analysis of the expressed TCR repertoire.* Curr Protoc Immunol, 2001. **Chapter 10**: p. Unit 10 28.
102. Singh, V., et al., *Melanoma progression despite infiltration by in vivo-primed TRP-2-specific T cells.* J Immunother, 2009. **32**(2): p. 129-39.
103. Zhu, Z., et al., *CD4+ T Cell Help Selectively Enhances High-Avidity Tumor Antigen-Specific CD8+ T Cells.* J Immunol, 2015. **195**(7): p. 3482-9.
104. Robbins, P.F., et al., *Cutting edge: persistence of transferred lymphocyte clonotypes correlates with cancer regression in patients receiving cell transfer therapy.* J Immunol, 2004. **173**(12): p. 7125-30.
105. Zhou, J., et al., *Persistence of multiple tumor-specific T-cell clones is associated with complete tumor regression in a melanoma patient receiving adoptive cell transfer therapy.* J Immunother, 2005. **28**(1): p. 53-62.
106. Badovinac, V.P. and J.T. Harty, *CD8(+) T-cell homeostasis after infection: setting the 'curve'.* Microbes Infect, 2002. **4**(4): p. 441-7.
107. D'Cruz, L.M., M.P. Rubinstein, and A.W. Goldrath, *Surviving the crash: transitioning from effector to memory CD8+ T cell.* Semin Immunol, 2009. **21**(2): p. 92-8.
108. Jameson, S.C. and D. Masopust, *Diversity in T cell memory: an embarrassment of riches.* Immunity, 2009. **31**(6): p. 859-71.
109. Masopust, D., et al., *Preferential localization of effector memory cells in nonlymphoid tissue.* Science, 2001. **291**(5512): p. 2413-7.
110. Sallusto, F., et al., *Two subsets of memory T lymphocytes with distinct homing potentials and effector functions.* Nature, 1999. **401**(6754): p. 708-12.
111. Gebhardt, T., et al., *Different patterns of peripheral migration by memory CD4+ and CD8+ T cells.* Nature, 2011. **477**(7363): p. 216-9.
112. Busch, D.H., et al., *Role of memory T cell subsets for adoptive immunotherapy.* Semin Immunol, 2016. **28**(1): p. 28-34.
113. Farber, D.L., N.A. Yudanin, and N.P. Restifo, *Human memory T cells: generation, compartmentalization and homeostasis.* Nat Rev Immunol, 2014. **14**(1): p. 24-35.
114. Gattinoni, L., C.A. Klebanoff, and N.P. Restifo, *Paths to stemness: building the ultimate antitumour T cell.* Nat Rev Cancer, 2012. **12**(10): p. 671-84.
115. Gattinoni, L., et al., *A human memory T cell subset with stem cell-like properties.* Nat Med, 2011. **17**(10): p. 1290-7.
116. Zhang, Y., et al., *Host-reactive CD8+ memory stem cells in graft-versus-host disease.* Nat Med, 2005. **11**(12): p. 1299-305.
117. Gebhardt, T., et al., *Memory T cells in nonlymphoid tissue that provide enhanced local immunity during infection with herpes simplex virus.* Nat Immunol, 2009. **10**(5): p. 524-30.
118. Flynn, J.K. and P.R. Gorry, *Stem memory T cells (TSCM)-their role in cancer and HIV immunotherapies.* Clin Transl Immunology, 2014. **3**(7): p. e20.
119. Rosenblum, M.D., S.S. Way, and A.K. Abbas, *Regulatory T cell memory.* Nat Rev Immunol, 2016. **16**(2): p. 90-101.
120. Jameson, S.C., Y.J. Lee, and K.A. Hogquist, *Innate memory T cells.* Adv Immunol, 2015. **126**: p. 173-213.
121. Behar, S.M. and S.A. Porcelli, *CD1-restricted T cells in host defense to infectious diseases.* Curr Top Microbiol Immunol, 2007. **314**: p. 215-50.

122. Berg, L.J., *Signalling through TEC kinases regulates conventional versus innate CD8(+) T-cell development.* Nat Rev Immunol, 2007. **7**(6): p. 479-85.
123. Cho, H., et al., *Nonconventional CD8+ T cell responses to Listeria infection in mice lacking MHC class Ia and H2-M3.* J Immunol, 2011. **186**(1): p. 489-98.
124. Oliveira, C.C., et al., *The nonpolymorphic MHC Qa-1b mediates CD8+ T cell surveillance of antigen-processing defects.* J Exp Med, 2010. **207**(1): p. 207-21.
125. Intlekofer, A.M., et al., *Effector and memory CD8+ T cell fate coupled by T-bet and eomesodermin.* Nat Immunol, 2005. **6**(12): p. 1236-44.
126. Pearce, E.L., et al., *Control of effector CD8+ T cell function by the transcription factor Eomesodermin.* Science, 2003. **302**(5647): p. 1041-3.
127. Hu, J., et al., *Memory phenotype CD8+ T cells with innate function selectively develop in the absence of active Itk.* Eur J Immunol, 2007. **37**(10): p. 2892-9.
128. Broussard, C., et al., *Altered development of CD8+ T cell lineages in mice deficient for the Tec kinases Itk and Rlk.* Immunity, 2006. **25**(1): p. 93-104.
129. Fukuyama, T., et al., *Histone acetyltransferase CBP is vital to demarcate conventional and innate CD8+ T-cell development.* Mol Cell Biol, 2009. **29**(14): p. 3894-904.
130. Horai, R., et al., *Requirements for selection of conventional and innate T lymphocyte lineages.* Immunity, 2007. **27**(5): p. 775-85.
131. Jordan, M.S., et al., *Complementation in trans of altered thymocyte development in mice expressing mutant forms of the adaptor molecule SLP76.* Immunity, 2008. **28**(3): p. 359-69.
132. Verykokakis, M., et al., *SAP protein-dependent natural killer T-like cells regulate the development of CD8(+) T cells with innate lymphocyte characteristics.* Immunity, 2010. **33**(2): p. 203-15.
133. Weinreich, M.A., et al., *KLF2 transcription-factor deficiency in T cells results in unrestrained cytokine production and upregulation of bystander chemokine receptors.* Immunity, 2009. **31**(1): p. 122-30.
134. Itsumi, M., Y. Yoshikai, and H. Yamada, *IL-15 is critical for the maintenance and innate functions of self-specific CD8(+) T cells.* Eur J Immunol, 2009. **39**(7): p. 1784-93.
135. Weinreich, M.A., et al., *T cells expressing the transcription factor PLZF regulate the development of memory-like CD8+ T cells.* Nat Immunol, 2010. **11**(8): p. 709-16.
136. Rafei, M., et al., *Development and function of innate polyclonal TCRalphabeta+ CD8+ thymocytes.* J Immunol, 2011. **187**(6): p. 3133-44.
137. Haluszczak, C., et al., *The antigen-specific CD8+ T cell repertoire in unimmunized mice includes memory phenotype cells bearing markers of homeostatic expansion.* J Exp Med, 2009. **206**(2): p. 435-48.
138. Huang, W., J. Hu, and A. August, *Cutting edge: innate memory CD8+ T cells are distinct from homeostatic expanded CD8+ T cells and rapidly respond to primary antigenic stimuli.* J Immunol, 2013. **190**(6): p. 2490-4.
139. Jameson, S.C., *T cell homeostasis: keeping useful T cells alive and live T cells useful.* Semin Immunol, 2005. **17**(3): p. 231-7.
140. Marleau, A.M. and N. Sarvetnick, *T cell homeostasis in tolerance and immunity.* J Leukoc Biol, 2005. **78**(3): p. 575-84.
141. Surh, C.D. and J. Sprent, *Regulation of mature T cell homeostasis.* Semin Immunol, 2005. **17**(3): p. 183-91.
142. Le Campion, A., et al., *Naive T cells proliferate strongly in neonatal mice in response to self-peptide/self-MHC complexes.* Proc Natl Acad Sci U S A, 2002. **99**(7): p. 4538-43.

143. Min, B., et al., *Neonates support lymphopenia-induced proliferation.* Immunity, 2003. **18**(1): p. 131-40.
144. Schuler, T., G.J. Hammerling, and B. Arnold, *Cutting edge: IL-7-dependent homeostatic proliferation of CD8+ T cells in neonatal mice allows the generation of long-lived natural memory T cells.* J Immunol, 2004. **172**(1): p. 15-9.
145. Ernst, B., et al., *The peptide ligands mediating positive selection in the thymus control T cell survival and homeostatic proliferation in the periphery.* Immunity, 1999. **11**(2): p. 173-81.
146. Goldrath, A.W. and M.J. Bevan, *Low-affinity ligands for the TCR drive proliferation of mature CD8+ T cells in lymphopenic hosts.* Immunity, 1999. **11**(2): p. 183-90.
147. Kieper, W.C. and S.C. Jameson, *Homeostatic expansion and phenotypic conversion of naive T cells in response to self peptide/MHC ligands.* Proc Natl Acad Sci U S A, 1999. **96**(23): p. 13306-11.
148. Hamilton, S.E. and S.C. Jameson, *The nature of the lymphopenic environment dictates protective function of homeostatic-memory CD8+ T cells.* Proc Natl Acad Sci U S A, 2008. **105**(47): p. 18484-9.
149. Cho, J.H., et al., *An intense form of homeostatic proliferation of naive CD8+ cells driven by IL-2.* J Exp Med, 2007. **204**(8): p. 1787-801.
150. Kieper, W.C., et al., *Il-12 enhances CD8 T cell homeostatic expansion.* J Immunol, 2001. **166**(9): p. 5515-21.
151. Sandau, M.M., C.J. Winstead, and S.C. Jameson, *IL-15 is required for sustained lymphopenia-driven proliferation and accumulation of CD8 T cells.* J Immunol, 2007. **179**(1): p. 120-5.
152. Schluns, K.S., et al., *Interleukin-7 mediates the homeostasis of naive and memory CD8 T cells in vivo.* Nat Immunol, 2000. **1**(5): p. 426-32.
153. Hamilton, S.E., et al., *The generation of protective memory-like CD8+ T cells during homeostatic proliferation requires CD4+ T cells.* Nat Immunol, 2006. **7**(5): p. 475-81.
154. Stockinger, B., G. Kassiotis, and C. Bourgeois, *Homeostasis and T cell regulation.* Curr Opin Immunol, 2004. **16**(6): p. 775-9.
155. Huang, T., et al., *Commensal microbiota alter the abundance and TCR responsiveness of splenic naive CD4+ T lymphocytes.* Clin Immunol, 2005. **117**(3): p. 221-30.
156. Akue, A.D., J.Y. Lee, and S.C. Jameson, *Derivation and maintenance of virtual memory CD8 T cells.* J Immunol, 2012. **188**(6): p. 2516-23.
157. La Gruta, N.L., et al., *Primary CTL response magnitude in mice is determined by the extent of naive T cell recruitment and subsequent clonal expansion.* J Clin Invest, 2010. **120**(6): p. 1885-94.
158. Obar, J.J., K.M. Khanna, and L. Lefrancois, *Endogenous naive CD8+ T cell precursor frequency regulates primary and memory responses to infection.* Immunity, 2008. **28**(6): p. 859-69.
159. Schluns, K.S. and L. Lefrancois, *Cytokine control of memory T-cell development and survival.* Nat Rev Immunol, 2003. **3**(4): p. 269-79.
160. Surh, C.D. and J. Sprent, *Homeostasis of naive and memory T cells.* Immunity, 2008. **29**(6): p. 848-62.
161. Tian, C., J. Bagley, and J. Iacomini, *Homeostatic expansion permits T cells to re-enter the thymus and deliver antigen in a tolerogenic fashion.* Am J Transplant, 2007. **7**(8): p. 1934-41.
162. Klebanoff, C.A., et al., *IL-15 enhances the in vivo antitumor activity of tumor-reactive CD8+ T cells.* Proc Natl Acad Sci U S A, 2004. **101**(7): p. 1969-74.

163. Berger, C., et al., *Adoptive transfer of effector CD8+ T cells derived from central memory cells establishes persistent T cell memory in primates.* J Clin Invest, 2008. **118**(1): p. 294-305.
164. Wang, A., et al., *The stoichiometric production of IL-2 and IFN-gamma mRNA defines memory T cells that can self-renew after adoptive transfer in humans.* Sci Transl Med, 2012. **4**(149): p. 149ra120.
165. Guyonneau, L., et al., *Expression of Cre recombinase in pigment cells.* Pigment Cell Res, 2002. **15**(4): p. 305-9.
166. Mueller, K., O. Schweier, and H. Pircher, *Efficacy of IL-2- versus IL-15-stimulated CD8 T cells in adoptive immunotherapy.* Eur J Immunol, 2008. **38**(10): p. 2874-85.
167. Anderson, M.J., et al., *Tolerization of tumor-specific T cells despite efficient initial priming in a primary murine model of prostate cancer.* J Immunol, 2007. **178**(3): p. 1268-76.
168. Lee, J.Y., et al., *Virtual memory CD8 T cells display unique functional properties.* Proc Natl Acad Sci U S A, 2013. **110**(33): p. 13498-503.
169. Sosinowski, T., et al., *CD8alpha+ dendritic cell trans presentation of IL-15 to naive CD8+ T cells produces antigen-inexperienced T cells in the periphery with memory phenotype and function.* J Immunol, 2013. **190**(5): p. 1936-47.
170. Renkema, K.R., et al., *Two separate defects affecting true naive or virtual memory T cell precursors combine to reduce naive T cell responses with aging.* J Immunol, 2014. **192**(1): p. 151-9.
171. Chiu, B.C., et al., *Cutting edge: Central memory CD8 T cells in aged mice are virtual memory cells.* J Immunol, 2013. **191**(12): p. 5793-6.
172. Rudd, B.D., et al., *Evolution of the antigen-specific CD8+ TCR repertoire across the life span: evidence for clonal homogenization of the old TCR repertoire.* J Immunol, 2011. **186**(4): p. 2056-64.
173. Baaten, B.J., et al., *Regulation of Antigen-Experienced T Cells: Lessons from the Quintessential Memory Marker CD44.* Front Immunol, 2012. **3**: p. 23.
174. Wherry, E.J., *T cell exhaustion.* Nat Immunol, 2011. **12**(6): p. 492-9.
175. Mazzucchelli, R., et al., *Development of regulatory T cells requires IL-7Ralpha stimulation by IL-7 or TSLP.* Blood, 2008. **112**(8): p. 3283-92.
176. Ray, R.J., et al., *Characterization of thymic stromal-derived lymphopoietin (TSLP) in murine B cell development in vitro.* Eur J Immunol, 1996. **26**(1): p. 10-6.
177. Drake, A., et al., *Interleukins 7 and 15 Maintain Human T Cell Proliferative Capacity through STAT5 Signaling.* PLoS One, 2016. **11**(11): p. e0166280.
178. Park, L.S., et al., *Cloning of the murine thymic stromal lymphopoietin (TSLP) receptor: Formation of a functional heteromeric complex requires interleukin 7 receptor.* J Exp Med, 2000. **192**(5): p. 659-70.
179. Wohlmann, A., et al., *Signal transduction by the atopy-associated human thymic stromal lymphopoietin (TSLP) receptor depends on Janus kinase function.* Biol Chem, 2010. **391**(2-3): p. 181-6.
180. Freeman, B.E., et al., *Regulation of innate CD8+ T-cell activation mediated by cytokines.* Proc Natl Acad Sci U S A, 2012. **109**(25): p. 9971-6.
181. Hinrichs, C.S., et al., *Human effector CD8+ T cells derived from naive rather than memory subsets possess superior traits for adoptive immunotherapy.* Blood, 2011. **117**(3): p. 808-14.
182. Amae, S., et al., *Identification of a composite enhancer of the human tyrosinase-related protein 2/DOPAchrome tautomerase gene.* Biochim Biophys Acta, 2000. **1492**(2-3): p. 505-8.

183. Tsukamoto, K., et al., *A second tyrosinase-related protein, TRP-2, is a melanogenic enzyme termed DOPAchrome tautomerase.* EMBO J, 1992. **11**(2): p. 519-26.
184. Guyonneau, L., et al., *Melanocytes and pigmentation are affected in dopachrome tautomerase knockout mice.* Mol Cell Biol, 2004. **24**(8): p. 3396-403.
185. McLane, L.M., et al., *Differential localization of T-bet and Eomes in CD8 T cell memory populations.* J Immunol, 2013. **190**(7): p. 3207-15.
186. Klose, C.S., et al., *The transcription factor T-bet is induced by IL-15 and thymic agonist selection and controls CD8alphaalpha(+) intraepithelial lymphocyte development.* Immunity, 2014. **41**(2): p. 230-43.
187. Berard, M., et al., *IL-15 promotes the survival of naive and memory phenotype CD8+ T cells.* J Immunol, 2003. **170**(10): p. 5018-26.
188. White, J.T., et al., *Virtual memory T cells develop and mediate bystander protective immunity in an IL-15-dependent manner.* Nat Commun, 2016. **7**: p. 11291.
189. Ilangumaran, S., et al., *Suppressor of cytokine signaling 1 attenuates IL-15 receptor signaling in CD8+ thymocytes.* Blood, 2003. **102**(12): p. 4115-22.
190. Tan, J.T., et al., *IL-7 is critical for homeostatic proliferation and survival of naive T cells.* Proc Natl Acad Sci U S A, 2001. **98**(15): p. 8732-7.
191. Bhatia, S.K., et al., *The effect of in vivo IL-7 deprivation on T cell maturation.* J Exp Med, 1995. **181**(4): p. 1399-409.
192. Grabstein, K.H., et al., *Inhibition of murine B and T lymphopoiesis in vivo by an anti-interleukin 7 monoclonal antibody.* J Exp Med, 1993. **178**(1): p. 257-64.
193. von Freeden-Jeffry, U., et al., *Lymphopenia in interleukin (IL)-7 gene-deleted mice identifies IL-7 as a nonredundant cytokine.* J Exp Med, 1995. **181**(4): p. 1519-26.
194. Goldrath, A.W., L.Y. Bogatzki, and M.J. Bevan, *Naive T cells transiently acquire a memory-like phenotype during homeostasis-driven proliferation.* J Exp Med, 2000. **192**(4): p. 557-64.
195. Tan, J.T., et al., *Interleukin (IL)-15 and IL-7 jointly regulate homeostatic proliferation of memory phenotype CD8+ cells but are not required for memory phenotype CD4+ cells.* J Exp Med, 2002. **195**(12): p. 1523-32.
196. Kurzweil, V., A. LaRoche, and P.M. Oliver, *Increased peripheral IL-4 leads to an expanded virtual memory CD8+ population.* J Immunol, 2014. **192**(12): p. 5643-51.
197. Cho, B.K., et al., *Homeostasis-stimulated proliferation drives naive T cells to differentiate directly into memory T cells.* J Exp Med, 2000. **192**(4): p. 549-56.
198. Berg, R.E., et al., *Memory CD8+ T cells provide innate immune protection against Listeria monocytogenes in the absence of cognate antigen.* J Exp Med, 2003. **198**(10): p. 1583-93.
199. Kambayashi, T., et al., *Memory CD8+ T cells provide an early source of IFN-gamma.* J Immunol, 2003. **170**(5): p. 2399-408.
200. Musso, T., et al., *Interleukin-15 activates proinflammatory and antimicrobial functions in polymorphonuclear cells.* Infect Immun, 1998. **66**(6): p. 2640-7.
201. Huntington, N.D., et al., *IL-15 trans-presentation promotes human NK cell development and differentiation in vivo.* J Exp Med, 2009. **206**(1): p. 25-34.
202. Kennedy, M.K., et al., *Reversible defects in natural killer and memory CD8 T cell lineages in interleukin 15-deficient mice.* J Exp Med, 2000. **191**(5): p. 771-80.
203. Lodolce, J.P., et al., *T cell-independent interleukin 15Ralpha signals are required for bystander proliferation.* J Exp Med, 2001. **194**(8): p. 1187-94.
204. Carson, W.E., et al., *Interleukin (IL) 15 is a novel cytokine that activates human natural killer cells via components of the IL-2 receptor.* J Exp Med, 1994. **180**(4): p. 1395-403.

205. Chae, D.W., et al., *Distribution of IL-15 receptor alpha-chains on human peripheral blood mononuclear cells and effect of immunosuppressive drugs on receptor expression.* J Immunol, 1996. **157**(7): p. 2813-9.
206. Zanoni, I., et al., *IL-15 cis presentation is required for optimal NK cell activation in lipopolysaccharide-mediated inflammatory conditions.* Cell Rep, 2013. **4**(6): p. 1235-49.
207. Dummer, W., et al., *T cell homeostatic proliferation elicits effective antitumor autoimmunity.* J Clin Invest, 2002. **110**(2): p. 185-92.
208. Hu, H.M., et al., *Development of antitumor immune responses in reconstituted lymphopenic hosts.* Cancer Res, 2002. **62**(14): p. 3914-9.
209. Li, Q., et al., *A central role for mTOR kinase in homeostatic proliferation induced CD8+ T cell memory and tumor immunity.* Immunity, 2011. **34**(4): p. 541-53.
210. Wang, L.X., et al., *Interleukin-7-dependent expansion and persistence of melanoma-specific T cells in lymphodepleted mice lead to tumor regression and editing.* Cancer Res, 2005. **65**(22): p. 10569-77.
211. Dudley, M.E., et al., *A phase I study of nonmyeloablative chemotherapy and adoptive transfer of autologous tumor antigen-specific T lymphocytes in patients with metastatic melanoma.* J Immunother, 2002. **25**(3): p. 243-51.
212. Muranski, P., et al., *Increased intensity lymphodepletion and adoptive immunotherapy--how far can we go?* Nat Clin Pract Oncol, 2006. **3**(12): p. 668-81.
213. Sukumar, M., et al., *Inhibiting glycolytic metabolism enhances CD8+ T cell memory and antitumor function.* J Clin Invest, 2013. **123**(10): p. 4479-88.
214. Kim, H.J., et al., *Inhibition of follicular T-helper cells by CD8(+) regulatory T cells is essential for self tolerance.* Nature, 2010. **467**(7313): p. 328-32.
215. Kim, H.J., et al., *CD8+ T regulatory cells express the Ly49 Class I MHC receptor and are defective in autoimmune prone B6-Yaa mice.* Proc Natl Acad Sci U S A, 2011. **108**(5): p. 2010-5.
216. Lin, S.J., et al., *Programmed death-1 (PD-1) defines a transient and dysfunctional oligoclonal T cell population in acute homeostatic proliferation.* J Exp Med, 2007. **204**(10): p. 2321-33.
217. Rifa'i, M., et al., *Essential roles of CD8+CD122+ regulatory T cells in the maintenance of T cell homeostasis.* J Exp Med, 2004. **200**(9): p. 1123-34.
218. Sakuraba, K., et al., *Naturally occurring PD-1+ memory phenotype CD8 T cells belong to nonconventional CD8 T cells and are cyclophosphamide-sensitive regulatory T cells.* J Immunol, 2013. **190**(4): p. 1560-6.